SIMULATION AND OPTIMIZATION OF SEAWATER INTRUSION IN COASTAL AQUIFERS DUE TO CLIMATE CHANGE AND SEA LEVEL RISE

By

NEBIYU DANIEL TIRUNEH

A DISSERTATION PRESENTED TO THE GRADUATE SCHOOL
OF THE UNIVERSITY OF FLORIDA IN PARTIAL FULFILLMENT
OF THE REQUIREMENTS FOR THE DEGREE OF
DOCTOR OF PHILOSOPHY

UNIVERSITY OF FLORIDA

2004

Once again, to my loving parents Daniel Tirunch and Yeshimebet Hawaz, who gave me life and raised me to be who I am. Although it is grossly inadequate to express my gratitude, I dedicate this to you both with love and respect.

ACKNOWLEDGMENTS

First and foremost, praise and glory be to almighty God who made every thing possible and established my thoughts (Prov 16,3)

I would like to extend my sincere thanks and appreciation to my mentor and advisor Dr Louis H Motz, who introduced me to the world of groundwater flow modeling and the problem of seawater intrusion His invaluable guidance and encouragement throughout the duration of my study have been driving forces behind the many hours spent working on computer programs and seemingly endless simulations.

My sincere thanks and appreciation also go to Dr Kirk Hatfield for being an invaluable source of support in many respects He has inspired me in many ways and instilled the appreciation for problem solving in groundwater transport modeling I have also benefited from his groundwater quality evaluation lectures

I would like to thank my committee members, Dr Scot Smith, Dr William Wise and Dr Elizabeth Screaton for their interest in my work, guidance, and for sharing my vision They have provided stimulating insights since the inception of the concept and problem formulation Their varied expertise and comments have shaped the research into what it finally turned out to be.

Special thanks to Dr Gualbert Oude Essink of Free University of Amsterdam and Dr Christian Langevin of the USGS for being extremely helpful by sharing their views data, and other resources.

I would finally like to thank my beloved parents, brothers, sisters and dear friends too many to name in a short acknowledgment. The love and care of my family and friends have seen me through the many tiresome and sleepless nights

Finally, my sincere thanks go to the staff and faculty of the Department of Civil and Coastal Engineering for their kindness and unreserved support, especially to Dr Mark Newman for sharing his experience

TABLE OF CONTENTS

LIST OF TABLES

LIST OF FIGURES

Abstract of Dissertation Presented to the Graduate School
of the University of Florida in Partial Fulfillment of the
Requirements for the Degree of Doctor of Philosophy

SIMULATION AND OPTIMIZATION OF SEAWATER INTRUSION IN COASTAL AQUIFERS DUE TO CLIMATE CHANGE AND SEA LEVEL RISE

By

Nebiyu Daniel Tiruneh

December 2004

Chair: Dr. Louis H. Motz
Cochair: Dr. Kirk Hatfield
Major Department: Civil and Coastal Engineering

Seawater intrusion, also synonymously referred to in some literature as saltwater intrusion, has become an increasingly dominant constraint on the utilization of groundwater in coastal aquifers. Climate change is a natural factor that has been identified to have serious impacts on the hydrologic regime and water resources. When coupled with extensive freshwater withdrawal through pumping, climate change could pose a serious threat to coastal freshwater resources.

The research presented in this dissertation has three basic components: generation of climate change impact scenarios; simulation of sea level rise sensitive variable-density groundwater flow; and optimization of freshwater withdrawal from coastal aquifers. The climate change scenario generation module was developed using the spatial modeling capabilities of raster based geographical information systems (GIS). The module specifically models sea level rise and generates new sea levels, shoreline translations, and impact maps.

The variable-density groundwater flow simulation module simulates the influence of sea level rise in altering the groundwater flow regime A scenario of climate change was selected and applied. Extensive sensitivity analyses were performed to test the significance of various parameters

The optimization model is based on the concept of genetic algorithms. The use of evolutionary algorithms to solve optimization problems in water resources is a fairly recent approach. The capability of evolutionary algorithms to handle non-linear problems has created interest in the application of these algorithms in the solution of simulation-optimization problems

The research methodology followed a systematic approach that involved investigation of climate change impacts, simulation of freshwater saltwater flow and optimization of freshwater withdrawals subject to the various constraints considered. A three-dimensional variable density groundwater flow model and a cross-sectional model were developed to simulate seawater intrusion

The primary objective of the research was to provide an integrated approach to the investigation of seawater intrusion in coastal aquifers and to develop a better understanding of the processes involved. The results obtained from the test cases considered clearly demonstrate the significance of sea level rise as a factor to be considered in the development of management strategies for coastal aquifers

CHAPTER 1
INTRODUCTION

Water is a very precious natural resource. It is estimated that 99.4% of the available water resources of the earth (1.4×10^9 km^3) are surface water. Groundwater accounts only for 0.6% (9×10^6 km^3) of the total. From the total amount of surface water, most of it (97%) is in the form of salt water in oceans and inland seas. Fresh surface water accounts for only 2% of the total volume of water (Bear et al., 1999).

If salt water is excluded, the proportion of surface and sub-surface freshwater resources becomes 78% and 22%, respectively. Most of the freshwater is in the form of ice locked in the ice caps of the polar regions. This amount is estimated to be 77% of the total volume of surface freshwater. The fresh surface-water resources that are readily usable for human consumption are a very small proportion, 0.3% in lakes and 0.003% in streams, whereas the groundwater is comparatively a very large 22%. Thus, because water shortages are unavoidable in the foreseeable future (Gleick, 1993), it would be very prudent to conclude that the future of mankind is dependent on a sustainable exploitation of groundwater.

In order to manage properly fresh groundwater resources in coastal areas, it is necessary to investigate the possibility of intrusion of salt water into coastal aquifers. Saltwater intrusion is described as a mass transport of saline waters into zones of the aquifer that were previously occupied by fresh water (Stewart, 1999). This degradation of the water quality is characterized by increases in salinity levels that exceed the

acceptable values for potable or agricultural uses. This problem requires a greater attention because about 70% of the world population lives in coastal plains.

Global climate change is one of the most pressing environmental issues we are facing today. The Intergovernmental Panel on Climate Change (IPCC) has undertaken a comprehensive assessment of the scientific evidence about global climate change. The results of the IPCC assessments were published in a series of reports since 1990. According to the reports, substantial changes in the environment have occurred in the past centuries as a result of human activities associated with advances in science and technology (IPCC 1995a, 2001a). There is also an overwhelming body of research conducted by climate researchers from around the world suggesting that human activities have contributed significantly to climate change (Kondratyev and Cracknell, 1998; and Storch and Floser, 1999).

Through the years, various agricultural and industrial practices have led to increased atmospheric concentrations of several greenhouse gases, including carbon dioxide, methane, nitrous oxide, and chlorofluorocarbons (CFC) in the lower part of the atmosphere. The basic heat-trapping property of these greenhouse gases is essentially undisputed, although there is considerable scientific uncertainty about exactly how and when the earth's climate will respond to enhanced greenhouse gases in the future.

Climate Change

The importance of studying climate change with the aim of establishing a better understanding of the climatic process and determining the contributions of natural causes and anthropogenic effects has been emphasized in the wake of the growing concern about the possible effects of CO_2, chlorofluorocarbons (CFCs), and other greenhouse gases. The physical and chemical factors that affect climate and bring about change have been

under investigation. The majority of climatological research in recent years has been conducted with the aim of predicting the impacts of human activities on the climate However, the difficulties involved in studying the effects of human activities directly have necessitated the modeling of climate change to be based primarily on predicting the climate change due to natural factors and then introducing anthropogenic effects (Kondratyev and Cracknell, 1998)

There are two main modeling approaches currently in use to forecast the impact of climate change The first one involves working out analogues from past climatic and hydrometric records. The second, which is more commonly used, employs mathematical simulations of climate known as general circulation models or global climate models (GCMs)

Climatic analogues are developed by choosing warmer than average years from the historical record and identifying what conditions were like to get an idea of the likely effects of global warming The limitation of this method is that the relatively short period of climatic data does not represent conditions that may come with future climate change For example, unprecedented long-term increases in temperature, particularly in wintertime, may not be in past records.

The GCMs simulate atmospheric circulation the energy exchanges, and other important land/ocean/atmosphere interactions However they cannot as yet model well other small scale processes such as biological processes, precipitation, and cloud cover These processes have significant effects on water resources The GCMs in current use project climate over several decades to more than a century ("climate" being based on

average weather conditions over 10 years or more) but give only large-scale predictions, not the regional ones needed for planning.

Results from the models used by climatologists generally agree that the temperature increase, as a global annual average, might be from 1°C to 4°C by the year 2100. They also agree that the effect would be greater in the higher latitudes, especially during the winter months and over large land masses. The warmer temperature would trigger other changes, such as a change in global precipitation patterns, a decrease in snow and ice coverage, and a rise in sea levels. GCMs simulating a climate that is based on a doubling of CO_2 suggest a global mean increase in precipitation and evaporation of between 3 and 15%. Yet the more useful information, i.e., the location and timing of these changes, is still uncertain.

Climate Change Detection and Modeling

The climate system is characterized by a complex system of interacting internal and external components. The internal interactive components include the atmosphere, the oceans, sea ice, the land and its features (including vegetation, albedo, biomass, and ecosystems), snow cover, land ice (including the semi-permanent ice sheets of Antarctica and Greenland and glaciers), and hydrology (including rivers, lakes, and surface and subsurface water) (IPCC, 1995a). The components of the climate system that are customarily regarded as external to the system include the Sun and its output, the Earth's rotation, Sun-Earth geometry, and the slowly changing orbit, the physical components of the Earth system such as the distribution of land and ocean, geographic features on the land, ocean bottom topography and basin configurations, and the mass and basic composition of the atmosphere and ocean (IPCC, 1996a). Figure 1.1 is a schematic representation of the components of the global climate system.

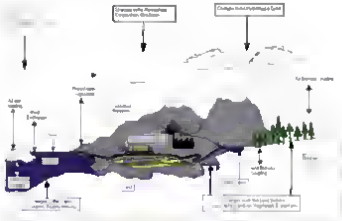

Figure 1-1 Schematic view of the components of the global climate system.

Impacts of Climate Change

Climate change as used by the IPCC refers to any change in climate over time, whether due to natural variability or as a result of human activity. The very nature of climate change makes it a global problem with long-term impacts that involve complex interactions between climatic, environmental, economic, political, institutional, social, and technological processes (IPCC, 2001c).

The impacts of climate change on the ecosystem are diverse and vary on a regional scale. Recent regional climate changes, particularly increases in temperature, have already affected many regional and biological systems (IPCC, 2001b). Some of the areas of vulnerability impacted by global climate change include the following:

- Hydrology and water resources,
- Agriculture and food security,
- Terrestrial and freshwater ecosystems,
- Coastal zone and marine ecosystems,
- Human health,
- Human settlements, energy, and industry, and

- Insurance and other financial services.

Impacts of Climate Change on Water Resources

Global warming due to greenhouse gases and anthropogenic climate change is likely to have significant impacts on the hydrological cycle (IPCC, 1995a). Water resources of the world, which are already stressed in some areas, are highly vulnerable to climate change (IPCC, 2001b). The major impacts of climate change on water resources and the hydrological cycle include the following

- Increased competition for water supply between various consumptive and non-consumptive uses,
- Variability in precipitation and evaporation,
- Variability in aquifer recharge,
- Increase in sea level rise and
- Loss of freshwater resources and increase in saltwater intrusion in coastal aquifers

Precipitation variability. Climate models in current use are still unable to make precise regional predictions. This inability of the models and the inherent complexity of the hydrological cycle have made better prediction a difficult task. However, it is understood that a change in precipitation may affect surface wetness, reflectivity, and vegetation, which then affect evapotranspiration and cloud formation, which in turn affect precipitation. Meanwhile, the hydrological system is also responding to other human activities such as deforestation, urbanization, and the over-use of water supplies.

Infiltration variability. Infiltration is one of the major processes of the hydrological cycle. These changes in seasonal patterns may affect the regional distribution of both ground and surface water supplies. Through infiltration, aquifers get recharge, and the vadose zone of the subsurface retains moisture necessary for agriculture, especially rain fed agriculture. When the precipitation pattern is affected by climate change, the processes of infiltration and recharge also will be affected. Long

spells of dry seasons result in the lowering of the water table and decrease in yield of production wells used for water supply or agriculture. Several models also suggest that precipitation will become more intense in some parts of the world, and as a result, there will be increases in the magnitudes of surface runoff and floods.

Increase in sea level rise. Global warming has been attributed to the thermal expansion of the ocean water and the melting of glacial deposits in the polar regions. These two factors are the major contributors to global sea level rise, which is expected to affect the livelihood of people living in coastal areas. Inhabitants of small islands might face the worst consequences of all as a result of land submergence due to increased sea level. Increase in sea level also affects the coastal dynamics of low-lying areas. The processes of beach erosion and deposition will be altered as a result of sea level rise.

Increase in seawater intrusion. The increase in sea level and the subsequent submergence of coastal areas is also expected to result in the loss of coastal freshwater resources. The upstream movement of saltwater in estuaries will affect freshwater well fields upriver. Coastal aquifers, which are already under stress in many areas, may be subject to increased levels of salinity due to seawater intrusion.

Sea Level Rise

There is a general consensus about the issue of average global sea level rise. There is a substantial wealth of research findings confirming that the average sea level has been rising globally at an average rate of about to 2 mm annually for at least the last century or so (Peltier and Tushingham, 1989, Trupin and Wahr, 1990, Douglas, 1991), and probably at a much smaller rate for the previous several millennia (Flemming, 1978, Flemming and Webb, 1986, Kearney and Stevenson, 1991, Sherman and Woodworth, 1992, Varekamp et al., 1992). Due to a number of contributing factors, primarily global

warming most researchers plausibly argue that the rate at which the sea level will rise globally in the future will be much greater than the present rate

Sea Level Rise Components

Sea level rise has two components First, what is known as eustatic sea level rise is the result of global warming due to natural and anthropogenic causes. The rise in global temperature induces thermal expansion of the ocean water, melting of mountain glaciers, and possibly the melting of continental ice sheets such as those of Greenland The second component is the relative sea level rise, which is attributed to the vertical movement of the land The dynamic nature of the continents has resulted in continental movement over long periods of time. This continental movement could be either a rise or fall in the land surface that results in a relative rise or fall of sea level with respect to the land surface Considering a localized scale, relative sea level rise could also be brought about by land subsidence as a result of pumping groundwater

Estimation of Sea Level Rise

There is a general consensus among researchers that the thermal expansion that occurs at all ocean temperatures is the major contributing factor for sea level rise in the 20th and 21st centuries (IPCC, 2001a) The IPCC report also states that the change in salinity has had a significant impact on the local density and local sea level but little effect on the global average sea level change

The analysis of observational data at different time scales has been very instrumental in assessing the impact of climate change on sea level rise. On the geological time scale, evidence from coral reefs, oxygen isotopes, and other records has demonstrated sufficiently the existence of a globally coherent connection between sea level and climate. This has enabled researchers to make valid speculations about an

imminent rise in global sea level of a few meters due to the long term global warming of several degrees Celsius (Tooley, 1993).

At the secular time scale,[1] tide-gauge data have been the primary sources for direct observations of relative sea level change (Warrick, 1993). On the basis of late Holocene sea level indicators and other data, Gornitz (1990) concludes that the rate of global sea level rise over the last 100 years was of the order of 1.0 to 2.0 mm/yr. Geological evidence of the past 10,000 to 20,000 years indicates that major temporal and spatial changes occur in relative sea level rise. Observed sea level changes near former sites of glaciation are brought about by glacio-isostatic effect.[2] On the other hand, changes observed at tectonically stable localities far from the former ice sheets approximate the global average sea level change (IPCC 2001a). The IPCC (1996b) estimates that sea level rise will be in the range of 20 to 86 cm from 1990 to 2100 with a best estimate of 49 cm (Warrick et al. 1996). Analysis of data from sites that have been subject to the glacio-isostatic effect indicate that the ocean volume may have increased to add 2.5 to 3.5 m to the global average sea level over the past 6,000 years (IPCC, 2001a). The geological sea level estimates may also include a component from thermal expansion and glacier mass changes. The contribution of ice sheets to sea level rise in the 20th and 21st centuries in response to earlier climate change is estimated to be from 0.0 to 0.5 mm/yr (IPCC 2001a). This has to be added to the effect of the 20th century and future climate change. AOGCM[3] experiments for the IS92a scenario including sulfate aerosols,

---

[1] The secular time scale in most cases refers to a range of decadal to century time lengths.

[2] Glacio-isostatic effect is the Earth's response to the past changes in ice and water loads.

[3] AOGCMs are Atmosphere-Ocean General Circulation Models and IS92a is a set of scenarios based on emission control policies agreed in 1991.

conducted for the hundred-year period from 1990 to 2090 show that the global average sea level rise from thermal expansion is in the range of 0 09 to 0.37 m. The results further indicate that there will be an acceleration through the 21st century Expansion for 2040 to 2090 is greater than for 1990 to 2040 by a factor of 1 4 to 2 1 (IPCC, 2001a)

The most recent assessment for the complete range of AOGCMs and SRES[4] scenarios, including uncertainties in land-ice changes, permafrost changes, and sediment deposition, projects the global average sea level rise to be from 0 09 to 0 88 m over the 1990 to 2100 estimate with a central value of 0 48 m (IPCC, 2001a) The central value gives an average rate of 2 2 to 4 4 times the rate over the 20th century The earlier assessment conducted using time-dependent sulfate aerosols, all of the IS92 scenarios with uncertainties, and a simple model with climate sensitivities of 1 5 to 4 5°C estimated the global average sea level rise to be in the range of 0 13 to 0 94 m (Warrick et al , 1996)

Groundwater Flow in Coastal Aquifers

Coastal aquifers constitute an important source of water in many parts of the world In addition to being the primary sources of water, the proximity of coastal aquifers to the seacoast puts them in a unique position. The geology of coastal aquifers and their unique relationship to the marine environment make the investigation of groundwater flow in coastal aquifers a technically challenging task. The flow of groundwater in coastal aquifers is characterized by variation in density, which becomes more pronounced closer to the coast The existence of this variation in density is brought about by the presence of dissolved solids in the groundwater

[4] SRES are marker scenario experiments reported in the IPCC Special Report on Emission Scenarios

The total dissolved solids (TDS) are used as a measure of concentration and density variation in groundwater. The most important of all the dissolved solids in terms of characterizing groundwater quality is chloride (Cl). In order to characterize the type of groundwater, classifications are based on the concentration of TDS and chloride. Two different classification tables are provided for the purpose of understanding. The first one uses the TDS as a measure of concentration while the second one uses Cl (see Tables 1-1 and 1-2). Table 1-1 is based on Fetter (2001) and Table 1-2 is based on Stuyzfand (1993).

Table 1-1 Classification of water based on total dissolved solids.

Class	TDS (mg/l)
Fresh	0 – 1000
Brackish	1,000 – 10,000
Saline	10,000 – 100,000
Brine	> 100,000

Table 1-2 Classification of fresh and saline groundwater on the basis of chloride concentration

Type of groundwater	Chloride concentration Cl (mg/l)
Oligohaline	0 – 5
Oligohaline-fresh	5 – 30
Fresh	30 – 150
Fresh-brackish	150 – 300
Brackish	300 – 1,000
Brackish-saline	1,000 – 10,000
Saline	10,000 – 20,000
Hyperhaline or brine	≥ 20,000

In addition to their unique geology and proximity to the marine environment, coastal aquifers are also susceptible to environmental stresses, anthropogenic climate change, and human activities. Climate change, for example, alters the hydrologic characteristics of the area and results in changes in precipitation, evaporation, and evapotranspiration. Sea level rise and changes in the tide gage records also would be

expected, which could result in shoreline retreat and flooding. Excessive pumping of freshwater aggravates the problem by exacerbating land submergence and destabilizing the balance of the saltwater-freshwater interface.

There are a number of factors that need to be considered on different scales while trying to understand the flow of groundwater in coastal aquifers. A thorough analysis requires investigating the hydrogeology of the aquifer using available geophysical methods, analyzing the constituents of the flow in terms of the dissolved solids, identifying the various boundary conditions, and applying a suitable variable density flow model. Figure 1-2 (modified from Oude Essink, 2000) details the factors that need to be considered in the investigation of groundwater flow in coastal aquifers.

There are numerous complexities involved in modeling density dependent flow in porous media. The complexities range from the inherent properties of the porous medium to the mathematical formulation of the process and the ensuing difficulties in obtaining analytical solutions. In order to be able to model groundwater flow, a number of issues involved in the modeling process have to be considered. The processes involved include:

- Understanding the hydrogeology of an area,
- Formulating a well posed problem, and
- Selecting efficient solution techniques.

Hydrogeology. Proper understanding of the hydrogeology of an area to be modeled is a crucial factor in the modeling process. Knowledge of the inherent hydraulic properties of the porous medium such as porosity, hydraulic conductivity, and transmissivity and geologic factors such as lithology, stratigraphy, and the geochemistry of the layer greatly facilitate the modeling process by providing the necessary information about the subsurface processes that govern the flow.

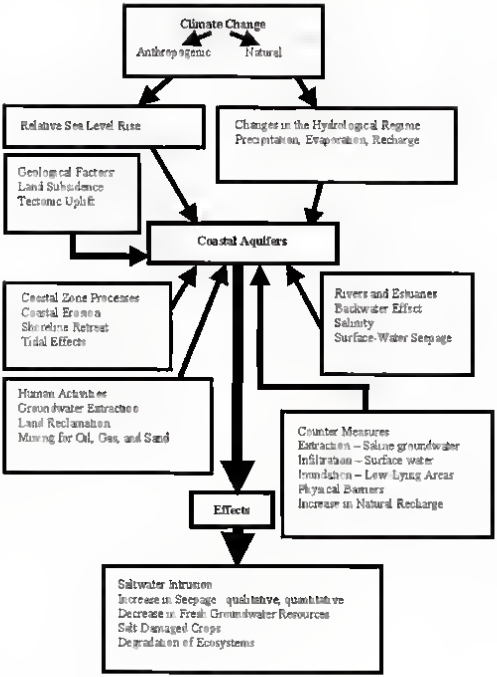

Figure 1-2 Factors affecting coastal aquifers

Problem formulation Formulating a well posed problem greatly enhances the modeling process Stating simplifying assumptions, choosing appropriate temporal and spatial scales, and deciding sufficient dimensions to appropriately represent the flow are some of the issues addressed by a well posed problem The processes involved in the modeling of density dependent flow such as advection, diffusion, and dispersion and the choice of appropriate state and boundary conditions constitute the major parts of a well posed problem

Solution techniques Analytical solutions to groundwater flow problems are very difficult to obtain owing to the heterogeneity of the medium and non-linearity of the differential equations This problem gets even more complicated when the flow is a density dependent flow As a result, for most two-dimensional and three-dimensional problems, numerical solutions are the only practical way to solve the problem The numerical methods employed can utilize finite-element or finite-difference discretization Also, the iterative processes involved in the solution require selection of an efficient numerical algorithm These numerical algorithms perform the iterative temporal and spatial processes on the basis of a specified set of convergence criteria. The spatial and temporal discretization plays a very important role in the accuracy of the result and numerical stability of the solution One has to keep in mind that higher spatial and temporal discretization involves higher computing and storage capabilities, and, as a result, faster and larger memory computers.

Application of Geographic Information Systems in Water Resources

Over the past couple of decades the field of Geographical Information Systems (GIS) has gained an increasing applicability in the field of hydrologic modeling GIS has proven to be an invaluable tool in enhancing the spatial dimensions of hydrologic models.

There are two basic data formats in GIS, Raster and Vector. Raster GIS works on the basis of cells defined by rows and columns. These cells contain the spatial location and refer to the attribute information in the database that contains the layer information. Vector GIS, on the other hand, uses points, lines, and polygons to define the layer information.

Raster GIS has many features that make it more suitable for performing hydrologic analyses. These advantages are as follows:

Speed. Raster GIS analyses take considerably less computer processor time as compared to Vector GIS analyses.

Adaptability. Hydrologic models have benefited from remotely sensed data. The data format in remotely sensed data such as satellite imagery is similar to the data format used in Raster GIS, thus making Raster GIS more easily adaptable in the attempt to couple remote sensing and GIS with hydrological models.

Suitability to represent continuous features. The spatial distribution of hydrologic parameters is not defined by a clear-cut boundary. It is rather continuous in nature and crosses boundaries and features. This unique property is best represented by cell-based data formats that represent the spatial gradual change in data attributes.

Display resolution. The resolution of computer monitors is measured in terms of pixels that are also cell based, thus making Raster suitable for high spatial resolution analysis and display.

Earlier applications of GIS utilized the display capability of the system. In other words, model results were imported into the database and displayed, thus enabling one to see the spatial distribution of the results of the modeling process across the area being

modeled. Later on, derived parameters such as slope and aspect were first computed as part of the GIS analysis, and then the results were used in hydrologic models.. The final analysis was again displayed using the advanced cartographic abilities of GIS

Advances in the geo-processing and analytical capabilities of the GIS software resulted in coupling hydrological models with GIS This was achieved either by coupling the hydrological model as part of a GIS analysis package or by integrating the GIS module within the framework of the larger hydrological model This requires substantial programming and testing in order to ensure a seamless coupling between the superior computational capabilities of mathematical models and the spatial modeling capabilities of GIS

The advantages of this method rely on the fact that the GIS component can be used as a pre- and post-processor of the model As a pre-processor, layers of data that are spatially referenced to the same geographical location are created, thus minimizing the need for an external data set to be called during execution of the model. As a post-processor, the GIS component imports the results of the mathematical model analysis and displays it and also performs spatial analysis in order to generate derived sets of data.

Spatially Distributed Modeling in GIS

Most hydrologic models, although computationally robust, generally experience difficulties in addressing the issue of spatial variability of the processes involved. This problem is not very pronounced in lumped models, in which there is no concern about the spatial variability of model parameters On the other hand, distributed models rely on the accurate representation of the spatial distribution of model parameters and hydrologic response units

In distributed modeling, the catchment is subdivided into smaller units of homogeneous properties and the contribution of each smaller unit, referred to as a Hydrologic Response Unit (HRU), is eventually accounted for to simulate the response of the whole catchment. This approach comes at the price of large amounts of data that need to be collected, stored, processed, and presented. Increased spatial variability magnifies the scale of this problem significantly. This calls for a method that reduces the size while maintaining the spatial discretization and precision required for a more accurate result.

GIS also helps integrate a very diverse array of spatially referenced data through the common denominator, which is their spatial location. For example, data layers of vegetation, rainfall, soil type, evaporation, and surface-water features can be used to estimate recharge. These spatially referenced data layers or coverages constitute the input for distributed hydrologic models.

Object Oriented Modeling in GIS

Recent advances in object-oriented programming have begun to influence the field of GIS as well. The recent paradigm is object orientation in GIS. This is based on the same premises as the other object oriented programming languages. Properties such as data hiding, encapsulation, polymorphism, and inheritance are employed.

In object oriented programming, data and procedures are treated as a single entity referred to as an "object." Data hiding and encapsulation refer to the ability of the process to hide the internal structure of an object from the user. With encapsulation, it is only possible to manipulate the object's data using a set of predefined functions, thus ensuring data independence. The internal definition of the data structure can then change without influencing what the user perceives.

One of the most important concepts in object-oriented systems is inheritance. In object oriented programming, inheritance refers to the ability to create a new type as an extension of the existing type. More general classes that contain the generic type of object are first defined, and then subclasses are created as specializations of the more generic class. These subclasses inherit all properties of the parent class and add some more of their own. For instance, when creating an object class to represent water network nodes, one might define subclasses to be a pump and reservoir, which would inherit generic water node characteristics such as code and location, along with their relationship with water pipes, and aggregate specific characteristics such as pump throughput and reservoir capacity.

Polymorphism is the other important feature of object orientation. This refers to a program's ability to use objects belonging to different classes in a transparent way, interpreting their characteristics on the run. For instance, if a program needs to have access to an attribute called code, which has been defined for several different object classes or for classes with common ancestry, it is not necessary to know the object's class beforehand.

The advantages of this recent modeling approach are numerous. The concept of data and class makes it possible to minimize the data allocation problem by categorizing data into classes. The property of inheritance ensures that one class denotes a number of subclasses, which inherit similar properties from the main class. Data hiding and encapsulation make it possible to treat data and process as a unit, thus making the process more efficient. Polymorphism makes it possible to create different data features that share the same name, thus minimizing the memory access time of the process. With the

tools of object oriented programming and advanced geo-processing capabilities of GIS software, the integration of GIS and hydrologic modeling enhance the modeling process significantly

Application of Optimization Methods in Water Resources

The management of water resources requires an integrated approach based on a careful investigation of both the hydrologic factors and human water use. Depending on the type of optimization problem to be addressed, the factors to be considered include the type of engineering adopted in the design, the management of the system, economical and legal issues concerning water rights and water use, ecological factors affected by the water use and development, and social factors involving the decision makers and stakeholders. A combination of the factors considered is employed to formulate a policy that enables management of water resources on a sustainable basis.

One important tool used in formulation of decision support systems, policy frameworks and management plans of different scales is optimization. There are a number of mathematical tools used to optimize the utilization of water resources subject to various constraints. The constraints in most cases require meeting some ecological needs quantitative and qualitative hydrologic factors, and a forecasted demand.

Optimization is a very rigorous process that requires a very careful outlining of the following

- Definition of the problem
- Identification of parameters.
- Formulation of the objective function.
- Formulation of the constraining conditions.

Definition of the problem. Problem definition requires understanding the process that needs to be optimized. At this stage, a thorough understanding of cause and effect is

required through a detailed analysis of the problem For example a general optimization problem in water resources requires identification of the water sources, investigation of the hydrological and consumptive stresses, and various options that could be looked into during the problem formulation Detailed historical records of hydrologic data and consumption records need to be analyzed, and forecasts need to be made Then a decision has to be made if the problem is a maximization or minimization problem

Identification of parameters. The parameters are the basis for the formulation of the objective function The parameters need to be identified as dependent and independent parameters.

Formulation of the objective function Formulation of the objective function requires writing a series of linear or non linear mathematical relationships that define the pumping requirements subject to the constraints as explained earlier Choosing the most appropriate formulation scheme impacts the final analysis very significantly Depending on how the objective function and the constraining functions are formulated, the optimization problem could be classified as integer programming (IP), quadratic programming (QP), linear programming (LP), non-linear programming (NLP), mixed integer programming (MIP), dynamic programming (DP), and so on. The solution techniques also differ from graphical methods used to solve systems of linear equations, non-linear equations, and differential equations. Definition of the solution space over which the solution is feasible is important in some cases. This region is generally bounded by the constraining equations of the objective function

Formulation of the constraining conditions The constraining conditions define the maximum value or the minimum value that could reasonably be achieved without

jeopardizing the system. For example, in a water supply system from a river, the maximum amount of water that could be withdrawn from the river could be constrained by the minimum flow requirement that needs to be maintained at all time.

Definition of convergence criteria. This criterion is a mathematical criterion that defines the conditions for the optimal value of the parameter to be optimized on the basis of some sets of mathematical rules. For example, if head is to be optimized, then the difference between the head value at one time step is compared with the head at the next time step and the difference compared with the convergence criterion. This is applicable in a more complicated optimization scenario.

Optimization modeling is a general class of problems, which require minimization or maximization subject to a set of constraints. A number of optimization models have been developed to address the issue of groundwater management. Most models are developed to formulate optimal pumping strategies by employing cost minimization or pumping maximization subject to water quality and quantity constraints.

Optimization algorithms developed for management of groundwater systems have to be coupled with a simulation model. The coupling of single-objective, linear groundwater optimization models is broadly classified on the basis of the approaches used. The two approaches are embedded and response matrix approaches (Gorelick, 1983).

Embedding methods involve development of a linear set of equations known as response equations from the partial differential equations of groundwater flow and transport. The solution of the resulting equations is obtained by using numerical methods

such as finite difference or finite elements Applications of this approach have been successfully tested by Aguado and Remson (1974) and Willis and Liu (1984)

The response matrix approach is developed from hydraulic or water-quality models of the aquifer system. The simulation model is used to generate the response of the aquifer system to pumping or recharge The resulting matrix of coefficients is used to convert pumping stresses into linearized changes in drawdowns and/or changes in concentration of the ambient water The set of unit responses is formulated for individual wells and superimposed to model multiple wells, which form a set of linear equations that is solved systematically However, if the problem is formulated as a non linear problem, then the solution is obtained iteratively The response matrix approach has been used to solve multi-objective optimization problems, (e.g , Louie et al , 1984 and Yeh et al , 1992).

Research Objectives and Methodology

There is a considerable amount of knowledge that describes the process of saltwater intrusion In the past couple of decades, different mathematical approaches have been developed to model the process of seawater intrusion. There are also well-documented research results and a number of GCMs that make climatic variability forecasts, usually on the time scale of a century

The majority of research on saltwater intrusion is primarily focused on assessing the effect of freshwater withdrawals from coastal aquifers. Although it has been established that climate change impacts influence the process of seawater intrusion, there is a gap in the dynamic linking of climate change impacts to seawater intrusion and quantification of the flow and transport processes There is also a gap in the development

of an integrated approach to manage coastal water resources by incorporating the impacts of climate change and freshwater withdrawal

The objectives of the research described in this dissertation were

- To obtain a better understanding of the impacts that climate change and sea level rise will have on seawater intrusion in coastal aquifers
- To bridge the gap of knowledge in the integrated assessment of coastal aquifers, particularly management on a time scale of a century
- To investigate the sensitivity of coastal aquifer parameters and hydrologic stresses to the process of saltwater intrusion coupled with the impacts of sea level rise

The research objectives described above address a wide array of subtopics As a result, each objective required the application of a combination of hydrologic, hydrogeologic, and spatially distributed numerical modeling methods

Investigation of the impacts of sea level rise involved transient modeling over a given area and as a result, a GIS approach was chosen to perform the task Investigation of the impacts of sea level rise and climate change on the groundwater flow regime in coastal aquifers required development of a groundwater flow model that incorporates the transient nature of sea level rise as a boundary condition Similarly, investigation of the management of freshwater withdrawals required application of optimization methods to develop optimal pumping strategies. Also bridging the gap of knowledge in the integrated management of coastal aquifers required development of a procedure that combines sea level rise modeling, groundwater flow simulation, and optimization

In order to proceed with the research, three major methodologies were identified, viz., GIS for sea level rise modeling, numerical modeling for groundwater flow simulation, and optimization for management of freshwater withdrawals After

identifying the methodologies, detailed procedures for each methodology were outlined. The general classes of methodologies used in this research are:

- Development of a GIS based sea level rise modeling method
- Development of a variable density groundwater flow modeling computer code that incorporates the effects of sea level rise by modifying an existing three-dimensional, variable density, groundwater flow simulation code.
- Development of an optimization model based on evolutionary algorithms
- Development of an approach for integrated coastal water resources management by combining sea level rise modeling, groundwater flow simulation, and optimization in one shell program.

As part of this research, a number of computer codes were developed for each methodology. A shell program that incorporates all the three components also was developed. The programming languages used in the development of the computer codes include Avenue, FORTRAN, and Visual Basic.

Sea level rise modeling was performed for coastal areas of south Florida. Groundwater flow simulation was performed for a coastal aquifer in south Florida and a coastal aquifer in Turkey. Optimization modeling was performed for a test case of a coastal aquifer under salinization.

Dissertation Organization

The first chapter of this dissertation describes the general background required for the simulation and optimization of water resources management problems and the application of GIS in water resources. The attempt is to give the reader a basic understanding of the topics rather than a detailed description of methods and concepts.

The process of seawater intrusion in coastal aquifers is described in the second chapter with special emphasis on numerical modeling. The general mathematical formulation of a variable density groundwater flow problem and the numerical solution

of the problem are discussed. The effects that climate change and sea level rise have on the groundwater flow regime are also briefly discussed. Also, the numerical three-dimensional groundwater flow model SEAWAT is described.

Chapter three describes optimization methods based on evolutionary computation. Specifically, Genetic Algorithms (GAs) are discussed, and their application and suitability in search and optimization are investigated.

In chapter four, a GIS model is developed to investigate the impacts that sea level rise has on coastal areas. The model framework is described in detail, and the computer code development process is explained. In addition, the IPCC scenarios are analyzed with special emphasis on global sea level rise and on methods to estimate relative sea level rise of an area from global sea level rise estimates.

Chapter five describes the method adopted to incorporate the impacts of sea level rise in the modeling of groundwater flow in coastal aquifers. The boundary conditions commonly used in groundwater flow modeling are discussed, and modifications to a three-dimensional variable density groundwater flow model are presented.

An optimization model based on genetic algorithms is developed and described in chapter six. Model components, solution techniques, and state and decision variables are discussed in detail. The coding aspects of the new groundwater flow optimization model GENOPT, which is based on genetic algorithms, also are explained.

Results of the simulation and optimization modeling are presented in chapter seven. The shift of the saltwater-freshwater interface, simulated heads and concentration values, and optimized model parameters are used to explain the results.

Chapter eight is the final chapter, where the conclusions drawn from the research are summarized and presented. Suggestions and recommendations for future research opportunities also are presented.

Appendix A presents the concept of integrated modeling as applied to the management of coastal aquifers subject to the impacts of climate change. The shell program that incorporates the three modules, viz., GIS, simulation, and optimization is presented. A discussion of software and data requirements and a series of transient plots also are included.

CHAPTER 2
SEAWATER INTRUSION IN COASTAL AQUIFERS

Concepts and Methods

Seawater intrusion, also known as saltwater intrusion is described as the mass transport of saline waters into zones of an aquifer that were previously occupied by freshwater (Stewart, 1999) Degradation of groundwater quality due to seawater intrusion is characterized by increased levels of salinity that exceed acceptable values for potable and/or agricultural purposes Seawater intrusion primarily affects coastal aquifers which serve as major sources of freshwater supply in many parts of the world. Estimates show that coastal plains are inhabited by about 70% of the world's population. The steadily increasing demand for potable water and the threat posed by saltwater intrusion have become serious issues of concern As a result, management of freshwater resources in coastal aquifers has emerged as a challenging problem to planners, policy makers, and water resources professionals.

The rate of mass transport of seawater and its pathway in the subsurface is determined by the hydraulic gradient and distribution of hydraulic conductivity (Stewart, 1999) The flow of saline water into the freshwater aquifer and the discharge of freshwater into the coastal boundary is a long-term process that takes a considerably long time to reach a new state of equilibrium (Van Dam, 1999) The dynamics of flow in the aquifer are governed by the existence of pressure gradients, which in turn are determined by aquifer boundary conditions and sources and sinks Under natural circumstances the boundary conditions are determined by components of the hydrologic cycle and relative

sea level rise. However anthropogenic factors such as increased pumping alter the process, and lead to seawater intrusion.

Salinity of water is usually measured in terms of either the Total Dissolved Solids (TDS) or the concentration of chloride ions (Cl^-). Total dissolved solids (TDS) describes the inorganic salts and small amounts of organic matter present in solution in water. The principal constituents are usually calcium, magnesium, sodium and potassium cations and carbonate, hydrogencarbonate (HCO_3), chloride, sulfate, and nitrate anions (WHO, 1996). Chlorides are distributed widely in nature as salts of sodium ($NaCl$), potassium (KCl), and calcium ($CaCl_2$). Tables 2-1 and 2-2 present a classification based on both methods. The data presented in Table 2-1 was obtained from Chemical Rubber Company (CRC, 1982).

Table 2-1. Properties of various concentrations of seawater

Solute mass fraction (percent)	Salinity (parts per thousand)	Chlorinity (parts per thousand)	Density (kg l^{-1} at 20 °C)	Absolute viscosity (centipoises, cP at 20 °C)	Kinematic viscosity (centistokes, cS at 20 °C)
0.00	0.00	0.00	0.9982	1.002	1.004
0.50	4.94	2.72	1.0019	1.010	1.008
1.00	9.92	5.48	1.0057	1.018	1.012
2.00	19.89	11.00	1.0132	1.036	1.022
3.00	29.86	16.53	1.0207	1.057	1.036
3.50	34.84	19.29	1.0245	1.070	1.044
4.00	39.82	22.05	1.0283	1.080	1.050
5.00	49.79	27.57	1.0358	1.103	1.065
10.00	99.63	55.18	1.0738	-	-

The Problem of Seawater Intrusion

The problem of seawater intrusion is characterized by the presence of two fluids of different solute concentration, freshwater and saltwater. There are two different approaches to the solution of the problem of seawater intrusion. The first approach

known as the sharp interface model involves assuming the two fluids are immiscible and that there exists a sharp interface that separates them. The second approach, known as the variable density model, considers the two fluids as miscible and incorporates a transition zone that separates the freshwater zone with the saltwater zone. This approach calls for a method that accounts for variability of density in the flow zone.

In a situation where the interface is approximated to be sharp, and with a simplifying assumption of a predominantly horizontal flow, the problem of finding the interface may sometimes be solved in closed form[1]. However, neglecting the existence of hydrodynamic dispersion and a mixing zone is generally inadequate in terms of accurately representing the flow regime. As a result, most of the recent two and three-dimensional models of seawater intrusion account for the transition zone and vertical flow.

The mathematical formulation of the coupled transport and flow terms that represent the governing partial differential equations in three dimensions is generally solved using numerical methods. The major difficulty involved in finding analytical solutions is the non-linearity of the parameters. There are some quasi-analytical and analytical solutions for one and two-dimensional problems.

The numerical methods used in solving seawater intrusion problems generally use either finite-difference or finite-element methods and solve for hydraulic head and solute concentration. The hydraulic head is customarily known as environmental head as it can

[1] An equation is said to be a closed-form solution if it solves a given problem in terms of functions and mathematical operations from a given generally accepted set. For example, an infinite sum would generally not be considered closed-form. However, the choice of what to call closed-form and what not is rather arbitrary since a new "closed form" function could simply be defined in terms of the infinite sum.

be head either in the fresh or saltwater zone of the aquifer and can readily be measured by using a piezometer. Many solution techniques solve for the hydraulic head in terms of the equivalent freshwater head, which can then be converted to environmental head by using the concentration and density terms as required. The equivalent freshwater head is a measure of the environmental head in the saltwater zone representing the level to which the water level would rise if the piezometer were filled with freshwater.

The primary concern in studying the problem of seawater intrusion is the permanent loss of a freshwater aquifer due to excessive levels of salt in the aquifer. Once an aquifer is subject to intrusion, reversing the process and reclaiming the aquifer is a very difficult and expensive undertaking. There have been some attempts to mitigate the impacts of aquifer loss to seawater intrusion in the western coast of the United States. Two such examples are the projects in Orange and Los Angeles counties in California, where there are efforts underway to contain the advance of seawater intrusion by creating subsurface hydraulic barriers.

Mathematical Modeling of Seawater Intrusion

The pioneering work in the investigation of saltwater intrusion was done by Baden Ghyben (1888) and Hertzberg (1901). The Ghyben-Hertzberg formula, as it has become to be known, established a relationship between elevation of water table in an unconfined aquifer to the elevation of the boundary known as saltwater-freshwater interface. Looking at Figure 2-1, the relationship between position of the interface and the water table head is written as

$$z = \frac{\rho_f}{\rho_s - \rho_f} h \qquad (2\text{-}1)$$

where ρ_f and ρ_s are densities of fresh and salt water respectively, z is the depth of the interface below the measuring point, normally mean sea level, and h is the elevation of the water table. Assuming a density of 1,025 kg/m^3 for the saltwater and 1,000 kg/m^3 for the freshwater, the depth of the interface is approximately 40 times the value of h. This serves as a preliminary estimate for the position of the interface in many cases

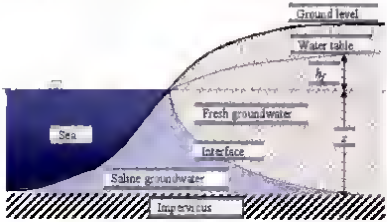

Figure 2-1 Definition sketch for the saltwater freshwater environment.

Sharp Interface Approach

The simplified assumption of a sharp interface is by no means the most accurate representation. When the thickness of the freshwater saltwater transition zone is small compared to the thickness of the aquifer, then it is possible to assume that the freshwater and saltwater domains are separated by a sharp interface (Essaid, 1999). The two domains of saltwater and freshwater are coupled by the interfacial boundary condition of continuity of flux and pressure (Essaid, 1999). In situations where the thickness of the interface is significant, the sharp interface ceases to exist, leading to a mixing zone where hydrodynamic dispersion takes place. Although a sharp interface approach reproduces the regional flow dynamics and the response of the sharp interface to stresses, it does not

provide information on the nature of the transition zone. In three-dimensions, the interfacial boundary condition is highly non-linear (Bear, 1979), as a result, both the flow and the aquifer have to be assumed to be horizontal in order to find a solution (Essaid, 1999). In order to obtain the three-dimensional solution, the horizontal flow is integrated vertically.

Hubbert (1940) developed equations that related densities of freshwater and saltwater with the elevation of a sharp interface in terms freshwater heads using the concept of a potential function. The freshwater-saltwater relationship was developed by equating pressure at a point on the interface. Equating the pressure at the interface for both the freshwater and saltwater environments, the freshwater head is computed as

$$h_f = \frac{P}{\rho_f g} + Z \tag{2-2}$$

and the saltwater head is computed as:

$$h_s = \frac{P}{\rho_s g} + Z \tag{2-3}$$

where h_f and h_s are freshwater and saltwater heads, ρ_f and ρ_s are densities of fresh and salt water respectively, and z is the elevation of the interface above a datum. The schematic description of the approach formulated by Hubbert (1940) and modified by Reilly and Goodman (1985) is presented in Figure 2-2.

Two cases are considered in Figure 2-2 to represent the motion of freshwater and saltwater. Both the freshwater and saltwater are assumed to be two immiscible fluids of different densities. Case 1 represents the situation when one fluid flows while the other is static while Case 2 depicts the condition when both fluids are in motion. Notation of the subscripts adopted in the sketch is such that for any parameter a_{ij}, the i represents the

fluid type while j represents the parameter number. Thus, Φ_{1j} is the potential of freshwater while Φ_{2j} is saltwater potential. Similarly, q_1 is freshwater flow vector, while q_2 is saltwater flow vector. The angle of inclination of the interface is represented by α and z represents the elevation. For the system to be in equilibrium, the saltwater has to be stationary (Case 1), and under equilibrium conditions, the elevation of a point on the interface above a datum could be determined by the formula

$$z = \frac{\rho_f}{\rho_f - \rho_s} h_f - \frac{\rho_s}{\rho_f - \rho_s} h_s \tag{2-4}$$

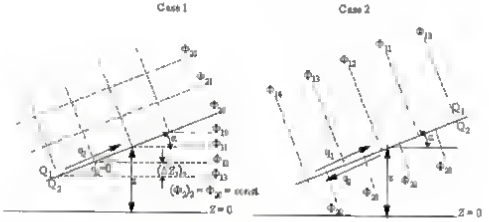

Figure 2-2 Description of the potential surface approach

The sharp interface approach is further classified into two groups as illustrated in Figure 2-2. The first case assumes the saltwater to be static while the freshwater is in motion. This essentially reduces the problem to a one fluid flow with a free surface boundary condition. The saltwater is assumed to move in response to the flow of freshwater. Glover (1959) developed a sharp interface model to study the pattern of freshwater flow in a coastal aquifer. Bennett and Giusti (1971) investigated coastal

groundwater flow in Ponce, Puerto Rico using the same approach. The saltwater beneath an oceanic island was studied by Fetter (1972) assuming sharp interface. Similar studies include Voss (1984a), Guswa and LeBlanc (1985), and Reilly et al. (1987b).

The second group of sharp interface problems assumes that both freshwater and saltwater are in motion as described in Case 2 of Figure 2-2. The two fluid approach requires the flow system to be treated as a two separate systems with a common free-surface boundary (Reilly, 1993). The solution of these types of problems requires solution of two different partial differential equations that govern the flow. The position of the interface is determined by equation 2-4 (Hubbert, 1940). The governing sets of mass balance equations are written in terms of the freshwater (equation 2-5) and saltwater (equation 2-6) are

$$S_f \frac{\partial h_f}{\partial t} = -\nabla \cdot q_f \pm Q_f \tag{2-5}$$

$$S_s \frac{\partial h_s}{\partial t} = -\nabla \cdot q_s \pm Q_s \tag{2-6}$$

where the operator $\nabla = \left(\frac{\partial}{\partial x}\right)_i + \left(\frac{\partial}{\partial y}\right)_j + \left(\frac{\partial}{\partial z}\right)_k$ with unit vectors i, j, k in the x, y, and z directions, h is head (L), q (LT^{-1}) is specific discharge, S is specific storage (L^{-1}), Q is a sink/source term (T^{-1}). The specific discharge for both freshwater and saltwater is expressed in terms of Darcy's equation of flow for constant density fluids as

$$q_f = -K \nabla h_f \tag{2-7}$$

and

$$q_s = -K \nabla h_s \tag{2-8}$$

The second case of the sharp interface approach was used to model saltwater intrusion in the southern part of Long Island, New York (Pinder and Page, 1977). A finite-difference solution of the sharp interface with two flow fields was also developed to model areal flow of freshwater and saltwater separated by an interface (Mercer, Larson, and Faust, 1980). Similarly, a sharp interface quasi-three-dimensional numerical model SHARP was developed and solved using finite-difference simulation (Essaid, 1990a and 1990b).

Variable Density Approach

The variable density conceptualization of the saltwater-freshwater problem is based on the mixing of the two fluids, thus influencing the density and viscosity of the fluid. Due to the variability in density of the fluid as a result of different levels of concentration in different zones, the flow is essentially a variable density flow problem. Solution of a variable density flow problem normally requires solving the non-linear mass balance equations for fluid and salt. The governing equations are solved for fluid pressure or hydraulic head and concentration. In order to find the solution, the fluid is assumed to be incompressible. Isothermal conditions also are assumed for the majority of flow problems in varying hydrogeologic settings.

The variable density system conceptualization used in the development of the numerical model SUTRA (Voss, 1984b) is presented to describe a variable density flow formulation. The primary step in the formulation of a variable density model is conservation of mass. The fluid mass balance is expressed as the sum of pure water mass and solid matrix mass as

$$\frac{\partial(n\rho)}{\partial t} = -\nabla\cdot(n\rho v) + Q \qquad (2\text{-}9)$$

where n is porosity (dimensionless) ρ is fluid density (ML^{-3}), Q is fluid mass source ($ML^{-3}T^{-1}$), v is average fluid velocity (LT^{-1}) obtained by dividing the specific discharge q by the porosity n, and t is time (T). The average fluid velocity depends on fluid pressure and density. Using Darcy's law and variable density, it is expressed as:

$$v = -\left(\frac{k}{n\mu}\right)(\nabla P - \rho g) \tag{2-10}$$

where k is the aquifer permeability (L^2), μ is the fluid viscosity ($ML^{-1}T^{-1}$) and g is the gravity vector with magnitude $|g|$ which is defined to relation to the vertical elevation as,

$$g = -|g|\,\nabla(elevation) \tag{2-11}$$

In order to make use of the fluid potential, the hydraulic conductivity K is defined for a constant density fluid as:

$$K = \left(\frac{k\rho|g|}{\mu}\right) \tag{2-12}$$

Substituting the constant density Darcy equations 2-6 and 2-7 into equation 2-8 yields

$$\frac{\partial(n\rho)}{\partial t} = +\nabla\left[\left(\frac{k\rho}{\mu}\right)(\nabla P - \rho g)\right] + Q \tag{2-13}$$

The left hand side of the mass balance equation can also be expressed in terms of pressure and concentration. But first, the storativity of a saturated aquifer is related to pressure and defined as:

$$\frac{\partial(n\rho)}{\partial P} = S_{ss} \tag{2-14}$$

where the term $S_{ss} = (1-n)\alpha + n\beta$ is the specific pressure storativity (LT^2M^{-1}), α is the aquifer matrix compressibility (LT^2M^{-1}) and β is the fluid compressibility (LT^2M^{-1})

When the left hand side of equation 2-8 is expanded in terms of fluid pressure P and solute concentration C (expressed as mass of solute per mass of total fluid), it becomes:

$$\frac{\partial(n\rho)}{\partial t} = \frac{\partial(n\rho)}{\partial P}\frac{\partial P}{\partial t} + \frac{\partial(n\rho)}{\partial C}\frac{\partial C}{\partial t} \tag{2-15}$$

Substituting equation 2-10 in equation 2-11 yields:

$$\frac{\partial(n\rho)}{\partial t} = S_{sp}\rho\frac{\partial P}{\partial t} + n\frac{\partial \rho}{\partial C}\frac{\partial C}{\partial t} \tag{2-16}$$

Substituting equation 2-12 into the fluid mass balance equation (2-8), the final equation in terms of pressure and concentration becomes:

$$(S_{sp}\rho)\frac{\partial P}{\partial t} + n\frac{\partial \rho}{\partial C}\frac{\partial C}{\partial t} - \nabla\cdot\left[\left(\frac{k\rho}{\mu}\right)(\nabla P - \rho g)\right] = Q \tag{2-17}$$

The solute mass balance for a single species is:

$$\frac{\partial(n\rho C)}{\partial t} = -\nabla(\rho n C) + \nabla\cdot[n\rho(D_m I + D)\nabla C] + QC^* \tag{2-18}$$

where

D_m = apparent molecular dispersivity of solutes in solution in a porous medium including effects of tortuosity ($L^2\,T^{-1}$),

I = identity tensor;

D = dispersion coefficient tensor (L^2T^{-1})

C = fluid solute mass fraction (ML^{-3}) and

C^* = the solute concentration of fluid sources (ML^{-3})

The dispersion term can be conceptualized in many ways. One method requires assuming constant dispersion, and the other considers it to be either dependent or independent of the flow direction. The constant dispersion method assumes dispersion tensor D to be independent of velocity. The flow direction independent approach on the

other hand assumes the dispersion coefficients to be proportional to the velocity in the systems with isotropic permeability In the formulation of the two-dimensional SUTRA code, a dispersion tensor for two-dimensional flow was defined as

$$D = \begin{bmatrix} D_{xx} & D_{xy} \\ D_{yx} & D_{yy} \end{bmatrix} \tag{2-19}$$

where the dispersion tensor is symmetric with diagonal elements

$$D_{xx} = \frac{1}{v^2}\left(d_L v_x^2 + d_T v_y^2\right) \tag{2-20}$$

$$D_{yy} = \frac{1}{v^2}\left(d_T v_x^2 + d_L v_y^2\right) \tag{2-21}$$

and off diagonal elements

$$D_{xy} = D_{yx} = \frac{1}{v^2}\left(d_L - d_T\right)\left(v_x v_y\right) \tag{2-22}$$

where

v = magnitude of velocity (LT^{-1}),

v_x = magnitude of horizontal component of v (LT^{-1}),

v_y = magnitude of vertical component of v (LT^{-1});

d_L = the longitudinal dispersion coefficient (L^2T^{-1}), and

d_T = the transverse dispersion coefficient (L^2T^{-1})

The longitudinal dispersion coefficient is used to represent dispersion in the direction of the flow whereas the transverse dispersion coefficient represents dispersion in the direction perpendicular to flow The dispersion coefficients are functions of the velocity in a groundwater flow system

$$d_L = \alpha_L v \tag{2-23}$$

$$d_T = \alpha_T v \tag{2-24}$$

where

α_L = the longitudinal dispersivity of the solid matrix(L), and

α_T = the transverse dispersivity of the solid matrix (L).

A three-dimensional version of the variable density groundwater flow model SUTRA was released in 2003 (Voss and Provost, 2003). The new code still maintains the basic features of the two-dimensional model (Voss, 1984) and simulates fluid movement and the transport of either energy or dissolved substances in a subsurface environment. The new code employs a two- or three-dimensional finite-element and finite-difference method to approximate the governing equations that describe the two interdependent processes that are simulated. The simulated processes are fluid density-dependent saturated or unsaturated groundwater flow and solute transport or transport of thermal energy in groundwater and solid matrix of the aquifer.

Huyakorn et al., (1987) developed a three-dimensional finite element model to simulate saltwater intrusion. The governing equations of the model consisted of a variable density fluid flow equation and an advective-dispersive transport equation. The freshwater hydraulic head and concentration are treated as dependent variables. The three-dimensional miscible flow model is written as:

$$\frac{\partial}{\partial x_i}\left[K_{ij}\left(\frac{\partial h}{\partial x_j}+\eta C e_j\right)\right] = S_s\frac{\partial h}{\partial t}+\phi\eta\frac{\partial C}{\partial t}-\frac{\rho}{\rho_0}q \qquad (2\text{-}25)$$

where K_{ij} = the hydraulic conductivity tensor (LT^{-1}), h = reference hydraulic head referred to as the freshwater head (L), x_j (j=1,2,3) = Cartesian coordinates (L), η = density coupling coefficient, C = solute concentration ($0 \le C \le 1$)(ML^{-3}), $e_j = j^{th}$ component of the gravitational unit vector ($e_1 = 0$, $e_2 = 1$, $e_3 = 0$), S_s = specified storage

(L^3); t = time (T), ϕ = porosity, q = volumetric flow rate of the sources per unit volume of the porous medium ($L^3T^{-1}L^{-3}$), ρ and ρ_0 = density of the mixed fluid (freshwater and seawater) and reference (freshwater) density respectively (ML^{-3}). It must be noted that the solute concentration is zero at the minimum (reference) density

The reference head and density-coupling coefficient in Equation 2-1 are defined as,

$$h = \frac{p}{\rho_0 g} + z \tag{2-26}$$

and

$$\eta = \frac{\varepsilon}{C_s} \tag{2-27}$$

where p = fluid pressure ($ML^{-1}T^{-2}$), g = gravitational acceleration (MLT^{-2}), z = elevation above datum (L), ε = density difference ratio defined as

$$\varepsilon = \frac{\rho_s - \rho_0}{\rho_0} \tag{2-28}$$

and C_s = solute concentration (ML^{-3}) corresponding to the maximum density ρ_s (ML^{-3})

The actual hydraulic conductivity K_{ij} in (1) which depends on fluid density and viscosity, is generally a function of solute concentration. It is defined as

$$K_{ij} = \frac{k_{ij}\rho g}{\mu} \tag{2-29}$$

where k_{ij} = intrinsic permeability tensor (L^2), μ = dynamic viscosity of the fluid ($\mu = \mu_0$) ($ML^{-1}T^{-1}$), and μ_0 = viscosity of the freshwater ($ML^{-1}T^{-1}$)

The density of the fluid in the mixed region is treated as a linear function of concentration and can be expressed as

$$\rho = \rho_0 \left(1 + \frac{\varepsilon C}{C_s}\right) \tag{2-30}$$

The advective-dispersive equation used to describe the salt transport is expressed in the following form

$$\frac{\partial}{\partial x_i}\left(D_{ij}\frac{\partial C}{\partial x_j}\right) - V_i = \phi\frac{\partial C}{\partial t} + q(C - C^*) \tag{2-31}$$

where $D_{ij} = \phi D_{ij}$, with D_{ij} being the dispersion tensor (L^2T^{-1}) defined by (Bear 1979), V_i = Darcy velocity vector (LT^{-1})

The Darcy velocity vector is expressed as

$$V_i = -K_{ij}^0\left[\frac{\partial h}{\partial x_j} + \eta C e_j\right] \tag{2-32}$$

where K_{ij}^0 = the hydraulic conductivity at the reference (freshwater) condition (LT^{-1})

Henry (1964) developed a semi-analytical model that defines the location and shape of the saltwater-freshwater interface under the condition of a constant seaward flux of freshwater toward an oceanic boundary. This semi-analytical model, in which dispersion is assumed to be constant, still serves as one of the standard benchmark problems for testing newly developed numerical models.

There has been a significant improvement in the modeling of variable density groundwater flow. This development was greatly enhanced by the development of numerical models and the advent of computers. The numerical models currently in use include the U.S. Geological Survey two-dimensional finite element model SUTRA (VOSS 1984b), the three-dimensional finite difference model HST3D (Kipp, 1997), MOCDENSE (Sanford and Konikow, 1985), and SEAWAT (Guo and Langevin, 2002).

In terms of the representation of the saltwater-freshwater interface, the generalized categorization of mathematical models currently in use falls under three major groups (Bear, 1999). These are

1 Three-dimensional sharp interface models,
2 Two-dimensional sharp interface models, and
3 Three-dimensional transition zone models

SEAWAT- Variable Density Groundwater Flow Model

The numerical model that was utilized in this study is a three-dimensional variable density, finite difference model called SEAWAT (Guo and Langevin, 2002). SEAWAT was developed by combining two widely used flow and transport models, *i.e.*, MODFLOW (McDonald and Harbaugh, 1988) and MT3DMS (Zheng and Wang, 1998). Similar to MT3DMS, SEAWAT has the capability to use a variety of solution techniques, and it maintains the modular structure of MODFLOW and MT3DMS. As a result, input files developed for MODFLOW and MT3DMS can be used directly as input files for SEAWAT with only little modification. A version of SEAWAT based on MODFLOW 2000 was released very recently (Langevin, Shoemaker and Guo, 2003). SEAWAT 2000 was designed by combining a modified version of MODFLOW-2000 and MT3DMS into a single computer program. The concept of process used in MODFLOW-2000 was also used in the development of SEAWAT-2000. A process is defined as part of the code that solves a fundamental equation by a specified numerical method. SEAWAT-2000 contains all of the processes distributed with MODFLOW-2000 and also includes the variable-density flow process and the integrated MT3DMS transport process.

The development of SEAWAT required modifying MODFLOW so that it is based on the principles of mass conservation, instead of the original formulation of fluid volume conservation. Furthermore, instead of using environmental heads, SEAWAT uses

equivalent freshwater heads (Lusczynski, 1961) In order to understand the concept of equivalent freshwater head, consider two piezometers as shown in Figure 2-3, one filled with freshwater and the other filled with saltwater The height of the water level in piezometer 1 above the datum is $\frac{P}{\rho_f g}$, where ρ_f is the density of freshwater The freshwater head at the measuring point (bottom of the piezometers) is equivalent to the elevation of the water level in piezometer 1, which is expressed using the energy equation as described in Equation 2-2 Similarly the head in the saltwater piezometer is expressed as Equation 2-3 Where h_f is equivalent freshwater head (L), h is head (L), P is pressure ($ML^{-1}T^{-2}$), ρ_f is freshwater density (ML^{-3}), ρ_s is saltwater density (ML^{-3}), g is acceleration due to gravity (LT^{-2}) and Z is elevation above datum (L)

The basic assumptions involved in the development of SEAWAT are based on Darcy's law for flow through porous media, Fick s law of diffusion for the dispersive transport, the prevalence of isothermal conditions and applicability of the specific storage concept to confined aquifers The porous medium is assumed to be fully saturated with water, and a single, fully miscible liquid phase of very small compressibility is also assumed to fill the porous medium.

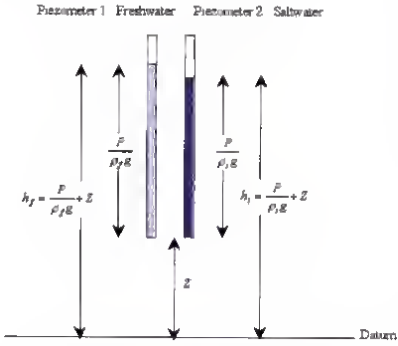

Figure 2-3 Schematic representation of the concept of equivalent freshwater head

The process of diffusion enables particles to be transferred from zones of high concentration to zones of low concentration. Fick's law of diffusion states that the mass flux of particles is proportionate to the concentration gradient.

$$\Phi = -d_0 \nabla C \tag{2-33}$$

where ϕ is the mass flux of particles and d_0 is the molecular diffusion coefficient in water. The classical dispersion theory has been developed by Taylor (1953), Josselin de Jong (1958), Saffman (1959/1960), Scheidegger (1960), Bear and Bachmat (1967), and Fried and Combarnous (1971). The mathematical representation of the dispersive transport process is analogous to that of Fick's law and accounts for the mixing involved. With the dispersion coefficient of the medium defined as D, the mass flux is expressed as.

$$\Phi = -D\nabla C \tag{2-34}$$

The head values calculated by SEAWAT are equivalent freshwater heads as represented in piezometer 1, and therefore the environmental heads which actually represent the level to which the saltwater will rise as shown in piezometer 2 have to be calculated. These values will be used to interpret results and calibrate models. Eliminating the pressure terms and solving for heads, the conversion equations are derived from equations (2-2) and (2-3) to be

$$h_f = \frac{\rho_s}{\rho_f} h_s - \frac{\rho_s - \rho_f}{\rho_f} Z \tag{2-35}$$

$$h_s = \frac{\rho_f}{\rho_s} h_f + \frac{\rho_s - \rho_f}{\rho_s} Z \tag{2-36}$$

Considering a representative elementary volume in a porous medium (Figure 2-4) the mathematical expression for the conservation of mass is written as

$$-\left(\frac{\partial(\rho q_x)}{\partial x} + \frac{\partial(\rho q_y)}{\partial y} + \frac{\partial(\rho q_z)}{\partial z}\right) + \overline{\rho} q_s = \frac{\partial(\rho \theta)}{\partial t} \tag{2-37}$$

where ρ is the fluid density [ML^{-3}], $\vec{q}$ is the specific discharge vector [LT^{-1}], $\overline{\rho}$ is the density of water entering from a source or leaving through a sink [ML^{-3}], q_s is the volumetric flow rate per unit volume of aquifer representing sources and sinks [T^{-1}], θ is porosity [dimensionless], and t is time [T]

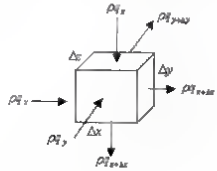

Figure 2-4 Representative Elementary Volume (REV)

The specific storage term is also written as.

$$\frac{\partial(\rho\theta)}{\partial t} = \rho S_p \frac{\partial P}{\partial t} + \theta \frac{\partial \rho}{\partial C}\frac{\partial C}{\partial t} \tag{2-38}$$

where S_p is the specific storage in terms of pressure [$M^{-1}LT^2$]

The flow equation for variable-density ground-water flow in porous media becomes

$$-\nabla \cdot (\rho q) + \overline{\rho q}_s = \rho S_p \frac{\partial P}{\partial t} + \theta \frac{\partial \rho}{\partial C}\frac{\partial C}{\partial t} \tag{2-39}$$

The corresponding mass fluxes are expressed in terms of the fluid density and the specific discharge, or volumetric flow per unit cross-sectional area of bulk porous medium. Darcy's law for a fluid of variable density is thus modified to be

$$q_x = -\frac{k_x}{\mu}\frac{\partial P}{\partial x} \tag{2-40}$$

$$q_y = -\frac{k_y}{\mu}\frac{\partial P}{\partial y} \tag{2-41}$$

$$q_z = -\frac{k_z}{\mu}\left[\frac{\partial P}{\partial z} + \rho g\right] \tag{2-42}$$

and finally, the governing equation for variable-density flow in terms of freshwater head as used in SEAWAT becomes (Guo and Langevin, 2002):

$$\frac{\partial}{\partial\alpha}(\rho K_{f\alpha}[\frac{\partial h_f}{\partial\alpha}+\frac{\rho-\rho_f}{\rho_f}\frac{\partial Z}{\partial\alpha}])+\frac{\partial}{\partial\beta}(\rho K_{f\beta}[\frac{\partial h_f}{\partial\beta}+\frac{\rho-\rho_f}{\rho_f}\frac{\partial Z}{\partial\beta}])$$
$$+\frac{\partial}{\partial\gamma}(\rho K_{f\gamma}[\frac{\partial h_f}{\partial\gamma}+\frac{\rho-\rho_f}{\rho_f}\frac{\partial Z}{\partial\gamma}])=\rho S_f\frac{\partial h_f}{\partial t}+\theta\frac{\partial\rho}{\partial C}\frac{\partial C}{\partial t}-\bar{\rho}q_s \qquad (2\text{-}43)$$

where the subscripts α and β represent the principal directions of permeability parallel to the bedding, γ represents the direction normal to the bedding. The terms k_α, k_β and k_γ are the permeabilities in these directions [L^2], and δ_α, δ_β, and δ_γ are the angles between the respective coordinate axes and the upward vertical direction, as described in the documentation of SEAWAT.

Variable density groundwater flow causes the redistribution of solute concentration, which in turn alters the density field. This redistribution significantly affects the groundwater movement. Therefore, it is important to describe the solute transport process, couple it with the flow equation, and solve the resulting equation.

The transport of solute mass in groundwater flow is brought about by advection, diffusion and dispersion. The three dimensional equation that describes this process is described as (Zheng and Bennett, 1995)

$$\frac{\partial C}{\partial t}=\nabla\cdot(D\nabla C)-\nabla\cdot(\bar{v}C)-\frac{q_s}{\theta}C_s+\sum_{k=1}^{N}R_k \qquad (2\text{-}44)$$

where D is the hydrodynamic dispersion coefficient [L^2T^{-1}], $\bar{v}$ is the fluid velocity [LT^{-1}], C_s is the solute concentration of water entering from sources or sinks [ML^{-3}], and R_k (k=1, ,N) is the rate of solute production or decay in reaction k of N different reactions [$ML^{-3}T^{-1}$].

SEAWAT solves concentration in terms of total dissolved solids (TDS). The formulation of a density term from the concentration is based on an empirical relationship (Baxter and Wallace, 1916)

$$\rho = \rho_f + EC \tag{2-45}$$

where the term E represents a dimensionless constant with an approximate value of 0.7 for salt concentrations ranging from zero to that of seawater (roughly 35,000 ppm).

The term C represents the salt concentration [ML^{-3}]. When the empirical equation of Baxter and Wallace (1916) is differentiated with respect to C, the resulting relationship becomes

$$\frac{\partial \rho}{\partial C} = E \tag{2-46}$$

When the term that relates density and concentration is substituted into the variable density flow equation of SEAWAT, the governing flow equation becomes:

$$\begin{aligned} &\frac{\partial}{\partial \alpha}(\rho K_{\beta\alpha}[\frac{\partial h_f}{\partial \alpha} + \frac{\rho - \rho_f}{\rho_f}\frac{\partial Z}{\partial \alpha}]) + \frac{\partial}{\partial \beta}(\rho K_{\beta\beta}[\frac{\partial h_f}{\partial \beta} + \frac{\rho - \rho_f}{\rho_f}\frac{\partial Z}{\partial \beta}]) \\ &+ \frac{\partial}{\partial \gamma}(\rho K_{\beta\gamma}[\frac{\partial h_f}{\partial \gamma} + \frac{\rho - \rho_f}{\rho_f}\frac{\partial Z}{\partial \gamma}]) = \rho S_f \frac{\partial h_f}{\partial t} + \theta E \frac{\partial C}{\partial t} - \overline{\rho} q_s, \end{aligned} \tag{2-47}$$

The linear formulation of Baxter and Wallace (1916) is considered applicable for normal seawater concentration ranges. However, if the concentration is much higher or the composition of seawater is different, then another more appropriate formulation would have to be developed. The governing partial differential equation is numerically solved using the appropriate boundary and initial conditions.

CHAPTER 3
SEARCH AND OPTIMIZATION IN WATER RESOURCES MANAGEMENT

Optimization Concepts and Methods

Optimization modeling is part of a general class of problems that require minimization or maximization of an objective function subject to a set of constraints. There are several types of optimization modeling based on the objective function and the constraints to be imposed (Walker et al., 1998). The mathematical techniques of search and optimization provide a formal means to make decisions on problems that require considering various options or best alternatives (Spall, 2003). In general, search and optimization methods are used to obtain local or global optimal values or a set of feasible solutions for a given problem. Global optimization is a search process where the objective is finding the best possible set of parameters to optimize an objective function. Global optimization problems generally fall within the broader class of nonlinear programming. There are two groups of optimization problems, combinatorial (or discrete) and continuous variable problems (Collette and Siarry, 2003). Search methods currently in use can broadly be classified as calculus-based, enumerative, and random (Goldberg, 1989).

Calculus based search methods search for the optimal value of an objective function in two ways, either directly or indirectly (Goldberg, 1989). The indirect way requires finding local extrema by solving a set of equations that is usually non-linear by setting the gradient of the objective function to zero. The search in this case is restricted to points where the slope is zero in all directions. The direct approach, on the other hand,

searches for local optima by picking points on the function and moving in a direction related to the local gradient. In other words, this is a hill climbing technique where the local best is obtained by climbing the function in the steepest permissible direction. Because of their local scope in the gradient analysis, calculus-based techniques yield local optima. Moreover, obtaining gradients and derivatives is not always possible. For these reasons, the general class of calculus-based methods lacks robustness.

Enumerative methods work within a finite search space or a discretized infinite search space to search for the optimal value (Goldberg, 1989). The algorithm considers the objective function values at every point in space one at a time. One such example is dynamic programming. Due to the requirement of function value evaluation at every point in space, (whether it is finite search space or discretized infinite space) enumerative techniques are not very efficient.

Random techniques try to obtain the global optima by randomly searching and saving a set of optimal values and continuing the somewhat stochastic process using an algorithm until the stopping criterion is met (Goldberg, 1989). The search does not require differentiating the objective function to obtain gradients, thus increasing the suitability and applicability of Random techniques. Overall Random search techniques are computationally intensive and fall short with regard to efficiency due to the inherent nature of the search method. With current high speed and large memory computers the efficiency problem could be minimized.

Through the years numerous techniques of optimization have been developed to solve a general class of optimization problems. Some of the major techniques of optimization are described very briefly in the following paragraphs.

Discrete Optimization

Discrete optimization is used to describe a category of optimization methods where the best alternative is selected from a finite set of feasible solutions as defined in the objective function. The variables used in the objective function of discrete optimization are restricted to assume only integer values. The most common techniques used in solving discrete optimization problems included integer programming, heuristic search techniques such as genetic algorithms, simulated annealing and artificial neural networks, and global search techniques

Continuous Optimization

Continuous optimization refers to a general class of optimization problems in which all the variables are allowed to take values from subintervals of the real line. Thus, continuous optimization allows decision variables defined in the objective function to have real or continuous values.

The major optimization methods used in both discrete and continuous optimization are briefly described in the following paragraphs

Linear Programming Linear programming is based on linear objective function and constraints with continuous decision variables. The objective of an LP problem is to find the minimum or maximum of a linear objective function subject to linear constraints

Integer Programming Integer programming is a technique that utilizes linear objective function and constraints with integer decision variables

Mixed Integer Programming The optimization technique of mixed integer programming was developed to solve linear objective functions with linear constraints and integer and continuous decision variables. MIP is an extension of integer

programming where the problem has one or more integer, real or binary decision variables

Dynamic Programming Dynamic programming is a technique used to optimize multistage processes The applicability of dynamic programming in water resources optimization problems was promoted by the capability of dynamic programming to translate nonlinear and stochastic problems into a dynamic programming formulation This was achieved by decomposing complex problems with large number of variables into a series of sub problems which are solved iteratively

The primary advantage of dynamic programming technique lies in its capability to handle discrete variables and nonconvex, nonconitinuous, and nondifferentiable functions It can also take into account stochastic variability by a simple modification of the deterministic procedure In order to obtain a solution, dynamic programming requires the objective function to satisfy conditions of separability and monotonicity An objective function is said to be separable if decomposed components of the objective function are independent of each other Similarly, an objective function is said to be monotonic if improvements in the decomposed individual components of the objective function lead to improvements in the objective function The major drawback of dynamic programming is dimensionality due to the large number of possible solution designs The size is generally an exponential function of locations and periods However, differential dynamic programming overcomes the problem of dimensionality by eliminating the need for discretization of the control and state vector, and by introducing stepwise decomposition Differential dynamic programming is characterized by a linear growth in

computing effort with respect to the number of stages or planning periods and it also exhibits quadratic convergence

Nonlinear Programming When both the objective function and the decision variables are nonlinear, the problem can be solved using the techniques of nonlinear programming. Many groundwater planning and management models involve nonlinear objective functions and constraints. The nonlinearities could be due to nonlinear cost functions, nonlinear equations governing the flow, particularly for unconfined aquifers, nonlinearities in the governing equations for solute transport in groundwater, other types of nonlinear physical, and managerial objective functions and constraints

Combinatorial optimization deals with problems that have a linear or nonlinear function defined over a finite but large set of problem space. Examples of combinatorial optimization problems include network problems, scheduling, and transportation, facility location and layout, and optimal design of waterways and bridges. If the function is piecewise linear, the combinatorial problem can be solved exactly with a mixed integer program method, which uses branch and bound. Combinatorial optimization problems generally consist of finding the optima for a function with constraints and encoded as integer vectors or binary variables. The methods used to solve combinatorial optimization problems include branch and bound, fixed heuristics, and meta heuristics. In the general class of heuristic methods, evolutionary algorithms such as simulated annealing, tabu search, and genetic algorithms have been successfully used to solve combinatorial optimization problems

Evolutionary Algorithms

Evolutionary algorithms are a new class of heuristic search and optimization methods. These methods have been called global optimization methods or gradient free

methods The term evolutionary algorithms has also been used to describe some of them since they are derived from natural, biological principles Evolutionary methods and artificial intelligence have been gaining increasing attention in the past few years Evolutionary methods try to emulate the evolution of life through natural selection and use similar procedures to obtain the best fitting optimal solution for a given problem. Artificial intelligence methods on the other hand try to train the system through examples, in a fashion similar to the way a child learns about the environment Then, once a sufficient knowledge database has been acquired through training, the system is required to recognize the best solution or simulate outputs for a given set of inputs Genetic algorithms (GAs) are one of the popular evolutionary algorithms used Artificial neural networks (ANNs) on the other hand have become increasingly applicable as artificial intelligence methods to perform simulation and optimization in a number of fields

Simulated annealing

Simulated annealing is a process based on the principles of thermodynamics, the basis of which is a process in which the temperature of a solid is raised to bring its molecules into a highly mobile state and then cooled to form a low-energy crystalline structure Simulated annealing was introduced by Metropolis et al. (1953) and is used to approximate the solution of very large combinatorial optimization problems (Kirkpatrick, 1983) The technique originates from the theory of statistical mechanics and is based upon the analogy between the annealing of solids and solving optimization problems.

The four key ingredients for the implementation of simulated annealing are; the definition of configurations, a generation mechanism, i e., the definition of a

neighborhood on the configuration space, the choice of a cost-function, and a "cooling" schedule.

Tabu search

Tabu search is a combinatorial optimization method, analogous to gradient-descent search with memory, and it is designed to avoid local minima (Glover 1986 1990). The memory preserves a number of previously visited states along with a number of states that might be considered unwanted. This information is stored in a tabu list. The definition of a state, the area around it and the length of the tabu list are critical design parameters. In addition to these tabu parameters, two extra parameters are often used aspiration and diversification. Aspiration is used when all the neighboring states of the current state are also included in the tabu list. In that case, the tabu obstacle is overridden by selecting a new state. Diversification adds randomness to this otherwise deterministic search. If the tabu search is not converging, the search is reset randomly.

Genetic algorithms

Genetic algorithms are search algorithms that are based on the principles of evolution. Therefore, the formulation of a genetic algorithm involves natural selection, inheritance, and mutation. Through these processes, GAs utilize survival of the fittest among string[1] structures with a structured yet randomized information exchange to form a search algorithm (Goldberg, 1989). The development of GAs as search and optimization tools was first pioneered by Holland, at the University of Michigan in 1975 (Goldberg, 1989). The driving force behind the application of GAs was robustness, which is the balance between efficiency and efficacy (Goldberg 1989).

---

[1]Strings are a set of artificial creatures formed from bits and pieces of the fittest of the old generation.

Genetic algorithms differ from the traditional optimization methods in many ways. The following are unique features of GAs (Tang and Mays, 1998, and Goldberg 1989)

- Ability to use the objective itself, not its derivatives,
- Ability to search from a population of decision variable sets, not a single variable set;
- Inherent random property that helps avoid local optima, and
- The use of probabilistic transition rules as compared to deterministic rules

As a result, GAs are very suited to handle convex and non linear problems by ensuring a global or near global optimal solution.

There are five components in the development of a GA solution for optimization problems (Adeli and Hung, 1995) These steps are encoding, initialization of the population, fitness evaluation, evolution performance, and working parameters

Encoding Encoding involves generating a set of decision variables of the problem and encoding it into a string called a chromosome The most common method uses a binary string to represent this vector of decision variables. Sometimes, integer and real coding are also utilized instead of binary coding. If there are m decision variables in an optimization problem and each variable is encoded as a binary string of length n, then the resulting chromosome will be an $n \times m$ string

Population Initialization The initialization is generally performed by random number generation by assigning an equal probability of selection to each bit.

Fitness Evaluation The fitness evaluation helps determine the probability that a chromosome will be selected as a parent chromosome to generate new chromosomes This is achieved through the use of a scaling function δ, which maps objective function values to an appropriate positive fitness value

Evolution Performance Generally there are three operators to perform evolution between two consecutive chromosome populations. These are selection, crossover and mutation.

Working Parameters The development of working parameters requires predefining a set of parameters to guide the GA. The parameters are chromosome length, population size, crossover rate, mutation rate, and stopping criterion.

Application of Optimization in Groundwater Management

There are a number of mathematical tools used to optimize the utilization of water resources subject to various constraints. The constraints in most cases require meeting some ecological needs, quantitative and qualitative hydrologic constraints, forecasted demands and in some cases risks

The formulation of practical water resources optimization problems is characterized by convexity and non-linearity As a result, obtaining second-order, and even in some cases first-order, derivatives of the objective functions that are required by many traditional optimization methods is difficult if not impossible (Tang and Mays, 1998) Moreover, it is difficult to ensure that the solution obtained is the globally optimal solution for a given problem. A number of optimization models have been developed to address the issue of groundwater management Most models are developed to formulate optimal pumping strategies by employing cost minimization or pumping maximization subject to water quality and quantity constraints

Optimization Coupling Methods in Groundwater Systems

Optimization algorithms developed for management of groundwater systems have to be coupled with a simulation model The coupling of single-objective, linear groundwater optimization models is broadly classified on the basis of the approaches

used. The two approaches are embedded and response matrix approaches (Gorelick, 1983)

Embedding methods involve development of a linear set of equations known as response equations from the partial differential equations of groundwater flow and transport. The solution of the resulting equations is obtained by using numerical methods such as finite difference or finite elements. Applications of this approach have been successfully tested by Aguado and Remson (1974) and Wilhs and Liu (1984)

The response matrix of groundwater optimization problems is developed from hydraulic or water-quality models of the aquifer system. The simulation model is used to generate the response of the aquifer system to pumping or recharge. The resulting matrix of coefficients is used to convert pumping stresses into linearized changes in drawdowns and/or changes in concentration of the ambient water. The set of unit responses is formulated for individual wells and superimposed to model multiple wells, which form a set of linear equations. The resulting set of equations is solved systematically. However, if the problem is formulated as a non-linear problem, then the solution is obtained iteratively. Examples of response matrix application in multi-objective optimization include (Louie et al., 1984) and (Yeh et. al., 1992)

Linear programming techniques have been used in groundwater optimization problems where both the objective function and constraints were linear functions. Aguado et. al. (1974) applied linear programming to predict optimum number and locations of wells, and rates of pumping needed to maintain ground water levels below specified elevations under steady state conditions. The objective was to minimize total pumping while maintaining steady state groundwater heads below some assigned value

during dewatering of a large dry dock excavation area. Gorelick and Remson (1982) incorporated the steady state finite difference form of the solute transport equation as an embedded constraint to maximize waste disposal at two locations while protecting water quality at supply wells and maintaining an existing waste disposal facility. The technique has been used extensively in groundwater optimization problems. Linear programming based management models were developed by embedding the governing differential equations as constraints in the formulation (Aguado and Remson, 1974). The objective function was formulated as maximization of the hydraulic heads at specific locations subject to sum of production rate and non decreasing head directional monotonicity constraints.

Mixed integer programming has been used to solve optimization problems with linear objective function and linear constraints in which some of the variables can take only integer values. These types of requirements arise in situations where the decision variables of the management problem require a logical decision prompt such as yes or no, or in situations where the decision variables decide parameters such as the number of installations and locations. In instances where all the variables take only integer values the problem invariably reduces to an integer programming problem. A mixed-integer programming with the response matrix approach was used to determine an optimal dewatering scheme in the foundation design of an electronuclear plant (Galeati and Gambolati, 1988). The response matrix was generated using a three-dimensional finite element model for steady state flow conditions. The best locations for a specified number of pumping wells were determined by using the branch and bound method to solve the MIP objective function (Rosenwald and Green, 1974). A planning model for

the optimal conjunctive use of groundwater and surface water resources was formulated and applied using MIP (Willis, 1976). Other applications of MIP in groundwater management are presented in Rosenwald and Green (1974) and Aguado and Remson (1980). Similar applications include (Aguado and Remson, 1980), (Misirli and Yazicigil, 1997), and (Datta and Dhiman, 1995).

Most groundwater optimization problems, especially unconfined aquifers, exhibit nonlinearity. There are a number of factors that make the groundwater system nonlinear. These factors include nonlinear cost functions, nonlinear flow and transport equations, and nonlinear objective functions and constraints. Nonlinear programming has been used to solve nonlinear optimization problems in water resources management. Gorelick et al. (1984) developed a planning model to determine the optimal design of reclamation schemes for contaminated groundwater systems. The model combined a nonlinear, distributed parameter groundwater flow and solute transport simulation model (SUTRA) with a nonlinear optimization model (MINOS). Colarullo et al. (1984) developed a hydraulic management and plume stabilization model for a partially contaminated aquifer used for both water supply and waste disposal. Their model consisted of a quadratic objective function with groundwater velocity constraints.

The exponential form of fixed charges (installation cost) was incorporated into the objective function and the problem was solved as a concave minimization problem (Karatzas and Pinder, 1993). They applied the outer approximation method to concave global minimization problem over a convex compact set of constraints. The cost analysis of an aquifer restoration system was also performed using quadratic programming (Lefkoff and Gorelick, 1986). The design and cost analysis of aquifer restoration systems

were formulated by assuming advective groundwater flow and incorporating retardation of solutes due to sorption. Other applications of nonlinear optimization include Wang and Ahlfeld (1994), and Halloji and Yazicigil (1996).

The objective function defined in terms of minimizing the present value of pumping costs was solved using quadratic programming combined with an algebraic technological function (Maddock, 1972a). These technological functions or response coefficients were defined as the changes in drawdown induced by unit pumping at each well. Maddock (1972b) also used quadratic programming with a nonlinear objective function and linear constraints to solve the problem of management of an unconfined aquifer. Mixed-integer quadratic programming was used to minimize the pumping costs plus fixed costs for well and pipeline construction.

Dynamic programming provides tools to solve multistage decision problems (Das and Datta, 2001). Solving multistage problems using dynamic programming techniques requires decomposing the multistage problems into single stage problems. Individual single-stage problems may then be solved by any method of optimization. The advantage of using the dynamic programming is its capability to deal with non-convex, non continuous and non-differentiable functions, and discrete variables. A penalty function approach was used in conjunction with a dynamic programming technique to obtain solutions to the constrained optimal control problem with a large number of constraints (Chang et al.,1992). A hyperbolic penalty function was used to incorporate the constraints. A time varying optimization of groundwater remediation with variable management and simulation periods was also solved using differential dynamic

programming (Culver and Shoemaker, 1992) Yakowitz (1982) has given a detailed review of various DP approaches used in water resources management

A differential dynamic programming algorithm was used to solve unsteady nonlinear groundwater management problem where the management problem was formulated as an optimal control problem (Jones et. al , 1987) Culver and Shoemaker (1992) presented a differential dynamic programming algorithm for time varying optimization of groundwater remediation in which management periods were different from the simulation periods.

Combinatorial optimization techniques search for optimal values within a well defined discrete problem space. Evolutionary methods generally fall under the heuristic methods Application of evolutionary methods in groundwater optimization problems have been researched and documented in the past two decades Some examples include Zheng and Wang (1996), Johnson and Rogers (2000), Marryott et. al (1993), Morshed and Kaluarachchi (1998), and Cheng et al (2000)

Formulation of Multi-objective Optimization Problems

Groundwater management problems often require considering more than one, and usually conflicting, management objectives. For example, a management problem where it is required to maximize the amount of water to be pumped from an aquifer and minimize the drawdown represents a problem with conflicting management objectives Due to the nature of the management issues involved groundwater management problems are often formulated as multi-objective optimization problems Multi-objective groundwater management models are often formulated as mathematical programming

problems with many conflicting objectives that require a set of Pareto optimal[2] non-dominated, or non-inferior (efficient) solutions (Das and Datta, 2001)

The mathematical definition of global optimality or Pareto optimality for a vector of decision variables x^* defined in a set of solutions C is given as follows:

A vector $x^* \in C$ is said to be (globally) Pareto optimal, or a (globally) efficient solution, or a non-dominated, or a non inferior point for multi objective optimization problem (MOP) if and only if there is no $x \in C$ such that the functional value of the objective function $f_i(x) \leq f_i(x^*)$ for all $i \in \{1,2, \ldots n\}$ with at least one strict inequality[3] Multi-criteria optimization methods typically assume that a multi-criteria problem is converted into an auxiliary parametric single-objective problem whose solution provides a Pareto-optimal point. The Pareto optimal solutions are represented by a trade-off curve relating two conflicting objectives (Das and Datta, 2001) Multiple objective management models generally attempt to develop such trade-off curves. Multi-objective optimization problems are mostly solved by combining the multiple objectives into one scalar objective whose solution is a Pareto optimal point for the original multi-objective problem.

A multi-objective groundwater quality management model was developed for a regional unconfined aquifer (Willis, 1977) The multi-objective model was formulated to minimize the operational cost of pumping, minimize the minimum hydraulic head within the injection zone of the aquifer, and maximize the injection rate The response equations

[2] A solution is called Pareto-optimal (or efficient) solution, if there is no other solution for which at least one criterion has a better value while values of remaining criteria are the same or better. In other words one can not improve any criterion without deteriorating a value of at least one other criterion.

[3] Pareto optimal points are also known as *efficient, non-dominated* or *non-inferior* points. http://www.fp.mcs.anl.gov/otc/Guide/OptWeb/multiobj/

were used as embedded constraints in the multi-objective optimization model. The optimization model was bounded by constraints of water demand and waste load, storage capacity, maximum pumping, maximum and minimum permissible heads, response equations, and non negativity of the state and decision variables.

A multi-objective linear programming coastal aquifer management model was developed to manage the problem of saltwater intrusion (Shamir et al., 1984). The management model had four objective functions which included, groundwater contour, location of the toe of the seawater freshwater interface, concentration distribution, and minimum energy for pumping and recharge. An approximate linearized expression was used to incorporate the location of the seawater freshwater interface, and a constraint method of multi-objective analysis (Cohon and Marks 1975) was used to obtain trade-off functions between pairs of objectives.

Multi-objective programming methods were used to determine the optimal groundwater management schemes in a hypothetical multi aquifer system (Yazicigil and Rasheeduddin, 1987). The management problem was solved by using a combination of embedding technique and linear programming. A single objective case was applied to a transient aquifer management while the multi-objective model was developed for a steady state aquifer management. Trade-off curves were developed for hydraulic heads and water withdrawal targets using constraints and weighting methods. Similarly, a multi-objective management model was used to determine the optimal management of a multi layer aquifer system (Yazicigil, 1990).

CHAPTER 4
DEVELOPMENT OF A GEOGRAPHIC INFORMATION SYSTEMS MODEL TO INVESTIGATE THE IMPACTS OF SEA LEVEL RISE

Concepts and Methods

Geographic Information Systems (GIS) provide the tools and methods required to perform spatial analysis on georeferenced data. Using GIS facilitates investigation of the impacts of sea level rise. The visual dimension provided by GIS makes it possible to better understand the changes in sea level with respect to space and time for a given area. The primary interest in such analyses is to determine how far seashore would move inland if the sea level were to rise by a certain magnitude. Subsequent investigations could focus on identifying and delineating areas that would be affected as a result of sea level rise, assessing the landuse and landcover that would be impacted, and quantifying the loss of habitat due to submergence. Application of GIS to model components of the ecosystem have been described in Singh and Fiorentino (1996), Tooley and Jelgersma (1992), Battaglin et al. (1993). Goodchild et al. (1995) and Michener et al. (1994).

The analysis of sea level rise primarily relies on elevation data and digital elevation data processing techniques. Digital Elevation Models (DEMs) have been used extensively to analyze terrains and derive design parameters. Elevation data in DEMs is stored in raster format, which is one of the data formats currently in use. Raster GIS deals with data stored and manipulated on a cell by cell basis. The DEM of an area therefore consists of cells where the required data are stored in a recognizable format. The Environmental Systems Research Institute (ESRI) is one of the leading GIS software

developers and solution providers ArcView is one of the desktop GIS analysis softwares developed by ESRI An ArcView extension called Spatial Analyst makes it possible to perform spatial analysis on Raster data

In order to create maps of areas vulnerable to sea level rise using selected scenarios, the simulation requires analyzing input values on a cell by cell basis The cell by cell analysis is a computationally intensive process that ArcView is not well equipped to handle as a stand-alone software As a result, the core computations have to be performed using a separate tool that is computationally robust and that can interface with ArcView

ArcView was originally written in an object oriented language called Avenue, although currently ESRI is shifting to the more widely used language Visual Basic The primary task in the sea level rise modeling process was therefore customizing ArcView by writing source codes to read the required input data then to export the digital elevation data and other relevant information to an external program to perform the computation, obtain the processed data, create raster files of the result, and generate maps

GIS Model Framework

The GIS model developed in this research consists of an ArcView interface written in Avenue and a core computational algorithm written in FORTRAN The model currently can be used to investigate impacts of sea level rise However, any spatially referenced parameter in raster format could be studied by appropriate modification of the core algorithm. For example if the user wants to study spatial variability of rainfall, the core algorithm that performs the analysis is modified to compute the required results while the main interface is modified to read the required raster file and rainfall data. In the current configuration, the input data to the model consists of the DEM of an area, a

selected scenario of climate change, a selected simulation period, and the local sea level trend. The IPCC scenarios provide global sea level rise values that are used to calculate the relative sea level rise for the area. The output of the model is displayed as a map that could be exported to serve as a boundary definition map for a groundwater flow model. The processes involved in the model developed as part of the research described in this dissertation are described in the flow chart presented in Figure 4-1. The simulation model is named CCGEN (Climate Change scenario GENerator).

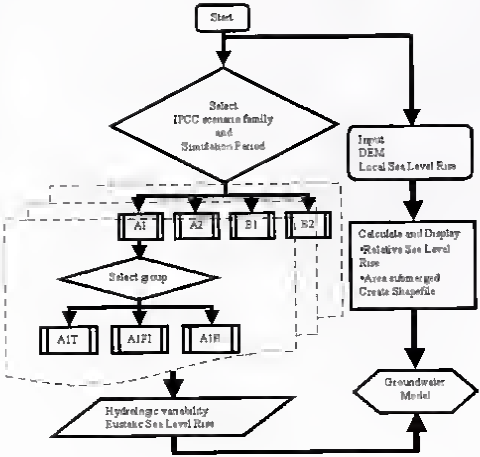

Figure 4-1 Process flowchart of climate change and sea level rise model

As displayed in Figure 4-1, the simulation model has a modular structure that allows further development and addition of raster based analysis packages. CCGEN was developed and tested on a personal computer running Windows 2000 and can be run on any computer that runs Windows versions 98 and above, a memory (RAM) of at least 128 MB, and ArcView 3x with Spatial Analyst. The model was compiled in such a way that the FORTRAN code is embedded within the Avenue calling program. The whole package was developed as an ArcView project, but it can also be recompiled as an extension for ArcView 3x to make it easily portable.

Algorithm Development and Programming

The primary factor in the development of a sea level rise modeling algorithm is choosing a suitable mathematical representation that defines the coastal geometry and processes. Sea level rise primarily results in shoreline retreat due to the combined effects of shore erosion and inundation. Inundation is the result of continuous and progressive submergence while erosion is removal of materials from the shores and beaches. The rise in sea level and the subsequent retreat in shoreline are presented schematically in Figure 4-2.

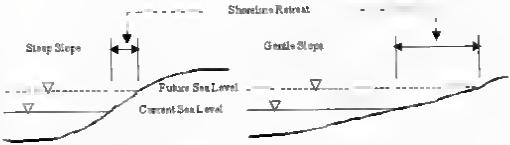

Figure 4-2 Schematic representation of shoreline retreat due to sea level rise

Changes in shoreline profile due to sea level rise could be quantified using a variety of approaches. The simplest method in use is based on the concept of drowned valley (Dean et al., 1987), in which the preexisting topography along the shore is fixed and combined with sea level rise to project the profile of the new shoreline (Kana et al., 1984). Since slope is the controlling variable in this approach, coastal areas with gentle slopes will be subject to larger flooding and shoreline retreat while shores with steep slopes will experience little horizontal shoreline displacement.

There are a number of techniques to estimate the shoreline retreat primarily due to erosional potential of sea level rise, a few of the methods documented in (Dean et al. 1987) are described as follows:

1. Historical Trend Analysis (Leatherman, 1984). Extrapolation of historical trends or historical trend analysis is a calibration method based on historical records. The method accounts for variability in shoreline response to coastal processes, sedimentary environments and coastline exposures.

2. The Bruun Rule (Bruun, 1962). Bruun's rule is based on what is known as the equilibrium beach profile, which refers to a statistical average profile that maintains its form apart from small fluctuations, including seasonal effects at a particular water level (Bruun, 1954). The equilibrium profile is expressed as

$$h = Ax^{2/3} \tag{4-1}$$

where h is the water depth, x is the horizontal distance from the shore, and A is a constant for each profile. The Bruun rule can be stated in a modified form (Hands, 1981) as

$$R = \frac{SWG_o}{h_*} \tag{4-2}$$

where R is shoreline recession, S is sea level rise, W is the width of the active portion of the profile subject to adjustment, G_o is the overfill ratio factor, and h_* is the vertical

distance over which the adjustment occurs. A schematic representation of Bruun's rule is presented in Figure 4-3

3 Sediment budget method (Everts, 1985) The sediment budget analysis is a method based on quantification of sources and sinks. The details of the source and sink approach are documented in U.S. Army Corps of Engineers Shore Protection Manual published in 1984

4 Dynamic equilibrium model (Dean, 1983) The dynamic equilibrium model considers changes in the forcing function and the resulting transient response characteristics of a beach profile.

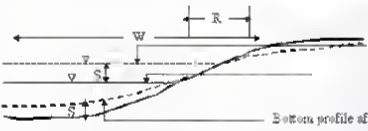

Figure 4-3 Schematic representation for the Bruun rule

Sea level rise at a particular location has a number of components. These components include global (eustatic) sea level rise, local subsidence, any spatial variability from the spatial average, local meteorological changes, and changes in the frequency of extreme events (Church et al., IPCC 2001a). Local projections of sea level rise are thus obtained by combining the local factors with the eustatic sea level rise projections. One such simplified approach suggests extrapolating the historical observations and adding global eustatic projections (Titus and Narayanan, 1995). The method suggested by Titus and Narayanan assumes that the global sea level rose 12 cm over the last century, and that the net subsidence at a particular location was 1-2 mm/yr less than the observed rate of relative sea level rise measured by tidal gauges. As a result, the relative sea level can be estimated as:

$$Local\,(t) = global\,(t) + (trend - 0.12)(t - 1990) \qquad (4\text{-}3)$$

In equation 4-3, *local(t)* is the rise in sea level by year t at a particular location (cm), *global(t)* is the global sea level rise projected by a particular scenario and trend is the current relative sea level rise trend at a particular location. The translation in shoreline is computed in terms of the rise in relative sea level and the slope of the coast. Schematic representation of the translation is presented in Figure 4-4.

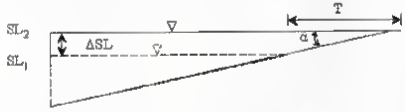

Figure 4-4 Schematic representation of translation of shoreline

The translation distance T is defined as (Hennecke and Cowell, 2000),

$$T = \frac{\Delta SL}{\tan \alpha} \tag{4-4}$$

where ΔSL represents the change in sea level, α represents the slope of the coast, and T represents the translation of the shore. In order to implement Equation 4-4 in grid analysis, the total translation at any transect has to be discretized into individual cell size translations and summed up for a given transect to obtain the total translation. The total translation along a transect is thus calculated as:

$$T = \sum \Delta T_i \tag{4-5}$$

where ΔT_i represents the incremental translation at cell i of a grid with cell size x. A schematic representation of the grid analysis of translation is presented in Figure 4-5.

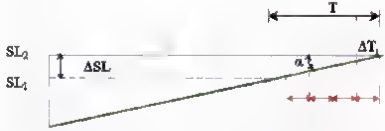

Figure 4-5 Discretization of incremental translation in grid analysis

The slope is calculated as the maximum rate of change of each cell from its neighbors using the Spatial Analyst extension of ArcView. The algorithm as defined by Equation 4-4 can sometimes encounter a numerical error while trying to compute translation for cells for which the slope value is zero or an extremely small value close to zero. In order to avoid the numerical error the slope of a transect is calculated as the average of all cells along the transect. This method ensures numerical stability and provides an averaged transect slope suitable for calculating the translation.

During a close examination of the methods used to determine translation, it became apparent that if the spatial discretization were sufficiently small, then the translation for a given cell could be estimated as the width of the cell along the transect. The final value of total translation along a transect could be computed as the sum of contiguous cell translations. In order to implement this method one has to code the algorithm to check for each cell and keep track of the cells that meet the criteria and then sum their values for a given transect. Therefore, the cell width method is recommended as a more stable method, given a reasonable cell dimension that ensures the underlying assumption is satisfied.

IPCC Climate Change Modeling Scenarios

The most recent assessment of global climate change and its impacts conducted by the IPCC was released in 2001. The assessment was published in three volumes that summarize the findings of the three working groups of scientists. The contribution of working group I was published under the title Climate Change 2001: The Scientific Basis. This report is based on the IPCC Special Report on Emission Scenarios: SRES 2000. The scenarios report that SRES 2000 presented a set of possible scenarios for greenhouse gas emissions on the basis of a very diverse set of factors.

The scenarios were primarily divided into four families (storylines), i.e., A1, A2, B1, and B2. The first family A1 is further divided into three groups, i.e., A1T, A1FI, and A1B. All SRES scenarios were designed as quantitative interpretations (quantifications) of the SRES qualitative storylines. Each scenario is a particular quantification of one of the four storylines. The quantitative inputs for each scenario involved, for instance, regionalized measures of population, economic development, and energy efficiency, the availability of various forms of energy, agricultural productivity, and local pollution controls. The following brief description is reproduced from SRES 2000:

The A1 storyline and scenario family describes a future world of very rapid economic growth, low population growth, and the rapid introduction of new and more efficient technologies. Major underlying themes are convergence among regions, capacity building, and increased cultural and social interactions, with a substantial reduction in regional differences in per capita income. The A1 scenario family develops into three groups that describe alternative directions of technological change in the energy system. These groups are A1FI, A1B, and A1T

The A2 storyline and scenario family describes a very heterogeneous world The underlying theme is self-reliance and preservation of local identities Fertility patterns across regions converge very slowly, which results in high population growth Economic development is primarily regionally oriented and per capita economic growth and technological change are more fragmented and slower than in other storylines

The B1 storyline and scenario family describes a convergent world with the same low population growth as in the A1 storyline but with rapid changes in economic structures toward a service and information economy, with reductions in material intensity, and the introduction of clean and resource-efficient technologies The emphasis is on global solutions to economic, social, and environmental sustainability, including improved equity, but without additional climate initiatives

The B2 storyline and scenario family describes a world in which the emphasis is on local solutions to economic, social, and environmental sustainability It is a world with moderate population growth, intermediate levels of economic development, and less rapid and more diverse technological change than in the B1 and A1 storylines While the scenario is also oriented toward environmental protection and social equity it focuses on local and regional levels.

All IPCC scenarios are in agreement in predicting an increase in the global average temperature and sea level For the full range of IPCC scenarios, the global sea level is projected to rise by 0 09 to 0 88 m between 1990 and 2100 with a central value of 0 48 m. The central value of this range gives an average rate that is 2.2 to 4 4 times the rate observed during the 20th century Figure 4-5 shows the ranges for the IPCC scenarios

Global sea level rise estimates and a local trend values are used to obtain relative sea level rise values for a given study area. The global estimates serve as a basis for the relative sea level rise. However, the local conditions of the study area dictate the most probable estimate of relative sea level rise. Availability of long-term tidal gage records and coastal geomorphology data improve the analysis of the coastal processes governing the rates of erosion and deposition.

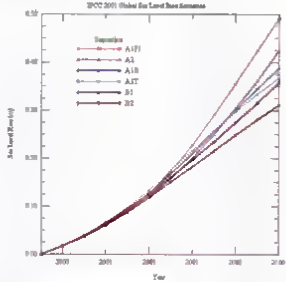

Figure 4-6. IPCC 2001 Global sea level rise scenarios.

Data Availability and Quality Issues

The data required to run simulations using GENOPT are of two types. The first is GIS data in the form of a DEM. The DEM of an area has two primary parameters that determine the precision of the analysis. These are the vertical resolution and the cell size. For sea level rise analysis, the vertical resolution of the DEM is preferred to be floating point data with about a meter resolution. The cell size of the DEM determines how precisely the horizontal translation and area submerged are to be calculated. Most DEMs

have a cell size of about 30 meters or more, but a cell size of about 10 meters gives a more precise estimate. The primary problem with DEM data of higher vertical and horizontal resolution is the size of the data file. By converting a 30-meter cell size data to a 10-meter cell size data, the file size can easily triple. The large data size requires a larger storage and computer memory.

The second data set comes from scenario results and local trend estimates. The IPCC scenario is readily available on a decadal basis. If the analysis requires simulations for smaller time steps, then the data series can be obtained by consulting the IPCC headquarters. The second approach involves fitting a curve and interpolating or extrapolating as required. From climate modeling point of view, extrapolation is a not a favorable method since the extrapolated figures are based purely on a mathematical foundation and a series of data, whereas the GCMs use a multitude of factors to make the estimates. Attempts to extrapolate the data for another 100 years have resulted in a polynomial set of equations with high coefficients of determination.

The polynomial sets of equations obtained by fitting to the data IPCC forecast data set for the period 1990 to 2001 were used to extrapolate global sea level rise values for the period 2100 to 2200. The results of the extrapolation and the corresponding coefficients of determination are presented Figure 4-6 and Table 4-1. The goodness of fit expressed in terms of coefficient of determination is well above the acceptable limit. In the absence of a reliable GCM model to forecast for the next two hundred years the forecast already in use for the one hundred years could be extrapolated and used with reasonable degree of acceptability.

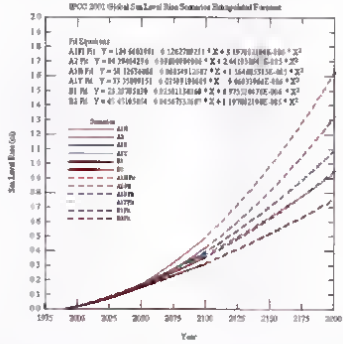

Figure 4-7. Extrapolated IPCC sea level rise values.

Table 4-1. Goodness of fit for polynomial curve fitting of the IPCC global sea level rise estimates.

Scenario	R^2
A1B	0.998480
A1FI	0.999413
A1T	0.996969
A2	0.999873
B1	0.998826
B2	0.999644

CHAPTER 5
DEVELOPMENT OF A VARIABLE DENSITY GROUNDWATER FLOW MODEL TO INVESTIGATE THE IMPACTS OF SEA LEVEL RISE ON COASTAL AQUIFERS

Boundary Conditions in Groundwater Flow Modeling

The development of a numerical groundwater flow model is highly dependent on the accurate representation of the system boundary conditions (Andersen and Woessner, 2002). Careful conceptualization of hydrogeologic boundaries is critical in properly representing the system using mathematical formulations (Wang and Anderson, 1982). In many cases, one hydrogeologic boundary could be represented by more than one system boundary condition (Reilly, 2001). Therefore, the modeler has to methodically define the groundwater flow system using appropriate governing equations and identify the most suitable boundary and initial conditions in order to solve those equations.

The equations governing groundwater flow are essentially boundary value problems where initial and boundary conditions need to be specified in order to obtain solutions. The general category of boundaries in flow models could be classified using the common mathematical boundary conditions as follows (Reilly, 2001):

1. Dirichlet boundary
2. Neumann boundary
3. Cauchy boundary

The Dirichlet boundary, also known as Type 1 boundary or specified head boundary, is a category that includes specified head and constant head boundaries. The specified head boundary is a more general type of boundary of which the constant head boundary is a special case. The specified head boundary requires the hydraulic head h to

be defined as a function of time and space, while in the case of constant head boundary, the head is held constant at a given location in space and time (Franke et al., 1987). In reality, a constant head boundary (also referred to as constant-potential or equipotential boundary) occurs where a part of the boundary surface of an aquifer system coincides with a surface of spatially and temporally uniform head values.

The Neumann Boundary also known as a Type 2 boundary or specified flow boundary, is a category that includes specified flux and no-flow boundaries (also known as streamline or stream surface). The more general case of a specified flux boundary is where flux q (discharge per unit cross-sectional area) varies with space and time. The flux could also be specified as constant in time but variable in space. A no-flow boundary on the other hand is a special case of the specified flux boundary where the flux is zero.

The Cauchy Boundary, also known as Type 3 or head dependent flow boundary includes the head dependent flux boundary. This type of boundary is encountered when the flow in an aquifer changes in response to the variability in head of the adjacent aquifer boundary.

A free surface boundary is characterized by a change in the head value with respect to elevation through time, i.e., $h = z$ or, more generally, $h = f(z)$. This type of boundary is used to represent a water table and the transition between freshwater and underlying seawater in a coastal aquifer (Franke et al., 1987). If the diffusive-dispersive process of solute transport is neglected and the saline groundwater located in the intruded seaward zone is assumed to be static, then the freshwater-saltwater transition zone can be treated as a sharp interface. The assumption of a sharp interface allows the interface to be

considered as a bounding stream surface (no-flow boundary) of the fresh groundwater flow system (Franke et al., 1987).

A seepage surface, or seepage face boundary, is encountered when a saturated flow field is exposed to the atmosphere, thus allowing free discharge to occur. In terms of mathematical representation, the seepage face is similar to the free surface where the head is the same as the elevation above a specified datum, i.e., $h = z$.

A generalized classification of the major boundary types (after Franke et al., 1987 and Reilly, 2001) is presented in table 5-1.

Table 5-1. Classification of boundary conditions

Boundary Type	Boundary Name	Boundary Mathematical Name	Mathematical Representation
Type I	Specified head Constant head	Dirichlet	$h(x,y,z,t) = constant$
Type II	Specified flux Stream line Stream surface	Neumann	$\frac{dh(x,y,z,t)}{dn} = constant$
Type III	Head dependent flux	Cauchy	$\frac{dh}{dn} + ch = constant$
	Free surface		$h = z$ OR $h = f(z)$
	Seepage face		$h = z$

Long-Term Response of Coastal Groundwater Flow to Tidal Fluctuations

Coastal aquifers are usually characterized by the dynamic interaction between seawater and groundwater, which is influenced to a certain degree by the fluctuation of tides. Studies conducted to investigate the influence of tides on groundwater flow in coastal aquifers have shown a lagged fluctuation in piezometric levels. In almost all of the studies, this response is observed to be significant on a smaller temporal scale primarily on an hourly basis (Erskine, 1991; White and Roberts, 1994; Millham and Howes, 1995; Chen and Jiao, 1999, Jiao and Tang, 1999). Tidal influence on

groundwater level is also dependent on the proximity of the observation point to the shore (Jiao and Tang, 1999) As part of the research conducted for this dissertation, studies were conducted using tidal and aquifer data for south Florida. The aim of the research was to determine whether tidal data should be part of the boundary condition for the groundwater flow model

The response of coastal aquifers to tidal influence also depends on the type of aquifer There is a marked difference in response to tidal fluctuation between confined and unconfined aquifers (White and Roberts, 1994) The spatial extent of the response zone measured from the open water may vary from a hundred meters or more for confined aquifers to about 30 or 40 meters for unconfined aquifers (Jiao and Tang, 1999) Although unconfined aquifers exhibit higher attenuation and negligible response, the leakage from overlying unconfined aquifers may affect the response of underlying confined aquifers. For the purpose of illustrating the amplitude of tidal fluctuation and groundwater head in coastal aquifers a schematic cross-section of a coastal aquifer with tidal effect on the potentiometric surface is presented in Figure 5-1

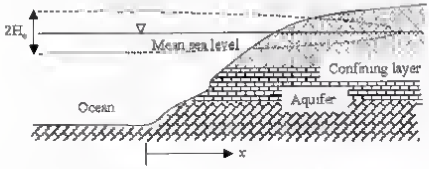

Figure 5-1 Coastal aquifer with tidal effect on the potentiometric surface

The tide varies between two extremes of high and low The time elapsed for the tide to vary between these two extremes is referred to as tidal period For a tide with

amplitude of tidal change H_o and a tidal period t_o, the amplitude of tidal fluctuation is given as (Jacob, 1950)

$$H_x = H_o \exp\left(-x\sqrt{\pi S / t_o T}\right) \tag{5-1}$$

where H_x is *the* amplitude of tidal fluctuation, a parameter that represents the variation in the piezometric head observed at the perpendicular distance x off the coast due to the tide at any distance x measured inland from the coast. The amplitude of tidal fluctuation was plotted for varying aquifer transmissivity values and presented in Figure 5-2 using storage of 0.001 and tidal period of 0.25 day (6 hours).

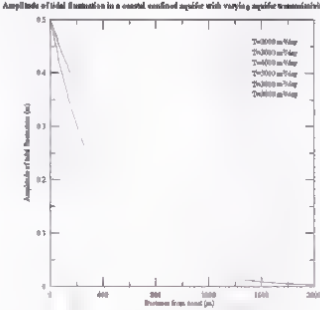

Figure 5-2 Amplitude of tidal fluctuation in a confined aquifer

The response of coastal aquifers to tidal fluctuations is not instantaneous, but rather, it is lagged by some time. Referring to Figure 5-1, for an aquifer of storativity S and transmissivity T, the time lag t_x is given by (Fetter 2001),

$$t_r = x\sqrt{t_o S/4\pi T} \tag{5-2}$$

From Equations 5-1 and 5-2 it is clear that the response of aquifers to tidal fluctuation exhibits exponential decrease as the location gets farther away from the coast. Similarly, the time lag decreases linearly with distance from the coast. Also, as demonstrated in Figure 5-2, the amplitude of the tidal fluctuation increases with increase in transmissivity of the aquifer.

The form of the relationship that exists between piezometer readings and tidal fluctuations is approximated to be sinusoidal. Once the time lag between piezometric level and tidal fluctuation is computed, then it is possible to superimpose the plot of one on another by applying a time lag and a tidal efficiency factor (Erskine, 1991). For a homogeneous confined aquifer sinusoidal oscillations in pressures propagate along the aquifer according to the following equation (Ferris, 1951):

$$h = h_o \exp\left(-x\sqrt{\pi S/t_o T}\right)\sin\left(2\pi/t_o - x\sqrt{\pi S/t_o T}\right) \tag{5-3}$$

where h = the groundwater head relative to mean sea level, x = distance from sea, t = time, t_o = period of tidal oscillation, h_o = amplitude of tidal oscillation, T = transmissivity of aquifer, and S = aquifer storativity. The time lag is defined as explained in Equation (5-2) and the tidal efficiency factor η is defined as (Erskine, 1991):

$$\eta = \exp\left(-x\sqrt{\pi S/t_o T}\right) \tag{5-4}$$

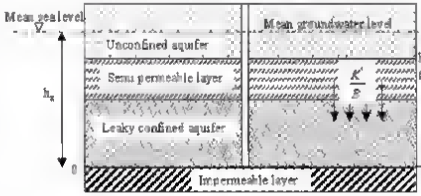

Figure 5-3 Leaky confined aquifer with tidal influence

Jiao and Tang (1999) derived an equation governing the fluctuation in hydraulic head due to tidal fluctuation for a leaky, confined, homogeneous, and isotropic aquifer governed by Dupuit's assumption with a uniform initial groundwater head of h_i measured from a specified datum as shown in Figure 5-3 (Jiao and Tang, 1999). With the assumption of a negligible storage of the semi permeable layer, the leakage is proportional to the difference in head between the two aquifers. For the specified set of conditions a one-dimensional groundwater flow equation is defined as (Jiao and Tang, 1999)

$$S\frac{\partial h}{\partial t}=T\frac{\partial^2 h}{\partial x^2}+\frac{K'}{B'}(h_i-h) \tag{5-5}$$

the head boundary condition is defined at the tidal boundary of the coast as,

$$h(0,t)=h_i+A\cos(\omega t+c) \tag{5-6}$$

Farther inland, as $x\rightarrow\infty$, the head boundary condition is

$$h(\infty,t)=h_i \tag{5-7}$$

where A is the amplitude of the tidal change, c is the phase shift, and ω is the tidal speed defined as $2\pi/t_0$. With the boundary conditions specified, the solution to equation 5-5 is (Jiao and Tang, 1999)

$$h(x,t) = h_s + A\exp(-\gamma x)\cos\left(\omega t - \frac{\omega S}{2pT} + c\right) \tag{5-8}$$

where p is a term defined as

$$p = \frac{1}{\sqrt{2}}\left[\left[\left(\frac{K/B}{T}\right)^2 + \left(\frac{\omega S}{T}\right)^2\right]^{1/2} + \left(\frac{K/B}{T}\right)\right]^{1/2} \tag{5-9}$$

for an aquifer with zero leakance then the solution reduces to

$$h(x,t) = h_s + A\exp\left(-\sqrt{\frac{\omega S}{2T}}x\right)\cos\left(\omega t - \sqrt{\frac{\omega S}{2T}}x + c\right) \tag{5-10}$$

In situations where the proximity of the wells and the length of time period of simulation warrants the use of tidal data, corrections need to be applied to compensate for tidal effects. The corrections are applied by filtering the observed piezometric data. In order to filter the data, tidal efficiency and time lag have to be determined using Equations 5-2 and 5-4

For a number of observation piezometers located at distances ranging from 50 m to 400 m from the seashore, Erskine (1991) used the following filtering equation.

$$h_F(t) = h(t) - \eta[T(t-t_\tau) - \bar{T}] \tag{5-11}$$

where $h_F(t)$ = filtered piezometric level at time t (m), $h(t)$ = piezometric level at time t(m), T = mean tide level (m). $T(t)$= tide level at time t (m)

As part of this study select tidal stations and monitoring wells were analyzed in the state of Florida. The locations and names of the stations are presented in Figure 5-4 and Figure 5-5. The tidal stations data was obtained from the Center for Operational Oceanographic Products and Services (COOPS), which is a data dissemination center of the National Oceanic and Atmospheric Administration (NOAA). The groundwater level data was obtained from the US Geological Survey and South Florida Water Management District.

From the available tidal stations for the state of Florida, those in the area of interest, which primarily consists of three counties in south Florida, were selected and corresponding groundwater monitoring sites were selected based on proximity. Although it was difficult to find corresponding sites where both a tidal station and groundwater monitoring site were located close to each other, it was possible to find some sites where the tidal stations and groundwater monitoring sites were within a few thousand meters of each other. Shorter time period time series and daily average tidal data for the year 2003 were plotted for the selected (see Figure 5-6). Corresponding daily groundwater level data also were plotted for the corresponding groundwater sites (see Figure 5-7).

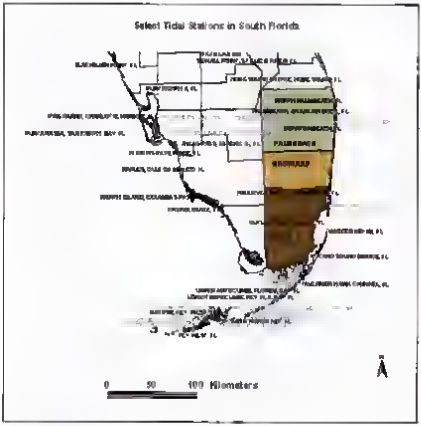

Figure 5-4 Select tidal stations in south Florida.

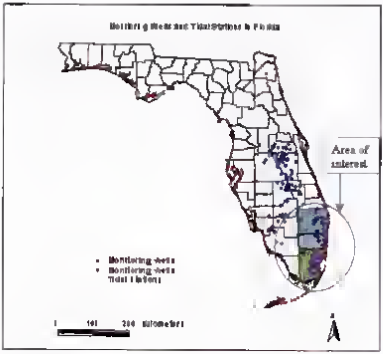

Figure 5-5 Tidal stations and select groundwater monitoring sites in Florida.

Referring to Figure 5-6, there is a clear trend in the tidal variation for the stations considered. The tide height usually attains its seasonal maximum some time in the month of October. Referring to Figure 5-7, the groundwater level plots superimposed on the tidal data reveal that the groundwater level maximum and minimum values are attained prior to the tidal maximum and minimum values. As a result, it is not possible to correlate the two parameters by considering the groundwater level to be dependent on the tidal fluctuation at a distance of a few thousands of meters. Perhaps a monitoring well located at a much closer distance would have resulted in different conclusions, but with the minimal data available for comparison, this is the only logical conclusion that can be made.

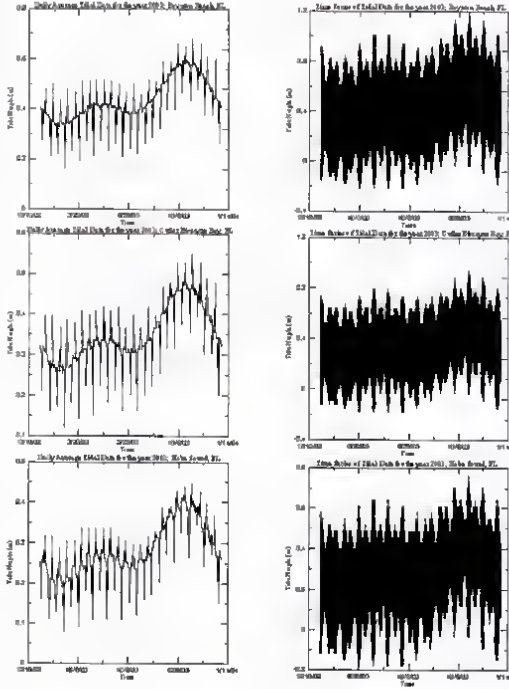

Figure 5-6 Tidal data of select stations in south Florida. A) Boynton Beach, Cutler Biscayne Bay and Hobe Sound B) Key West, Miami Beach, North Miami Beach C) North Palm Beach, Palm Beach, Vaca Key

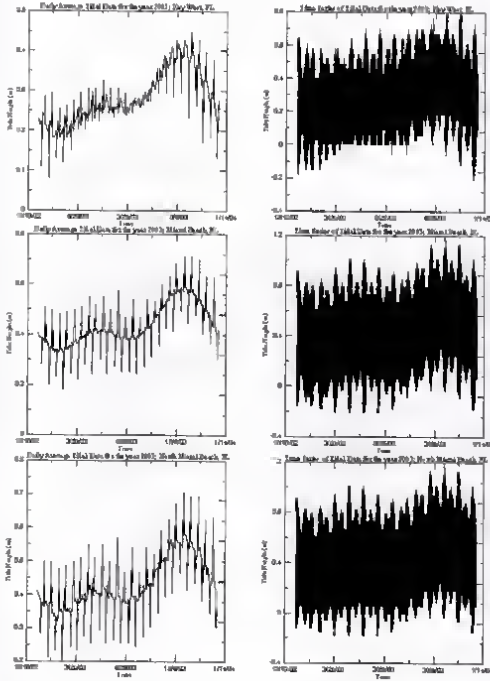

Figure 5-6. Continued.

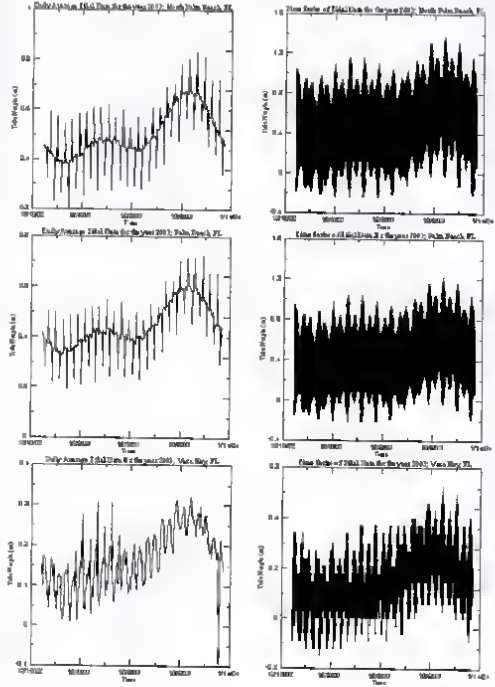

Figure 5-6. Continued.

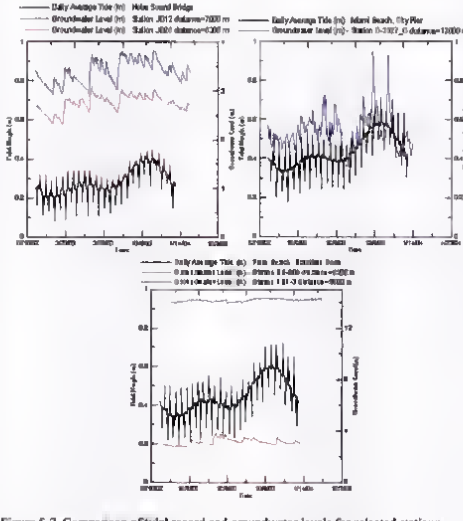

Figure 5-7 Comparison of tidal record and groundwater levels for selected stations

In order to analyze further the fluctuation in groundwater head due to tide, the Miami Beach data were used to determine the significance of their influence on the unconfined aquifer in the area. The water level data of monitoring well G-3327_G, which is located at about 12,000 m from the coast, were used. The groundwater head fluctuation was computed using Equation 5-3 (Ferris, 1951) and the calibration data of aquifer parameters for the Biscayne Bay regional model (Langevin, 2001). For the sake

of comparison, the groundwater head fluctuation was also computed again using the Equation 5-10 (Jiao and Tang, 1999) The data for both cases consisted of a surficial aquifer of average thickness 45 m, a hydraulic conductivity 9600 m/day, storage of 0 001, and an average tidal fluctuation of with varying periods of tidal oscillation that ranged from 0 5 hours to 24 hours

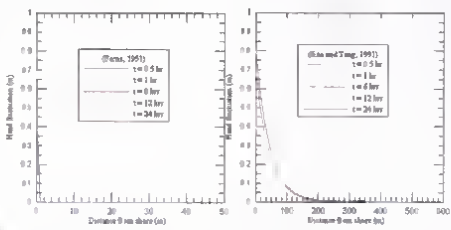

Figure 5-8. Groundwater head fluctuations due to tidal influence

The results from Equation 5-3 showed almost no fluctuation even at the coast, as the fluctuation was limited to less than 50 m. The results from Equation 5-10 showed small fluctuations up to a distance of 200 m, but after that, the oscillation becomes insignificant. At a distance of 12,000 m, there is no influence on the groundwater head

The calculations made to investigate the influence of tidal fluctuations demonstrated that the effects tidal fluctuations have on groundwater levels over a longer period of simulation that ranges from decades to centuries could be neglected Instead, the focus should be on the sustained rise in sea level The scale of a model also plays a significant role Groundwater head in areas beyond a couple of hundred meters in the case of confined aquifers, and perhaps less than fifty meters in the case of unconfined

aquifers does not seem to be influenced by tidal fluctuation. Usually regional models have spatial extents of a thousand meters or more, thus the influence is not significant to be considered due to attenuation.

The spatial and temporal scale of groundwater flow models varies depending on the requirements. If the spatial scale of the models is very small, the transect perpendicular to the seaside boundary is relatively short, and the time scale of modeling is also relatively small, then consideration of tidal influence might be required. In situations where tidal influence has to be considered, corrections need to be applied to the observed piezometric readings. Since most regional aquifer models have cell sizes of a few hundred meters, the adjoining cells at the seaside should be defined as a Dirichlet boundary, and the head and concentration should be specified accordingly. For the head boundary, the value should be set to vary in response to sea level rise.

Modification of Boundary Conditions to Account for Impacts of Sea Level Rise

The hydrogeologic boundaries of coastal aquifers are complex due to the presence of a seaside boundary in addition to the inland boundaries. During the investigation of seawater intrusion and sea level rise, the primary boundary condition of concern is the seaside boundary. The more customary way of specifying the seaside boundary condition involves defining a Dirichlet boundary condition where the head is specified or held constant. For a variable density model, concentration values at the seaside are also held constant. In order to define the change in the head boundary during transient simulations, numerical codes utilize a number of techniques. For example, in the USGS code MODFLOW, a linear relationship can be assumed between specified starting and final heads for each stress period. In between stress periods, the specified head boundary values are interpolated linearly between the specified starting and ending head values for

the different time steps within a given stress period. During a given time step, the head values are held constant and the interpolation algorithm is executed once every time step.

SEAWATSLR. Modification of SEAWAT to Model Sea Level Rise Impacts

The flow part of the three-dimensional variable density groundwater flow modeling code SEAWAT is based on MODFLOW. As described in Chapter 2, SEAWAT is formulated to yield values of groundwater head in terms of equivalent freshwater head. One of the flow packages incorporated in SEAWAT is the Time Variant Specified Head package (CHD). The CHD package is used to represent hydrogeologic/hydrologic features with static or nearly static head values. Customarily, the seaside boundary is incorporated into a groundwater flow model as a constant head boundary. The water hydraulic head on the seaside is expressed as equivalent freshwater head with hydrostatic variation.

The modified version of SEAWAT named SEAWATSLR accounts for time variant changes in the seaside boundary by incorporating incremental values of rise in sea level for each flow time step. The changes in time variant constant head are thus expressed as boundary changes due to sustained sea level rise through modification of the CHD algorithms.

SEAWATSLR incorporates a modified linear interpolation routine in the CHD package that has the same incremental trend as the rise in sea level. As a result, within a given stress period, the head is allowed to vary in response to an incremental increase of sea level specified by the user. The incremental sea level value is obtained from the relative sea level rise modeling results obtained by using CCGEN, as described in Chapter 4. The sea level rise estimated for a given forecast period is distributed as an

incremental increase and included in the constant head for the entire groundwater flow simulation period at every time step

The equivalent freshwater head in the time variant specified head boundary is written for every cell (i, j, k) at any time t as

$$h^t_{f(i,j,k)} = \frac{\rho^t_{s(i,j,k)}}{\rho_f} h^t_{s(i,j,k)} - \frac{\rho^t_{s(i,j,k)} - \rho_f}{\rho_f} Z_{(i,j,k)} \qquad (5\text{-}12)$$

Transient changes in the boundary head conditions result in a variation in the head term between successive time steps. The head at the next time step is related to the head at the current time step as follows

$$h^{t+1}_{f(i,j,k)} = h^t_{f(i,j,k)} + \psi \Delta t \qquad (5\text{-}13)$$

where ψ is the rate of sea level rise and Δt is the elapsed time at the given flow time step. Substituting for the head term in time step t+1, the equivalent freshwater head for the time variant constant head boundary becomes

$$h^{t+1}_{f(i,j,k)} = \frac{\rho^t_{s(i,j,k)}}{\rho_f} h^t_{s(i,j,k)} - \frac{\rho^t_{s(i,j,k)} - \rho_f}{\rho_f} Z_{(i,j,k)} + \psi \Delta t \qquad (5\text{-}14)$$

The head between two time steps is interpolated linearly in the current formulation of SEAWAT. However, the seaside boundary which in coastal aquifers is related to sustained sea level has a non linear variation through time. Referring to the best fit equations developed to extrapolate the global sea level rise scenarios in chapter 4, the relationship has been determined to be polynomial. According to the current formulation of SEAWAT, the head is linearly interpolated as

$$h^t_{f(i,j,k)} = h^{t-1}_{f(i,j,k)} + (h^{t+1}_{f(i,j,k)} - h^{t-1}_{f(i,j,k)}) \Delta t_p \qquad (5\text{-}15)$$

where Δt_F is a time fraction expressed as the proportion of stress period to the end of the current time step. This time fraction is calculated as the ratio of total elapsed time to the length of stress period.

$$\Delta t_F = \frac{PERTIM}{PERLEN} \tag{5-16}$$

where PERTIM is the total time elapsed during a stress period and PERLEN is the length of the stress period. With the current definition, equation 5-14 is updated to utilize the accumulated time in a given time step $\Delta t = PERTIM$ and it becomes

$$h^{t+1}{}_{(i,j,k)} = \frac{\rho^t{}_{s(i,j,k)}}{\rho_f} h^t{}_{s(i,j,k)} - \frac{\rho^t{}_{s(i,j,k)} - \rho_f}{\rho_f} Z_{(i,j,k)} + \psi \Delta t \tag{5-17}$$

The time component of the term that accounts for the rate of sea level rise is customarily expressed as per century or per year. Therefore, the user has to accordingly change it to days which is the more common time scale used in groundwater modeling. Also for a century long simulation using a time scale less than a day will make the computational efforts unnecessarily high. The length of a time step in a stress period is defined by the number of time steps and the time step multiplier, and the length of time step is defined as

$$DELT = \frac{PERLEN(1-TSMULT)}{(1-TSMULT)^{NSTP}} \tag{5-18}$$

where DELT is the time step length, TSMULT is the time step multiplier, and NSTP is the number of time steps. Using the concept of piecewise linearization, the linear interpolation scheme implemented in SEAWAT can be used without modification. The piecewise linearization within the specified time step of simulation is an acceptable approximation within the specified time step, which is usually smaller than the century

scale time frame implemented in the sea level rise simulation A generalized process flowchart for SEAWATSLR (modified from SEAWAT) is presented in Figure 5-9 Procedures in red boxes show components modified or added as part of this research

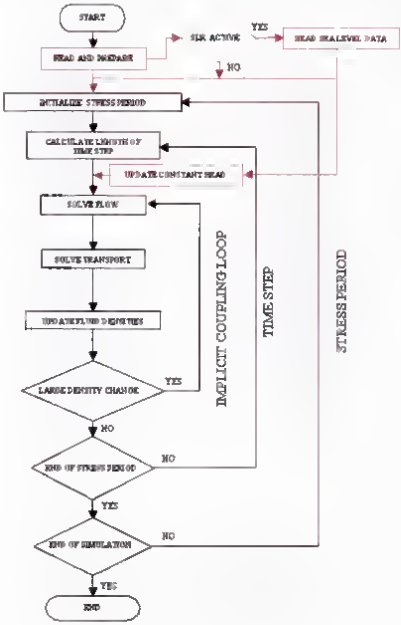

Figure 5-9 Generalized flowchart of SEAWATSLR.

CHAPTER 6
DEVELOPMENT OF EVOLUTIONARY ALGORITHM BASED GROUNDWATER FLOW OPTIMIZATION MODEL

Formulation of Objective Function and Constraints

The objective functions to be solved in optimization problems of coastal aquifers usually involve maximizing the benefits, minimizing the cost of pumping, minimizing the advancement of saltwater farther inland, minimizing drawdown due to pumping below a specified value, and maximizing the pumpage (Shamir et al., 1984, Willis and Finney, 1988, Finney et al., 1992, Hallaji and Yazicigil, 1996, Emch and Yeh, 1998, Das and Datta, 1999a, 1999b, Cheng et al., 2000, Benachim et al., 2000). Most optimization approaches used in coastal aquifers management focus on maximizing pumpage and minimizing cost subject to the constraints of drawdowns and saltwater intrusion criteria.

In this research, two approaches were considered for the purpose of demonstration, but only one was implemented in the development of the optimization model. The first approach is a sharp interface approach (Emch and Yeh, 1998), while the second approach is a variable density approach (Gordon et al., 2001). The sharp interface approach was modified to work with the formulation of SEAWAT just for the sake of demonstrating the feasibility of the approach for future research. The variable density approach was applied using genetic algorithms and the results are presented in Chapter 7. Both approaches are based on a multi-management period, multi-objective optimization problem formulation, but each one utilizes a different approach of constraint and objective function formulation.

Multi-objective optimization problems require finding a vector of decision variables that satisfy constraints and optimize a vector function whose elements represent the objective function (Osyczka, 1985). For a vector of n decision variables denoted mathematically denoted as x_i, $i = 1, n$, the vector notation of decision variables is defined as (Coello Coello et al , 2002):

$$\vec{x} = \begin{bmatrix} x_1 \\ x_2 \\ \cdots \\ x_n \end{bmatrix} \tag{6-1}$$

The constraints that need to be satisfied are defined are expressed as inequalities

$$g_i\left(\vec{x}\right) \geq 0 \quad i = 1, \ldots, m \tag{6-2}$$

or as equalities as

$$h_i\left(\vec{x}\right) = 0 \quad i = 1, \ldots, p \tag{6-3}$$

where the number of equality constraints p is less than the number of decision variables n in order to avoid the formulation of an over-constrained problem. The number of degrees of freedom is then defined as n-p, thus ensuring the number of unknowns is less than the number of equations.

The objective functions are defined as $f_1(\vec{x}), f_2(\vec{x}), \ldots f_k(\vec{x})$ where k is the number of objective functions in the multi-objective problem being solved. The objective functions are represented in vector form as

$$\vec{f}\left(\vec{x}\right)=\begin{bmatrix} f_1\left(\vec{x}\right) \\ f_2\left(\vec{x}\right) \\ \cdots \\ f_k\left(\vec{x}\right) \end{bmatrix} \tag{6-4}$$

The general multi-objective optimization problem is defined in Euclidean n-space as:

$$\vec{x}^{*}=\begin{bmatrix} x^{*}_1 \\ x^{*}_2 \\ \cdots \\ x^{*}_n \end{bmatrix} \tag{6-5}$$

which satisfies the m inequality constraints

$$g_i\left(\vec{x}\right)\geq 0 \quad i=1, \ldots, m, \; h_i\left(\vec{x}\right)=0 \quad i=1, \ldots, p$$

and optimizes the vector function

$$\vec{f}\left(\vec{x}\right)=\begin{bmatrix} f_1\left(\vec{x}\right) \\ f_2\left(\vec{x}\right) \\ \cdots \\ f_k\left(\vec{x}\right) \end{bmatrix} \tag{6-6}$$

Sharp Interface Approach

The first approach is based on the position of the saltwater freshwater interface and formulates the objective function on the basis of minimizing the cost and volume of saltwater in the aquifer. The original formulation (Emch and Yeh, 1998) used a sharp

interface approach, and the flow model was simulated using the USGS code SHARP (Essaid, 1990a) The optimization was performed using the commercial software MINOS (Murtagh and Saunders, 1987) In order to solve the nonlinear objectives and constraints, a projected augmented Eulerian Lagrangian algorithm was used and the nonlinear problem was reduced to a series of linearly constrained sub-problems. The reduced sub-problems were then solved using the reduced gradient algorithm.

The formulation of Emch and Yeh was modified for this discussion and reformulated on the basis of equivalent freshwater heads, the position of the saltwater freshwater interface, and freshwater withdrawal through pumping The simulation and optimization models could be coupled using the response matrix approach This approach requires generating the unit responses of aquifer to pumping stresses and utilizing these responses in the objective function to be optimized.

Minimizing the cost of pumping and maximizing the amount of water pumped require multi-objective criteria, thus satisfying the condition for a multi-objective optimization model The objective function could be formulated as a multi-objective, multi management period optimization problem.

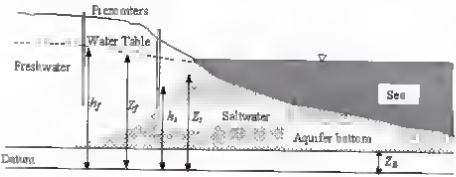

Figure 6-1 Representation of a coastal aquifer for objective function formulation

Consider the single layer aquifer shown in Figure 6-1. Let G be the set of all layered aquifers from which any layer $l \in G$ is considered. From continuity of fluid pressure the elevation of the saltwater-freshwater interface above the aquifer datum is

$$Z_l = \rho_f^* h_f^l - \rho_s^* h_s^l = (1+\delta^*) h_s^l - \delta^* h_f^l \tag{6-7}$$

where h_f^l and h_s^l are vertically averaged freshwater and saltwater heads, ρ_f and ρ_s are freshwater and saltwater densities, ρ_f^* and ρ_s^* are freshwater and saltwater density ratios; $\delta = \dfrac{\rho_f}{\rho_s - \rho_f}$, and Z_l is the elevation of interface above datum.

Assume there are n decision variables in the problem which are represented in vector form as

$$\overline{P} = (P_{1,1}, \cdots, P_{\omega,1}, P_{1,2}, \cdots, P_{\omega,2}, P_{1,\tau}, \cdots, P_{\omega,\tau}) \tag{6-8}$$

where $\omega = \omega_1 + \omega_2$ is the total number of supply sources and $n = \omega \times \tau$.

The state variables in the formulation suggested are freshwater heads, saltwater heads, and the position of the interface. In order to apply this approach using SEAWAT, the equivalent freshwater head and the position of the interface could be used. This requires isolating a specified isochlor as the defining interface boundary and based on that calculating the location of the Z_l boundary.

The cost objective requires minimizing the operation cost of pumping not including the cost of drilling the wells and constructing the supply system. The cost minimization could be formulated as

$$Min \quad Z_1 = \sum_{t=1}^{\tau} \left[\sum_{i \in \Omega_1} P_{i,t} \overline{C_i} (L_i - h_{i,t}) + \sum_{i \in \Omega_2} P_{i,t} \overline{C_i} \right] \tag{6-9}$$

where Z_j = elevation of the interface, $P_{i,j}$ = water supply rate from source i for time period j, $\overline{C_i}$ = unit cost of groundwater extraction per height of required lift or of surface water supply for source i, Ω_1 = set of groundwater sources, and Ω_2 is set of surface water sources.

The saltwater intrusion objective function was formulated in terms of the volume of saltwater in the aquifer

$$Min \quad Z_2 = \sum_{i=1}^{I} \left[\iint Z_j^i(x,y)\,dx\,dy \right] \tag{6-10}$$

The output from SEAWAT is in terms of the equivalent freshwater head therefore Equation (6-9) was reformulated accordingly. The position of the interface is similar to the saltwater head representation in SEAWAT, thus Z_j^i could be replaced by h_z, which was converted from the equivalent freshwater head formulation.

The reformulated objective function:

$$Min \quad Z_2 = \sum_{i=1}^{I} \left[\iint h_{z_j}^i(x,y)\,dx\,dy \right] \tag{6-11}$$

substituting for $h_{z_j}^i$,

$$Min \quad Z_2 = \sum_{i=1}^{I} \left[\iint (\rho_f^* h_{f_j}^i + \frac{1}{\delta} Z)(x,y)\,dx\,dy \right] \tag{6-12}$$

and the constraints include

Demand constraint,

$$\sum_{i \in \Omega} Q_{i,j} \geq D_{i,j} \tag{6-13}$$

Well capacity constraint

$$0 \leq Q_{i,j} \leq Q_i^{\max} \quad \forall i \in \Omega_1 \tag{6-14}$$

Drawdown constraints

$$s_{i,j} \geq s_i^{\min} \ \forall i \in \Omega_1 \tag{6-15}$$

Surface-water supply constraints

$$0 \leq Q_{i,j} \leq Q_{i,j}^{\max} \ \forall i \in \Omega_2 \tag{6-16}$$

Variable Density Approach

The second approach is based on the formulation of a regional scale optimization model (Gurdon et al., 2001). The objective of this optimization model is maximizing the amount of water pumped and minimizing the amount of salt mass extracted with the water. This requires performing a mass balance for the flow simulation and calculating the amount of salt mass extracted for each management period. The response matrix was generated from pumping stresses, mass of salt extracted through pumping, and the constraints on pumping for each management period.

Consider a regional aquifer with a number of pumping wells. It is assumed that the aquifer is already subject to saltwater intrusion and the objective is pumping the maximum amount of water without violating a set of predefined water quality and quantity constraints. Let N_w be the total number of wells and N_p be the number of time periods in the entire management period during which the pumping stresses are constant. In the current formulation these time periods are set to be the same as the stress periods of the flow model. The decision variables of the management model are the pumping rates with constraints on well pumping rates and total amount of water extracted.

The mathematical representation of the governing management model is formulated as follows (Gordon et al., 2001),

$$Max \quad F_1 = \sum_{ip=1}^{N_{ip}} \sum_{tp=1}^{N_{tp}} \left| Q_{ip,tp} \right| \tag{6-17}$$

$$Min \quad F_2 = \sum_{ip=1}^{N_{ip}} \sum_{tp=1}^{N_{tp}} \int \left| Q_{ip,tp} \right| C_{ip,tp}(t)\, dt \tag{6-18}$$

$$Q_{max,ip} \le Q_{ip,tp} \le 0 \tag{6-19}$$

$$Qa_{min} \le \sum_{ip=1}^{N_{ip}} \sum_{tp=1}^{N_{tp}} \left| Q_{ip,tp} \right| \le Qa_{max} \tag{6-20}$$

where $Q_{ip,tp}$ is the pumping rate of well ip in time period tp (in this case stress period) and is constant and considered negative to be consistent with the formulation of groundwater models, $C_{ip,tp}(t)$ is the concentration of salt in well ip during time period t, $Q_{max,ip}$ is the maximum pumping capacity of well ip, and Qa_{min} and Qa_{max} are the lower and upper bounds of the total amount of water that can be extracted from the aquifer

The presence of the concentration term in the objective function makes the problem defined above non-linear, non-convex, and non-smooth The solution adopted by Gordon et al , (2001) was the Bundle Trust method, which is a modification of the classical gradient methods. The constraints defined in (6-19) are incorporated directly into the optimization model while the constraints defined in (6-20) are incorporated as a penalty term giving a modified management model with a weighted sum of the two objective functions The modified objective function thus becomes:

$$Min \left\{ \begin{array}{l} I = -\sum_{ip=1}^{N_p}\sum_{jp=1}^{N_p}\left|Q_{ip,jp}\right| + P_1 \sum_{ip=1}^{N_p}\sum_{jp=1}^{N_p}\int\left|Q_{ip,jp}\right| C_{ip,jp}(t)\, dt \\ + P_2\, Max\left[0, Q_{min} - \sum_{ip=1}^{N_p}\sum_{jp=1}^{N_p}\left|Q_{ip,jp}\right|\right] \\ + P_3\, Max\left[0, \sum_{ip=1}^{N_p}\sum_{jp=1}^{N_p}\left|Q_{ip,jp}\right| - Q_{max}\right] \end{array} \right\} \qquad (6\text{-}21)$$

subject to $Q_{min,jp} \le Q_{ip,jp} \le 0$. The weights P_2 and P_3 are adjusted to make sure that the upper and lower pumping bounds are not violated.

GENOPT: A Genetic Algorithm Based Solution of Groundwater Flow Optimization Method

The formulation of practical water resources optimization problems is often characterized by convexity and non-linearity. As a result, obtaining second order and even in some cases first order derivatives of the objective functions, which are required by many traditional optimization methods, is difficult if not impossible (Tang and Mays, 1998). Moreover, it is difficult to ensure that the solution obtained is the globally optimal solution for the given problem. As explained in Chapter 3, Genetic Algorithms differ from the traditional optimization methods in many ways and are capable of handling convex and non-linear problems by ensuring global or near global optimal solution.

Once the objective function, the decision variables and the constraints are formulated, then the decision variables are encoded into strings referred to as chromosomes. Commonly these strings are coded as binary strings, but it is also possible to encode them as integer or real. Once the encoding is accomplished, then a random number generation algorithm is used to initialize the first population of possible solutions. Equal probability of survival is assigned initially for the entire ensemble. The objective function is used to define the fitness function of the problem. The fitness

function assigns a probability for each chromosome to generate new chromosomes and then tests its performance in between two successive generations by introducing selection, crossover, and mutation

The basic features of the core GA operations include creep mutations, elitism, niching, tournament selection, single point or uniform crossover. The detailed operations of the GA operation are presented in the process flowchart figure 6-2, the processes generally include the following

1 Randomly generate an initial seed population of binary strings representing possible designs This initial population of strings represents realizations of a set of decision variables Each string is coded as binary so that the alleles (particular locations on the strings) will have values of 0s and1s

2 Calculate the fitness of each string of the current generation using the objective function and the constraints. The strings are then ranked using their fitness values and assigned probabilities using tournament selection Using elitist strategy the string with the best fitness function value is copied to the new population

3 Produce subsequent generation starting from the current using crossover The strings are randomly selected for mating using single point or uniform crossover The mating between two strings is determined by the probability of crossover P_c

4 Perform mutation randomly on some of the alleles in order to prevent premature convergence using the probability of mutation P_m

5 Repeat steps 3 and 4 until convergence is achieved or the maximum number of generations is exceeded

The simulation optimization procedure is externally coupled thus first a simulation is run and the results that form the decision parameters and boundary constraints are extracted The main calling program has a subroutine that reads the binary and text files of the simulation and read the required concentration, head and pumping values. In addition to the values read from the simulation result, the user has to create the parameters required to run the core operations of the GA module

The objective function is formulated using the parameters and constraints. The optimization proceeds until the objective function is satisfied for the specified population size and number of generations. Once the optimization results are obtained the new parameter values are once again used in the simulation models to test acceptability of the optimization results in terms of satisfying the management objectives.

The optimization algorithm was developed on the basis of the more conventional GA methodologies in current use. The algorithm was designed to be a simple GA with robust working mechanisms. With the advent of newer techniques, individual functions and routines of the core algorithm in GENOPT could be modified in the future to create a faster and more efficient search algorithm.

The generation of random numbers is the first process in the algorithm. In order to generate random numbers, Knuth's algorithm was used (Knuth, 1981) as described in Press et al., (1992). The random number generating routine returns a uniform deviate between 0.0 and 1.0. The routine works by reading an initial seed value, after that a random number field is initialized and the first random number is generated. Subsequently, new random numbers are generated using a subtractive algorithm.

Determination of the population size was based on the average size of schema (the average number of bits per parameter (Goldberg, 1989). In a binary coding formulation of strings and for a schema of size k and string of length l, the population size n_{pop} is determined as (Goldberg, 1992):

$$n_{pop} = O\left[\left(\frac{l}{k}\right)\chi^{k}\right] \tag{6-22}$$

where χ is the number of possibilities for each chromosome (cardinality of chromosomes). For binary formulation the value of χ is 2.

Encoding of the decision variable into strings (referred to in GA as chromosomes) was accomplished by binary coding. It is also possible to use integer and real coding instead of binary coding. For m decision variables in an optimization problem, if the decision variables are binary coded as binary strings of length n, then the resulting chromosome will be an $n \times m$ string. The decoding of the string for the j^{th} decision variable x_j was performed as (Tang and Mays, 1998)

$$x_j = \frac{(x_{max} - x_{min})}{2^n - 1} \sum_{i=(j-1)*n+1}^{j*n} a(i) \cdot 2^{i-(j-1)*n-1} + x_{min} \tag{6-23}$$

where, $a(i) = (0,1)$ is the i^{th} binary digit value in the corresponding chromosome. For example, two decision variables each coded as binary string of 11 digits will have a sting of 22 binary digits that looks like 1000101110110101000110.

The fitness of a chromosome was evaluated to determine the probability that a chromosome will be selected as a parent chromosome to generate new chromosomes. This was achieved through the use of a scaling function δ, which maps objective function values to an appropriate positive fitness value. For a vector of decision variables X the objective function value $g(X(\mathfrak{a}))$ is mapped in to the fitness value $f(\mathfrak{a})$ using δ

$$f(\mathfrak{a}) = \delta(g(X(\mathfrak{a}))) \tag{6-24}$$

The fitness function $f(\mathfrak{a})$ that determines the reproduction of a chromosome is obtained from the modified objective function as described in Equation (6-21).

$$\begin{aligned} g(X(\mathfrak{a})) &\Rightarrow L(Q_{ip,jp}, C_{ip,jp}, Qa_{min}) \\ f(\mathfrak{a}) &= \delta(L(Q_{ip,jp}, C_{ip,jp}, Qa_{min})) \end{aligned} \tag{6-25}$$

For the fitness function described in Equation (6-25), the scaling function was based on a linear dynamic scaling (Tang and Mays, 1998). This method ensures non

negative fitness function for all chromosomes and the worst performing chromosomes that have zero fitness will be excluded from reproduction. The linear dynamic scaling method is formulated for a given chromosome a_k

$$\tilde{f}(f(\mathbf{a}_k)) = L(Q_{up,dp}, C_{up,dp}, Qa_{min}) - Min\left[f(\mathbf{a}_k) | \mathbf{a}_k \in N(t)\right] \tag{6-26}$$

Selection helps choose the survivor chromosomes that are fit for the new generation thus forming the parent chromosomes for the next generation. For the generated field of random numbers N, the total fitness S is calculated

$$S = \sum_{i=1}^{K} f(\bar{\mathbf{a}}_i) \tag{6-27}$$

where $f(\bar{a}_i)$ is fitness of the i^{th} chromosome in the old population. As a next step the k^{th} parent chromosome is selected if

$$\frac{\sum_{i=1}^{K-1} f(\bar{\mathbf{a}}_i)}{N} < N \leq \frac{\sum_{i=1}^{K} f(\bar{\mathbf{a}}_i)}{N} \tag{6-28}$$

A selection scheme was implemented based on the fitness of the individual chromosomes:

$$P_{select} = \frac{f(\bar{\mathbf{a}}_k)}{\sum_{i=1}^{K} f(\mathbf{a}_i)} \tag{6-29}$$

Crossover makes it possible for alleles of chromosomes to undergo changes that will allow them to create new individuals through bit combinations. As a result, crossover is considered to be a very important search operator in genetic algorithms. Since crossover combines useful segments of different parents it makes it possible for the new individual to benefit from advantageous bit combinations of both parents (Holland,

1975) Crossover probabilities of 0 6 to 0 7 were assigned and depending on the fitness of the selected parent chromosome crossover was performed

Mutation helps reintroduce lost alleles into the population Alleles are feature values assigned to chromosomes in natural systems or strings in artificial systems, so each string is assigned an allele The reintroduction helps bring back bit positions that have converged to a certain value throughout the population and therefore could never be regained again by means of recombination (Tang and Mays, 1998) The two common forms of mutation, creep and jump mutation, were implemented in the formulation of the solution. The overall probability of a jump mutation for an individual n_k and number of chromosomes (binary bits in a string) n_c was determined

$$(p_{jump})_{n_k} = 1-(1-p_{jump})^{n_c} \tag{6-30}$$

Similarly for creep mutation with number of parameters n_p, the creep mutation probability was determined

$$(p_{creep})_{n_k} = 1-(1-p_{creep})^{n_p} \tag{6-31}$$

For overall probability of mutation, probabilities of jump and mutation and creep were set to be equal, and creep mutation probability was expressed

$$(p_{creep}) = 1-(1-p_{jump})^{n_c/n_p} \tag{6-32}$$

If Equation (6-32) is expanded using binomial expansion and the lower order terms are neglected the relationship becomes (Carroll, 1996)

$$(p_{creep}) \cong \frac{n_c}{n_p} p_{jump} = \frac{n_c}{n_p}\left(\frac{1}{n_{pop}}\right) \tag{6-33}$$

The process flowchart of the GA operations is presented in Figure 6-2. The externally coupled simulation-optimization process flowchart is presented in Figure 6-3

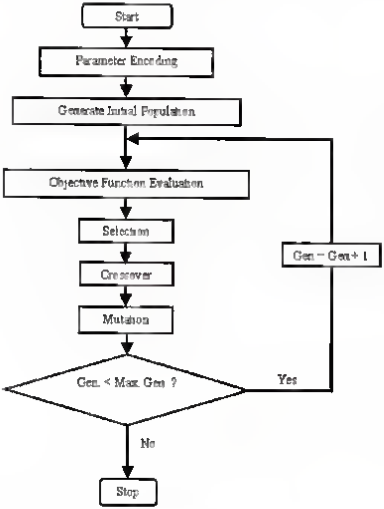

Figure 6-2 Flowchart of core operations of the GA algorithm.

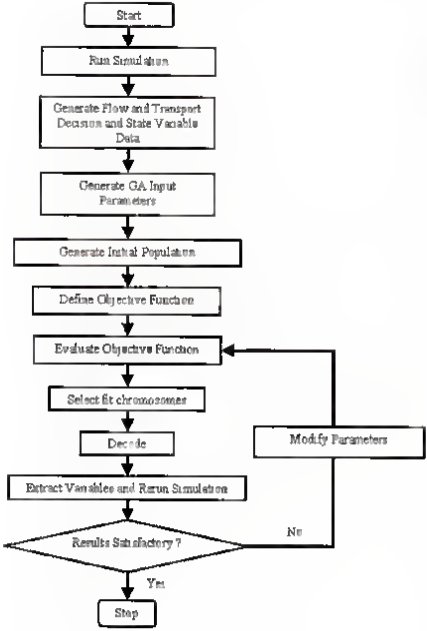

Figure 6-3 Flowchart of the simulation-optimization process

CHAPTER 7
NUMERICAL MODELING RESULTS

Application of CCGEN

The GIS-based climate change impacts simulation model was used to estimate relative sea level rise for selected stations in south Florida where the required geospatial data were available. The global sea level rise scenarios developed by the IPCC were used to select a mid-range scenario and determine the relative sea level rise for the specific location and period. The results are presented as vulnerability maps and a series of plots that show the various tidal gage data collected from observation stations.

Research conducted in different parts of the world over the past few decades clearly indicates that coastal areas are under the increasing threat of sea level rise. In the United States, the state of Florida is one of the states with a long shoreline (see Figure 7-1) that faces the possibility of being impacted by future sea level rise. The total length of coastline in the state of Florida is about 38,347,616 meters. This estimate includes inland coast and banks along rivers and estuaries. This long coastline makes Florida vulnerable to the impacts of climate change and sea level rise, especially in the highly populated coastal areas that face an increased threat due to the combined effects of both climate change and the effects of urbanization. For the subsequent sea level rise studies, three counties were selected from south Florida. Digital data obtained from the USGS and tidal data obtained from NOAA were used in combination with the eustatic sea level rise values of the IPCC to generate sea level rise scenarios for Palm Beach, Broward, and Miami-Dade counties. The analysis was performed using the mid range scenario A1T

and the respective mean sea level trends. Maps showing the extent of new sea level values and the translation in the location of seacoast for a simulation period of choice were generated.

Figure 7-1. Coastal Areas of Florida.

A vulnerability assessment conducted using a digital elevation model (DEM) for the entire state of Florida made it possible to quantify the extent of possible submergence due to sea level rise (Tirunesh and Motz, 2001). The study used a 90 meter cell DEM, the current sea level, and coastal elevations and identified vulnerable areas with respect to the proximity to sea level. The result showed that an estimated area of 19,862 km^2 is at sea level, and approximately 7,499 km^2 has an elevation of 1.0 m above sea level. Table 8-1

summarizes the elevation and corresponding approximate areas for elevations less than 5 meters above sea level

Table 7-1. Areas vulnerable to sea level rise

Elevation (masl)	Area (km^2)
0	19862
1	7499
2	6291
3	6709
4	9142

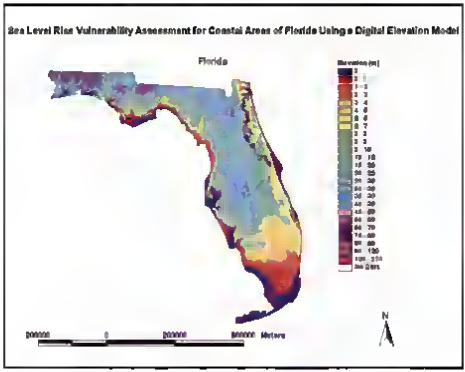

Figure 7-2. Vulnerability of Coastal Areas in Florida.

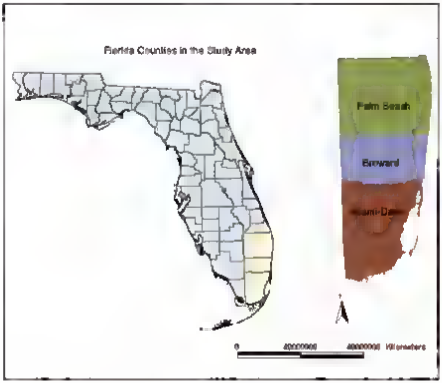

Figure 7-3 Counties of Florida included in the detailed study

The three counties shown in Figure 7-3 each were analyzed using a 30 m cell DEM. The length of coastline for each of these counties is tabulated in Table 7-2.

Table 7-2. Length of coastline for counties in the study area.

County	Coastal Length (m)
Palm Beach	779735
Broward	860927
Miami-Dade	1466769

The School of Marine and Atmospheric Sciences at the University of Miami has studied the impact of sea level rise on the coastal areas of Florida. The estimates suggest that sea level rise along the Florida's shoreline has accelerated at a rate of approximately 20 to 40 centimeters (8 to 16 inches) per century since 1932. This figure is more than six

times the rate recorded by earlier tide-gage records and estimates from the geological history of the past three thousand years The relative sea level rise along the shorelines of Florida is presented in Table 7-3 Relative sea level accounts for factors such as shoreline degradation, subsidence and other geological instabilities, and is therefore larger than eustatic sea level

Table 7-3 Estimated rates of relative sea level rise for selected sites in Florida

Location	Rate (cm/century)	Rate (in/century)
Key West	25.0	9.8
Miami Beach	24.0	9.4
Cedar Key	14.0	5.5
Fernandina Beach	22.1	8.7
Mayport	19.1	7.5
St. Petersburg	30.0	11.8
Pensacola	24.1	9.5

The Center for Operational Oceanographic Products and Services (CO-OPS) is the part of the National Oceanic and Atmospheric Administration (NOAA) responsible for collecting analyzing and distributing historical and real time observations and predictions of water levels coastal currents and other meteorological and oceanographic data. The water level records registered by the CO OPS stations are a combination of the fluctuations of the ocean and the vertical land motion at the location of the station. The sea level variations determined are the linear trend, average seasonal cycle, and inter-annual variability at each station. Mean sea level trends for selected stations in south Florida are presented in Table 7-4 Monthly data up to the end of 1999 were used in the calculation, and all stations had data spanning a period of 25 years or more.

Table 7-4 Mean sea level trends for stations in south Florida.

Station ID	Station Name	Mean Sea Level Trend (mm/year)	Standard Error (mm/year)	Mean Sea Level Data Duration
8723170	Miami Beach	2.39	0.22	1931-1981
8720030	Fernandina Beach	2.04	0.12	1897-1999
8720220	Mayport	2.43	0.18	1928-1999
8723970	Vaca Key	2.58	0.44	1971-1999
8724580	Key West	2.27	0.09	1913-1999
8725110	Naples	2.08	0.43	1965-1999
8725520	Fort Myers	2.29	0.45	1965-1999
8726520	St. Petersburg	2.4	0.18	1947-1999
8726724	Clearwater Beach	2.76	0.65	1973-1999
8727520	Cedar Key	1.87	0.11	1914-1999
8728690	Apalachicola	1.53	0.58	1967-1999
8729108	Panama City	0.3	0.64	1973-1999
8729840	Pensacola	2.14	0.15	1923-1999

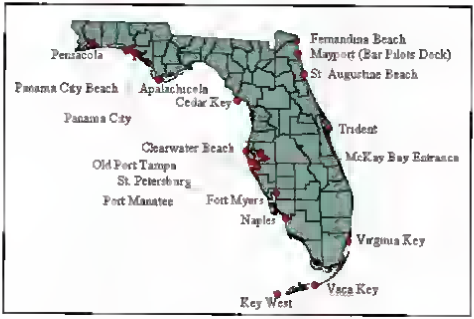

Figure 7-4 National Oceanic Service water level observation stations in Florida.

Observing the mean sea level trends presented in Table 7-4, it is clear that the mean sea level for coastal areas of Florida has been rising on average by about 2 mm per year

since the 1930s. When the observed local trend is combined with the eustatic sea level rise estimated by Global Circulation Models the corresponding estimates of probable relative sea level rise are obtained. The mean monthly sea level observations collected by the CO-OPS stations in Florida are presented in Figure 7-5. The values were averaged monthly from hourly tide records observed at the respective stations. The mean sea water level is defined with respect to the Mean Lower Low Water (MLLW). The MLLW is a tidal datum defined by the average of the lower low water height of each tidal day observed over the National Tidal Datum Epoch. For stations with shorter series simultaneous observational comparisons are made with a control tide station in order to derive the equivalent datum of the National Tidal Datum Epoch. The (NTDE) is a specific 19-year period over which tide observations are taken to determine Mean Sea Level and other tidal datums such as Mean Lower Low Water and Mean High Water. The latest update defines the 19-year period as 1983-2001. A tidal datum is a vertical reference based on a specific stage of tide, which serves as a baseline elevation to which sounding depths or topographic heights are referenced. The 19-year period includes an 18.6 year astronomical cycle that accounts for all significant variations in the moon and sun that cause slowly varying changes in the range of tide. The NTDE has been adopted so that tidal datum determinations throughout the United States will be based on one specific common reference period.

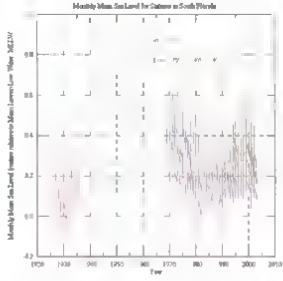

Figure 7-5 Monthly Mean Sea Level plot for stations in South Florida.

The monthly mean sea level plot presented in Figure 7-5 shows that there is a gradual rise for all the stations through the years of record. Comparatively, the highest trend in rise is near the Miami Beach and Biscayne Bay area. Estimates of relative sea level rise for select stations were performed using the trend values and all scenarios. The results presented in Figure 7-6 show a gradual rise of about 0 4 to 0 6 m depending on the specific scenario selected. A middle of the range value is obtained by scenario A1T, which has a reasonable probability of occurrence.

The study conducted and the results obtained clearly demonstrate that sea level rise will result in enhanced coastal erosion, coastal flooding, loss of coastal wetlands, and increased risk from storm surges, particularly in Florida and much of the U S Atlantic coast. This could be expected with a relatively high level of confidence especially given the unique topography of the coastal areas of Florida and the Atlantic coast

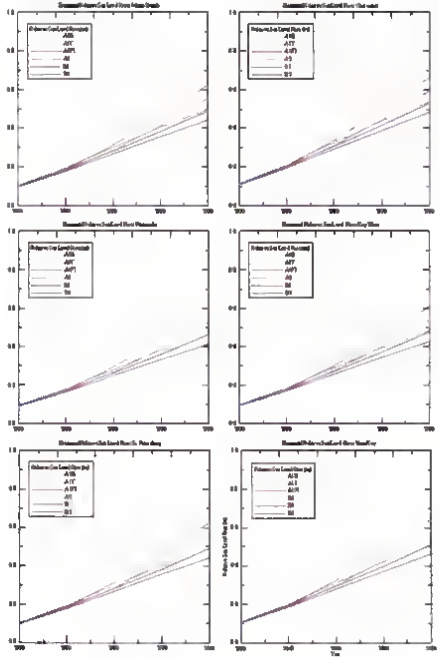

Figure 7-6 Estimated relative sea level rise for stations in Florida.

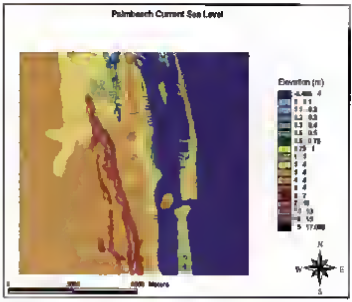

Figure 7-7 Current sea level for Palm Beach coast.

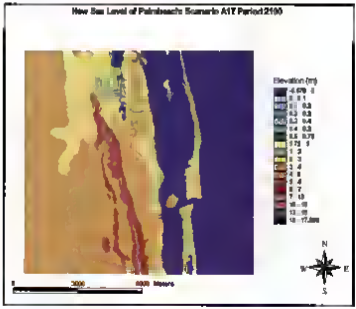

Figure 7-8 Palm Beach coast sea level forecast for the year 2100

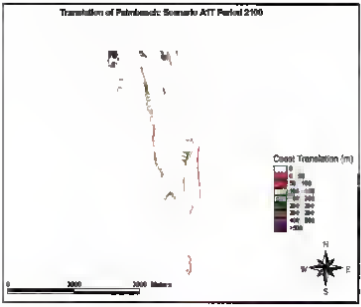

Figure 7-9 Palm Beach shoreline translation forecast for the year 2100

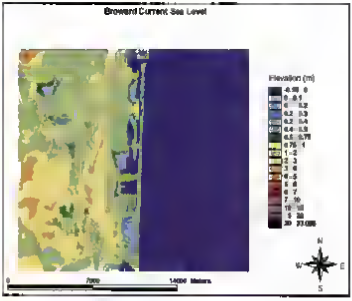

Figure 7-10 Current sea level for Broward coast

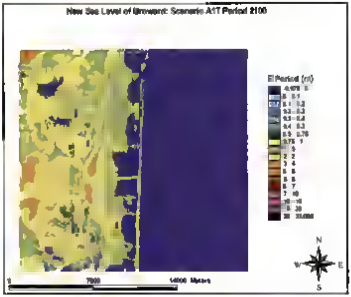

Figure 7-11 Broward coast sea level forecast for the year 2100

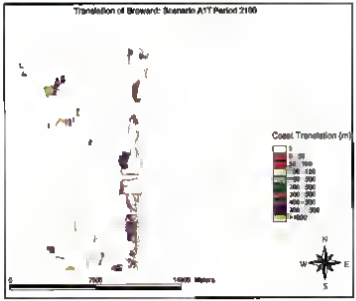

Figure 7-12 Broward shoreline translation forecast for the year 2100

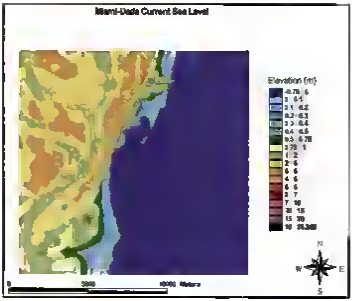

Figure 7-13 Current sea level for Miami-Dade const

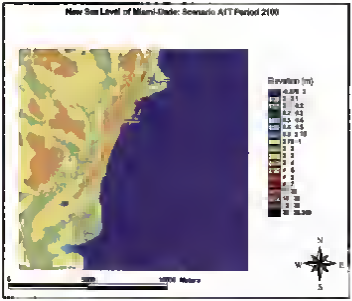

Figure 7-14 Miami-Dade const sea level forecast for the year 2100

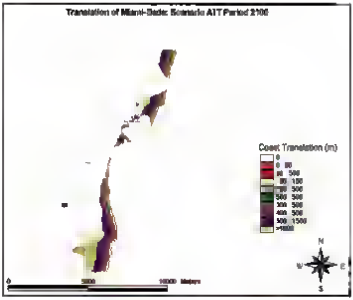

Figure 7-15. Miami-Dade shoreline translation forecast for the year 2100.

Scenario A1T being a mid-range scenario was chosen for further analysis; however, it has to be noted that the development of the IPCC scenarios, which is based on the SRES, does not place a likelihood or probability of occurrence on any of the scenarios. It is therefore suggested that any research to investigate the impacts of sea level rise should recognize the inherent uncertainties of long-term projections. While these projections provide a long-term context for the analysis of change expected to happen in the relatively near-term, the detailed analysis should consider the localization of the problem in greater details. As a result, the projections presented in the previous plots and in Table 7-5 should not be interpreted as "what is bound to happen." Instead, they should be interpreted as "what could happen." Moreover, the calculation of shoreline translation has to be done at a much smaller scale in order to account for the existence of localized infrastructures and mitigation impacts. The shoreline translation presented in Table 7-5

presents the maximum translation that could be expected for a given shoreline slope and the chosen scenario

Table 7-5 Estimates of shoreline translation for select slope values using extrapolated scenario A1T

Scenario A1T	Year							
	2025	2050	2075	2100	2125	2150	2175	2200
	Sea Level Rise (m)							
	0.152	0.281	0.423	0.576	0.742	0.919	1.109	1.311
Slope (%)	Shoreline Translation (m)							
0.1	152	281	423	576	742	919	1109	1311
0.2	76	141	211	288	371	460	555	655
0.3	51	94	141	192	247	306	370	437
0.4	38	70	106	144	185	230	277	328
0.5	30	56	85	115	148	184	222	262
0.6	25	47	70	96	124	153	185	218
0.7	22	40	60	82	106	131	158	187
0.8	19	35	53	72	93	115	139	164
0.9	17	31	47	64	82	102	123	146
1.0	15	28	42	58	74	92	111	131

Application of SEAWATSLR

The modified seawater intrusion code was used to model groundwater flow in select coastal aquifer cases and the results are compared with a no sea level rise scenario The models include a cross-sectional model from south Florida and a three-dimensional model from the Silifke Delta in Turkey

Due to the volume of work involved primarily due to the transient nature of the study and the limitation of space to present the results only one climate change scenario was used in the simulations. The A1T scenario that represents the mid-range was used for all the cases The results presented in this chapter show a comparison of simulations at the end of 20 years and 100 years from present. The transient simulations in between are plotted at 20 year intervals and presented in the appendix

Since analysis of this nature primarily focuses on changes in parts of the aquifer subject to saltwater intrusion, it becomes necessary to define a parameter that describes the spatial extent of changes in concentration for transient simulations. For the purpose of this analysis, a parameter here after referred to as zone of influence is used. A zone of influence is defined as part of the aquifer that will be subject to significant changes in terms of aquifer salinity due to transient changes of stresses. The zone of influence is characterized by a dimensionless aquifer salinity change ratio. The difference in monitored concentration at a given location x between time steps t and $t+1$ is given as

$$C_x^{(t)\Delta(t+1)} = C_x^{(t+1)} - C_x^{(t)} \tag{7-1}$$

while the dimensionless number of the zone of influence is given as

$$\overline{C}_x^{(t)\Delta(t+1)} = C_x^{(t)\Delta(t+1)} \Big/ C_{x\max} \tag{7-2}$$

Cross-Sectional Model

The cross-sectional model was originally developed to simulate the groundwater discharge patterns near the coast of Biscayne Bay (Langevin, 2001). The study area is part of the surficial aquifer system in south Florida. A brief description of the hydrogeology and stratigraphy documented in the report (Langevin, 2001) is presented here to give background information of the area.

South Florida presents unique hydrologic features primarily due to the dynamic interaction between surface water and groundwater. Rainfall and evapotranspiration in the area are generally high with marked seasonal variability of rainfall. For the study area, the average rainfall for the period from January 1989 to September 1998 was about 141 centimeters per year. About 75 percent of the rainfall was recorded during the wet

season that extends from June to October. Direct measurements of evapotranspiration in parts of South Florida resulted in a range of 122 to 130 centimeters per year. Although the measurements may not be representative of the entire southern region of Florida, the rates of ET are as high as 90 percent of the rainfall in some parts.

The hydrostratigraphy of southern Florida is primarily composed of the shallow surficial aquifer systems and the deeper Floridan aquifer system. As observed from the water table maps presented in the report (Langevin, 2001), the general flow of ground water is toward the coast, thus implying that the primary hydrologic component that enables the aquifer to maintain the water table is net recharge from rainfall. The Biscayne aquifer, which is part of the surficial aquifer system, consists of porous limestone from the Pliocene to Pleistocene epochs. The stratigraphic map of Florida created from data obtained from Florida Geological Survey is presented in Figure 7-17. A map showing the relations of geologic formations, aquifers, and semi-permeable units of the surficial aquifer system across central Miami-Dade County is presented in Figure 7-18 (Source: SOFIA website: http://sofia.usgs.gov/publications/wri/00-4251).

Coconut Grove

The Coconut Grove model modified as part of this research represents the coastal aquifer south of Miami in Miami-Dade County. The cross-section extends for 5,900 m inland and 2,100 m towards the sea. The base of the model extends to 40 m below sea level. For the model discretization, a uniform column width of 200 m and uniform layer thickness of 2 m were used. The model has a constant head boundary on the seaside and a constant flux boundary on the inland side. The freshwater head for the constant head boundary cells was calculated from a downstream stage value of 0.22 m, which represents an average value for sea level from 1989 to 1998. A net recharge value of 38

cm/yr was assigned to the overlying recharge boundary A constant seawater concentration of 35 kg/m^3 was used for the seaside boundary The model calibration data was obtained from the USGS, and on the basis of the calibration results, the following parameters were used for the simulation

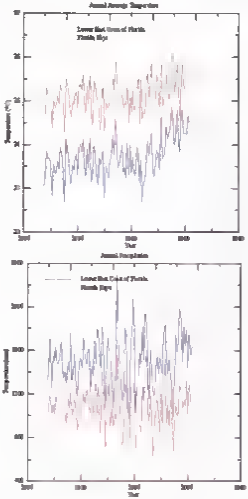

Figure 7-16 Time series plot of annual temperature and precipitation for lower east coast of Florida and Florida Keys

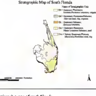

Figure 7-17 Stratigraphic map of south Florida.

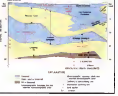

Figure 7-18 Relations of geologic formations, aquifers, and semi permeable units of the surficial aquifer system across central Miami-Dade County

Table 7-6 Model parameters used for Coconut Grove simulation

Model Parameter	Unit	Value
k_h (horizontal hydraulic conductivity)	m/day	9000
K_v (vertical hydraulic conductivity)	m/day	9
α_L (longitudinal dispersivity)	m	1
α_T (transverse dispersivity)	m	0.1
n_e (porosity)	dimensionless	0.2
Q/m (flux)	$m^3/d/m$	15
R, (net recharge)	m/yr	0.38
S_s (specific yield)	dimensionless	0.2

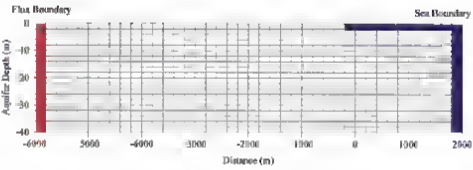

Figure 7-19 Discretization of Coconut Grove model

In order to establish a more realistic initial condition, a simulation was run for one million years using SEAWAT. Performing the simulation for such a long period made it possible for the system to attain a state of dynamic equilibrium. The hydraulic head and concentration values at the end of the million years simulation were used as initial conditions to perform simulations for the next 100 years. Simulations were run for a total of 100 years assuming uniform recharge and flux values to persist throughout. The constant head coastal boundary condition was modified to be time variant for the simulation using SEAWATSLR. The A1T sea level rise scenario was assumed, which resulted in a sea level rise of about 0.5 m by the year 2100. The transport component was solved using the method of characteristics. The results show a change in the position of

the transition zone due to the inclusion of a sea level rise component in the constant head boundary. Monitoring wells were introduced along the transition zone and hydrographs of concentration were plotted to see the transient change in the ambient concentration. The simulations were performed with steady values of parameters and no additional pumping stresses. The purpose of this approach was to see the response of the system to natural conditions.

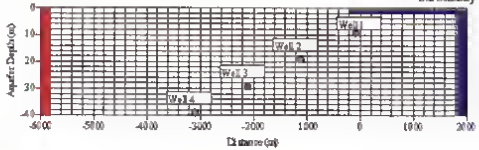

Figure 7-20 Location of monitoring wells.

The monitored concentration values plotted in Figure 7-21 exhibit changes in concentration due to sea level rise. The changes as presented in Figure 7-22 vary with the location of the monitoring wells. The general trend is that the rate of change tends to decrease as the monitoring location is further inland.

In order to have a more realistic initial condition, a no-sea level rise simulation of 5,000 years performed. The final concentration and head values were used to define the initial condition for the 100 years simulation of the period until the year 2100. The profiles of concentration were plotted for the entire period of simulation at specific time intervals by exporting the data to Surfer® and kriging to create contours. In order to identify the areas that will be subject to significant changes due to variability of stresses, the zones of influence were also plotted for the same time periods. The results show that

the portion of the aquifer that will be subject to significant changes due to sea level rise under natural conditions is the area that extends from 3,000 m to about 4,200 m inland. The areas extending from the shore up to 3,000 m inland will be subject to moderate changes in concentration under the conditions. The practical implication of this analysis is that, the better location of pumping wells from the seawater intrusion point of view would be areas farther than 4,000 m from the shore.

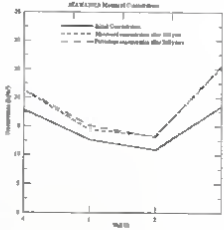

Figure 7-21. Plot of monitored concentrations for Coconut Grove monitoring wells.

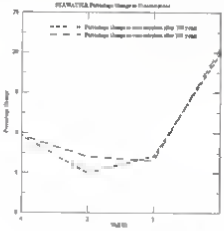

Figure 7-22. Plot of percent changes in monitored concentration due to sea level rise

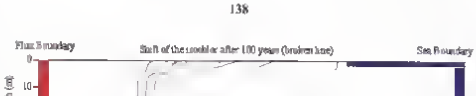

Figure 7-23. Profile of concentration after 100 years for Coconut Grove.

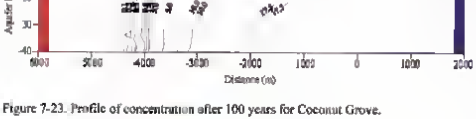

Figure 7-24. Zone of influence after 100 years.

In the plots of concentration from the monitoring wells, there is a noticeable fluctuation in values over the simulation period. In order to understand the phenomena, groundwater flow velocity and discharge were plotted for the cross-section. The results show that groundwater-seawater flux exchange occurs underneath the coast resulting in the observed oscillations in monitored concentration from wells close to the coast. The observed oscillations tend to dampen as the wells are located farther away from the coast. Accordingly, well 1, which is the closest to the surface, exhibits the highest oscillation, while well 4 exhibits the least oscillation. The groundwater discharge generally occurs

towards the sea while there is an inflow of seawater in the area adjacent to the sea. The plots of horizontal flow velocity and discharge are presented in Figures 7-25 and 7-26

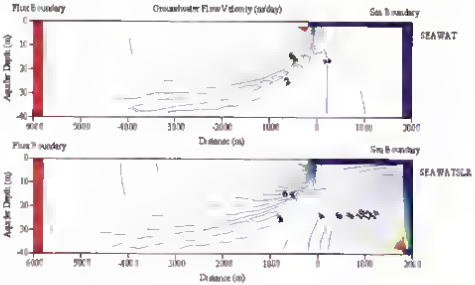

Figure 7-25 Horizontal flow velocity at the end of 100 years simulation.

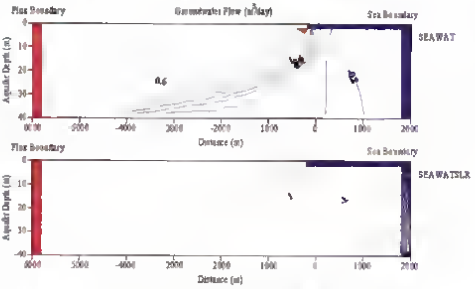

Figure 7-26 Groundwater flow at the end of 100 years of simulation.

The contours of head plotted in figure 7-27 show an increase due to the sustained sea level rise. The gradient, however, still follows the same trend with decreasing head values towards the coast. In the scenario where sea level rise was not considered, the contours tend to rise with a mild slope after the active zone of exchange, while in the sea level rise scenario the rise appears to be slightly higher. This increase shows the response of the constant head boundary and its significance in influencing the flow pattern.

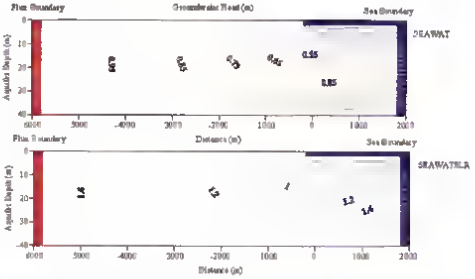

Figure 7-27. Profile of head at the end of 100 years simulation.

Three-Dimensional Model

The three-dimensional model presented in this study represents a deltaic aquifer close to the Mediterranean coast of Turkey. The available data for this model was very insufficient, and thus some approximations were made about the stratigraphy of the aquifer. The primary form of aquifer data was generated from digitized topographic maps and hand sketches of cross-sections obtained from geologists who have some

knowledge of the area. Some data on water use, aquifer water conductivity, and river stage were also obtained. Although the data were sparse and insufficient, care was taken to represent the current condition.

The conductivity data were converted to total dissolved solids (TDS) using appropriate regression equations. A two dimensional simulation of the Goksu Delta aquifer was performed earlier (Gordu, 2000). The study included determination of some aquifer parameters that helped in the development of the three dimensional model used in this study.

Goksu Delta at Silifke

The Goksu Delta is predominantly an alluvial deposit formed by the Goksu River, which is about 260 km long and has a drainage area of 10, 400 km^2. The Delta has an area of about 150 km^2 with a semi-arid Mediterranean climate (Gordu, 2000). The Goksu River with an annual average discharge of about 9.5 million m^3/day is a significant component of the hydrology of the delta. There are two lakes of significance in the delta namely Akgol and Paradeniz. Akgol is a freshwater lake with an area of about 12.45 million m^2 while Paradeniz is a saltwater lake with an area of about 4.05 million m^2. There is a man-made canal that connects the two lakes. The area is an agricultural area with water demands for both irrigation and water supply of the population.

The primary source of geologic data used by Gordu (2000) and the current case study is the hydrogeologic investigation conducted by Haar and Heunks (1992). The results of their investigation included lithological profiles from which it was concluded that the coarse grained medium ranging from 30 to 130 m in depth is the aquifer with connections to the adjacent karstic formations and intermediate thin layers of clay.

The investigation also included collecting both surface and ground water samples from which a water table map was constructed for the surficial phreatic aquifer. Based on the map there is a hydraulic gradient towards the sea where the water table is almost at sea level. The deeper aquifers are confined by an overlying semi-permeable clayey confining zone. It is also mentioned by Gordu (2000) that Menengic (1998) conducted a study about the potential risks of groundwater pollution in the Goksu delta. On the basis of the results documented by Haar and Heunks (1992) and Menengic (1998), Gordu (2000) presented a stratigraphic classification of the Goksu Delta. The classification is adapted in this study and presented in Table 7-7.

Table 7-7 Stratigraphic classification of the Goksu Delta (adapted from Gordu, 2000)

Epoch	Period/Stratigraphic Unit	Approximate thickness (m)	Lithology
Holocene and Recent	Quaternary sediments	3-4	Loose sand, silt
		20-25	Thin layers of different textured materials, mostly silt, sand, clay, silty clay and sandy clay
Pleistocene	Quaternary sediments	>130	Thick layers of fine and coarse material enclosed by thin clayey layers. Sand, gravel, clay, clayey sand
Pliocene	Tertiary deposits	Not available	Silty limestone
Miocene	Not available	750-800	Claystone, mudstone, limestone, and Miocene carbonate rock
Cretaceous	Not available	Not available	Carbonate rocks
Jurassic	Not available	Not available	Carbonate rocks
Devonian	Not available	Not available	Shale, sandstone conglomerates, quartzite, and reef limestone

Previous studies have estimated the hydraulic conductivities to range from 4 to 500 m/day in the horizontal direction and from 0 05 to 27 m/day in the vertical direction, and, thus, the aquifer is relatively homogeneous and anisotropic The dispersivity of an aquifer is a parameter known to be dependent on the scale of the flow model length along which the parameter is defined. Depending on the geometry of the cross-section, values of 1000 m and 50 m were used respectively in the study by Gordu (2000)

The spatial discretization of the model is based on a finite difference grid of 42 rows, 38 columns and 20 layers The spacing of the columns is kept at 500 m while the layer thickness is variable with maximum depth extending to 700 m below sea level. The boundaries include a constant head boundary with constant sea water concentration of 39 4 kg/m^3 (representative of the Mediterranean sea), a no-flow boundary that extends from northwest to southeast of the model area defining the bedrock, a general head boundary for the inland portion of the aquifer in the northwest, lakes and a network of drains The stage for the river and drains was set from elevation and stage data available For the purpose of detailed analysis, monitoring wells were strategically located close to the boundary and surface water features. The constant head boundary is set to extend for 500 m everywhere. Perhaps with the availability of bathymetric data in the future, this boundary will have to be specified differently. At this stage, the model is based on a coarse grid, which may have to be modified in the future with the availability of more geophysical and hydrologic data. The spatial discretization of the model is presented in Figure 7-28, and the model boundary features are presented in Figure 7-29 The model parameters used in the Sillifke model are presented in Table 7-8

In order to analyze the results of simulation for the Goksu Delta aquifer, two cross-sections were considered. The first cross-section (section Y-Y) was along row 20 with an east-west orientation, while the second cross-section was along column 19 (section X-X) with a north-south orientation.

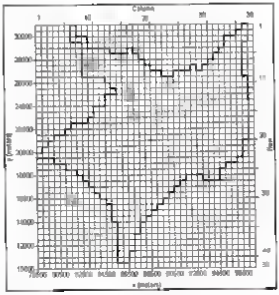

Figure 7-28 Spatial discretization of the Goksu Delta model

Table 7-8 Model parameters used for Silifke simulation.

Model Parameter	Unit	Value
K_h (horizontal hydraulic conductivity)	m/day	200
K_v (vertical hydraulic conductivity)	m/day	0.05
α_L (longitudinal dispersivity)	m	100
α_T (transverse dispersivity)	m	100
n, (porosity)	dimensionless	0.1
Q/m (flux)	$m^3/d/m$	0
R_n (net recharge)	m/yr	0-1.00375
S_y (specific yield)	dimensionless	0.1

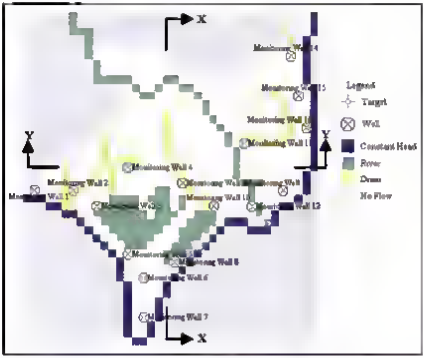

Figure 7-29 Hydrologic features used in the Goksu Delta model location of monitoring wells and cross-sections

The simulation results are presented in the form of cross-sectional plots along both directions Zones of influence were also constructed from the cross-sections considered. Plots of monitored concentration versus time are also presented to see the evolution of concentration through time at a given location

Contours of equivalent freshwater head are also plotted for the cross-sections considered and the transient variability is compared for both scenarios. Contours of equivalent freshwater head are also plotted for the first layer. This makes it possible to observe the gradient of the groundwater head and make some observations regarding the flow direction

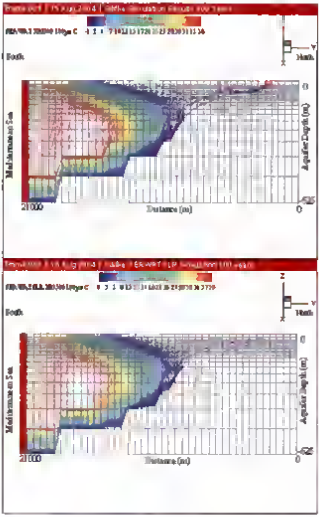

Figure 7-30 Concentration profile comparison along X-X after 100 years

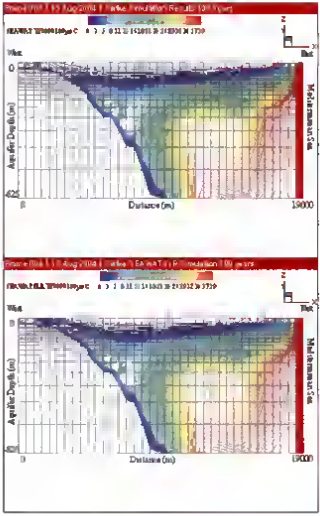

Figure 7-31 Concentration profile comparison along Y-Y after 100 years

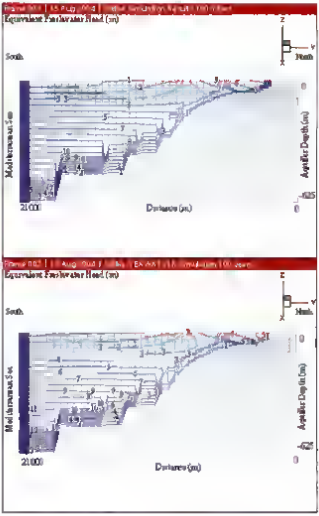

Figure 7-32 Equivalent freshwater head profile comparison along X-X after 100 years.

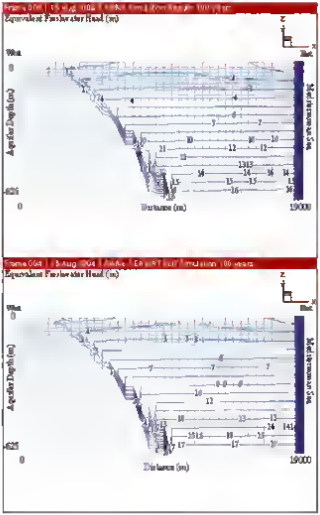

Figure 7-33 Equivalent freshwater profile comparison along Y-Y after 100 years.

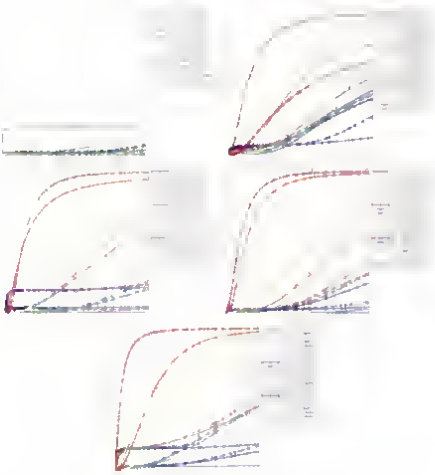

Figure 7-34. Plot of concentration vs time from Goksu monitoring wells after 100 years.

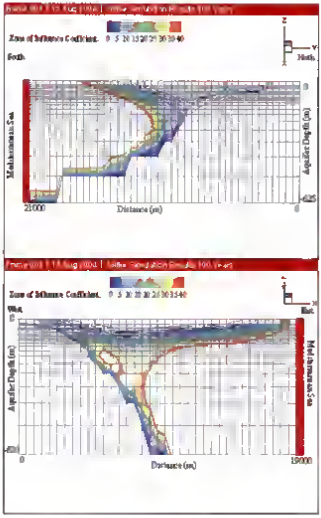

Figure 7-35 Zone of influence for Goksu Delta model along X-X and Y-Y after 100 years.

Observations from Figure 7-34 reveal that the difference in monitored concentration between the two scenarios tends to decrease vertically downwards. It is also observed that the lower layers reach higher values of concentration earlier than the upper layers. This is due to the density driven nature of flow that exchanges water between the sea and the ambient aquifer water. The fact that under steady stress

conditions the lower aquifers tend to reach a limiting value of concentration explains partially why the difference in concentration decreases vertically downwards. There are also localized concentration values above the maximum specified in the CHD suggesting deposition, but numerical dispersion seems the more likely cause. Similar phenomena of localized increase were observed in the simulation results of the Burdekin Delta in Australia[1] The simulations for the Burdekin Delta used the two-dimensional version of SUTRA

One interesting observation from the simulated concentration profiles is the significance of the geometry of the cross-section in influencing the shape of the transition zone profile Due to the existence of a no flow boundary with gradually decreasing extent, the shape of the transition zone exhibits a curvature that follows the geometry of the cross-section

As a result of the combination of the hydrodynamic and variable density processes induced by sea level rise parts of the aquifer that are expected to undergo significant changes in salinity are presented in Figure 7-35 Considering section X-X, the zone of influence extends from approximately 4,000 m from the seaside boundary With an average thickness of about 4,000 to 5 000 m it extends to about 400 m depth and starts a reversal due to the geometry of the no flow zone Considering section Y-Y, the zone of influence extends from about 1,500 inland to about 11,000 m where it expands significantly in the middle portion of the aquifer (about 200 to 400 m depth) and continues to thin out towards the west Therefore the influence of sea level rise on a century scale for Goksu Delta is not expected to be significant farther than about 5,000 m along X-X and 10,000 m along Y-Y

[1] Personal communication with Dr Kumar Narayan of CSIRO Australia November 2002

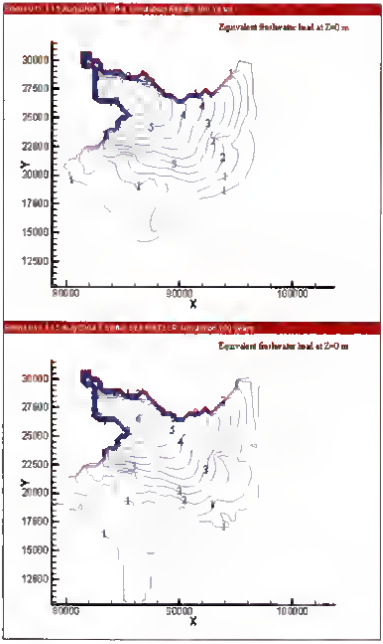

Figure 7-36 Simulated groundwater contours for Stiffke after 100 years

From the contour of groundwater observed from each layer the general flow trend is towards the sea with appreciable gradient oriented from northwest to southeast This is an indicative of groundwater discharge towards the Mediterranean Sea In order to confirm this theory it would be necessary to investigate the seasonality of the contours using data obtained from a network of monitoring wells. Also from the groundwater contour of layer1, the Goksu River appears to be a generally gaining river The results presented are to be used as preliminary simulation results obtained from a sparse data set, and therefore the Goksu Delta model needs to be refined in the future with more calibration work as additional data sets become available

Simulated Heads and Concentrations

The changes in simulated head and concentration values of a coastal aquifer system are the primary forms of the response to a rising sea level boundary The precise nature of the response could be described by a proper characterization of the seaside boundary General observations from the simulations performed make it possible to conclude that there is appreciable increasing trend in both simulated head and concentration due to sea level rise

In the current formulation of the constant head boundary component, the monitored head values are noted to respond to the linear increase of sea level rise However, if the increase in sea level is formulated to have an exponential trend the response is likely to be slightly different. The difference in head values between a no sea level rise scenario and the one that accounts for this is a factor of the rate of sea level rise incorporated in the simulation. Since the sea level rise scenario simulations are based on a futuristic assumption based on a number of factors, it is not possible to calibrate the model for a given scenario. It could also be argued that the linear increase in monitored head values

could have a different characteristic by introducing a distance dependent propagation factor. One way of determining this factor would be to conduct a controlled laboratory experiment where a static saltwater water column serves as a seaside boundary. This setup is similar to the analog models used by researchers a few decades ago. The results of this type of experiment will help determine the variation in monitored heads in response to a rise in the static water head. By applying appropriate similitude analyses, the results could be used to further refine the numerical model developed in this study. In any case, the fact remains that the time variant constant head boundary plays a significant role in influencing the flow regime and simulation values.

Shift of the Seawater-Freshwater Interface

Under steady natural stress conditions where there is no freshwater withdrawal, the shift of the seawater-freshwater interface is brought about by the dynamic interaction between the seawater and freshwater. The primary driving force in the vicinity of the coast appears to be the advective flux as it is observed in the flow velocity and groundwater discharge vectors. Traversing farther inland along a cross-section, the dispersive component begins to take effect resulting in appreciable spread in the transition zone.

The Impacts of Sea Level Rise on Groundwater Flow Regime

The general impact of sea level rise on the groundwater flow regime is characterized by the creation of a very active mixing zone close to the coast. In this zone, seawater enters at the bottom of the aquifer driven by the hydrostatic pressure variation and the density difference. After mixing with the ambient aquifer water, the general hydraulic gradient results in discharge of water towards the sea. In the long run, this process tends to shift the interface further until a state of dynamic equilibrium is reached.

Since aquifers are also subject to additional stresses such as pumping, it is rather difficult to say exactly how long it takes the aquifer to reach this state of dynamic equilibrium. Results obtained from a simulation performed for a period of 3,000 years were plotted and analyzed. The plots of monitored concentration versus time exhibited a steady state after approximately 2,500 years for most of the layers. Even after 3,000 years, there are portions of the aquifer that have not attained dynamic equilibrium as it is seen in layers 6 7 8, and 11. Based on this observation it appears that under natural constant stress conditions, the aquifer is likely to take much longer than 3 000 years to reach the state of dynamic equilibrium. When the impacts of a dynamic sea level change and pumping are included, the variation in aquifer stress is aggravated, thus increasing the time required to attain dynamic equilibrium

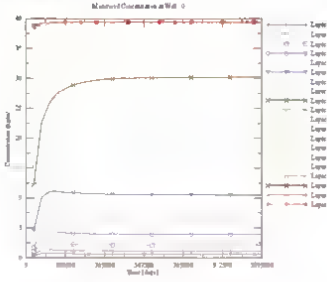

Figura 7-37 Monitored concentration at well 10 after 3000 years simulation.

The sensitivity of aquifers to sea level rise and the impact thereof are governed by a number of factors. One such factor is geometry of the aquifer. Aquifers with smaller

geometries are likely to undergo dynamic changes relatively faster than aquifers of larger geometry. The second factor is the inherent aquifer properties primarily hydraulic conductivity and transmissivity. Aquifers with smaller transmissivity values are likely to take longer to respond to changes in sea level.

The time required for a semi-confined or confined aquifer as compared to an unconfined aquifer is relatively shorter in small-scale modeling. In a regional scale modeling, this response time is generally within the scale of centuries. In effect, the impact of a sea level rise of 0.5 m is felt after many decades. Even the impossible condition of a sudden sea level rise is not likely to result in sudden rise in aquifer salinity due to the nature of groundwater flow velocity. The actual groundwater flow velocity is governed by the porosity of the medium and porosity also plays a significant role in the process. In coastal aquifers where there is a possibility of secondary porosity due to fracturing or if there are sedimentary deposits where localized reactions result in solution channels where the flow may not necessarily be governed by Darcy's law, the process is expected to be accelerated.

Based on the observations from the various simulations performed to understand the process of saltwater intrusion and the factors that govern it, generalized qualitative observations were made. The observations are plotted in Figure 7.38 to describe the significance with time. The impacts are classified as high, moderate, or low and the time scale is presented in a scale ranging from century to millennia. The figure depicts the trend of response in terms of aquifer salinity.

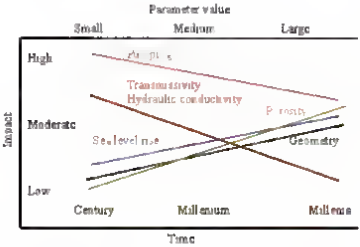

Figure 7-38 Schematic presentation of trend of response of coastal aquifers to stress impacts.

The interpretation of the qualitative description presented in Figure 7-38 is as follows. Pumping is a major factor in the process, and as a result it has higher impacts on a century scale. However if pumping is continued at a given rate for a longer time the aquifer will eventually reach the state of dynamic equilibrium on a time scale of millennia at which time the rate change becomes smaller. Even if pumping is increased throughout, there will be a point where the aquifer becomes completely saline or dry as the case may be and the pumping will have no additional impact to measure.

Aquifers with higher transmissivity and hydraulic conductivity values are likely to attain a state of dynamic equilibrium within centuries. On the other hand aquifers with smaller transmissivity values might take millenia to do the same. Porosity of an aquifer on a time scale of a century may not result in significant influence on the state of dynamic equilibrium. But on a scale of millennia it is likely to have a moderate effect in

inducing dynamic equilibrium especially if a time scale is long enough for factors such as secondary porosity to take effect.

The geometry of the aquifer has a low but significant influence on the state of dynamic equilibrium on a time scale of a century. As time scale increases this influence also increases. For example if two aquifers of the same hydraulic parameters are set to have different geometries where one is larger and the other is smaller, then the smaller geometry aquifer is likely to respond faster in terms of dynamic equilibrium compared to the larger geometry aquifer.

Model Sensitivity Analysis

Sensitivity analysis performed to evaluate the significance of the various aquifer parameters and boundary conditions makes it possible to see how the various parameters influence the flow regime. The parameters used in the sensitivity analysis were hydraulic conductivity, flux boundary, dispersivity, recharge and pumping. The cross-sectional models developed for the sensitivity analysis were all variations of the surficial aquifer model explained earlier. For the pumping sensitivity analysis, five pumping wells were located at equal distances from each other as shown in Figure 7-39. All sensitivity analyses were performed for a period of 100 years using the A1T sea level rise scenario.

The hydraulic conductivity of the models was modified for a homogeneous aquifer. Similarly, tests for heterogeneity were performed by changing the orientation of the individual layers. Layers of varying hydraulic conductivity were first arranged horizontally and then vertically (see Figure 7-40).

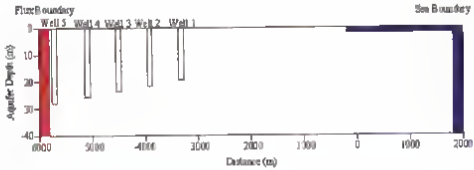

Figure 7-39 Location of pumping wells for sensitivity analysis.

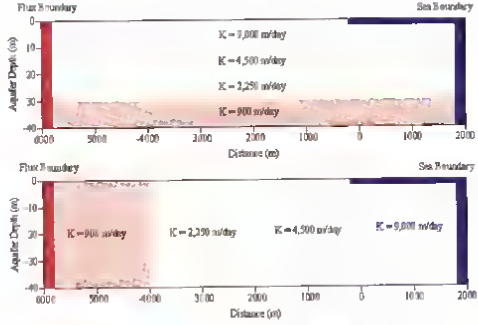

Figure 7-40 Representation of heterogeneous layers for sensitivity analysis

The shift in the interface was plotted for select values of horizontal hydraulic conductivity K_h. The results show that increase in K_h has moderate effect on the simulated concentrations and heads. Increasing the value of K_h from 90 m/day to 9000 m/day resulted in shift of the 0.1 isochlor by about 3500 m inland (see Figure 7-41). Similarly reducing the values of K_h shifts the interface towards the seaside boundary

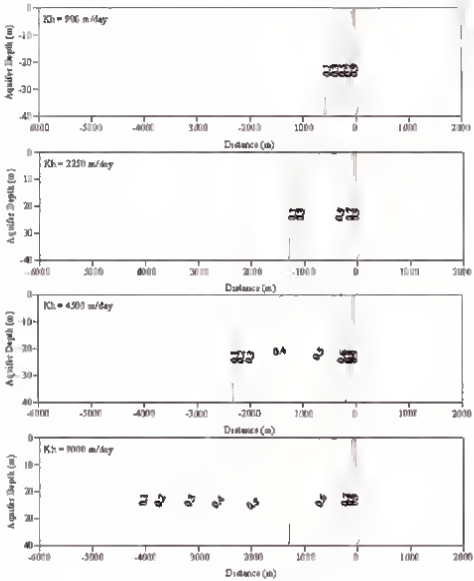

Figure 7-41 Sensitivity plots for horizontal hydraulic conductivity

The sensitivity to K_H is noticed to be more significant on isochlors less than 0.5 as it is observed in Figure 7-41. For higher values of isochlors, especially close to 0.95, the change seems to be insignificant as the isochlors are held at the coast. Thus, lower values

of K_h will result in a narrower transition zone for the same set of aquifer parameters and boundary conditions. Vertical hydraulic conductivity K_v doesn't seem to have significant effect on the simulated concentration values (see Figure 7-42). The isochlors shifted very little for a change in values of K_v ranging from 1 m/day to 90 m/day.

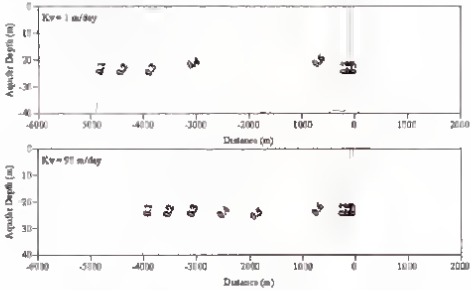

Figure 7-42. Sensitivity plots for vertical hydraulic conductivity

Sensitivity to aquifer heterogeneity was also tested for horizontal and vertical layers of varying hydraulic conductivities as described in Figure 7-40. As observed in Figure 7-43, the vertically layered heterogeneous aquifer exhibited appreciable results in minimizing the shift of the isochlors farther inland. The horizontal layering performed comparably well, although it was not as significant as the vertical layering. The practical significance of creating physical barriers either from impervious materials or layers of very low hydraulic conductivity is a method being investigated by researchers. The creation of physical barriers helps to mitigate the impacts of seawater intrusion by blocking the advancing saltwater front.

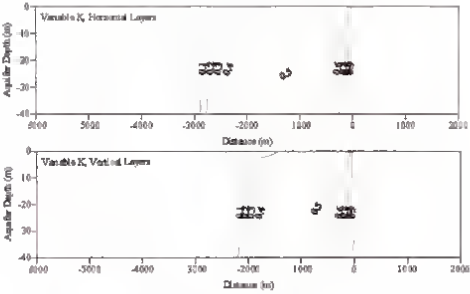

Figure 7-43 Sensitivity plots for aquifer heterogeneity

Sensitivity to flux boundary was tested by modifying the specified flux boundary on the left hand side of the model. As observed in Figure 7-44, increasing the magnitude of flux resulted in shifting of the isochlors seaward. For a flux of 15 m^3/day/m of coastline the 0.1 isochlor was at a distance of about 4100 m while increasing the flux magnitude by from 15 to 30 m^3/day resulted in shift of the 0.1 isochlor by about 1 000 m towards the coast. Decreasing the flux magnitude had the opposite effect on the isochlors and they shifted inland. The isochlors less than the 0.6 are observed to be more sensitive while the ones close to 0.95 seem to be locked at the coast. Comparatively the influence of increasing flux is a similar to reducing horizontal hydraulic conductivity and vice versa.

From the flux boundary sensitivity analysis, it is also possible to deduce the significance of a hydraulic barrier in mitigating the impact of saltwater intrusion. If an aquifer already subject to saltwater intrusion is injected with freshwater, then it is

possible to slow down the process of aquifer salinization. In fact, it is possible to reverse the process of salinization by creating a hydraulic block (Tiruneh and Motz, 2003)

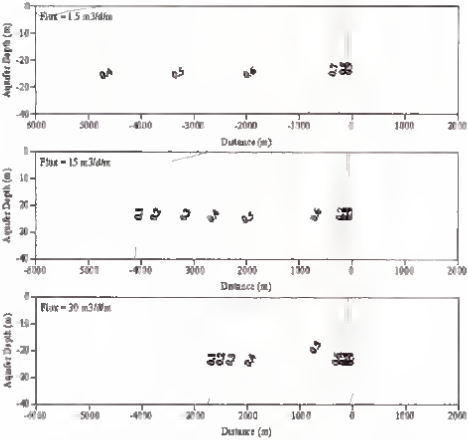

Figure 7-44 Sensitivity plots for flux boundary

Longitudinal dispersivity α_L was found to influence the salinity as its values were increased. The sensitivity exhibited a significant change as the values of α_L approached the rule of thumb values of about 1/10 of the length of the cross-section. With an increase in α_L, the salinity values tend to spread out further inland, especially within the 1/10 length range. Transverse dispersivity α_T on the other hand does not seem to affect the salinity values significantly. With increase in dispersivity, the isochlors tend to be

more straight and vertical. Also, when the dispersivity value was kept very low, the resulting concentration values exhibited hydrodynamic dispersion.

Two types of sensitivity analysis were performed to investigate sensitivity to recharge. The first was uniform recharge rate applied throughout the simulation period, but increased for different tests. The second was variable recharge rate that alternated between wet and dry decades during the entire simulation. For the first type of sensitivity analysis, a sustained uniform rate of recharge resulted in a shift of the isochlors seaward for increasing rates of recharge (see Figure 7-45). For the second type of analysis, which is more realistic compared to the first, no appreciable change in the position of isochlors was noticed.

It is understood that pumping plays a very significant role in the dynamics of saltwater intrusion. In order to quantitatively analyze the process the same aquifer was subject to varying pumping stresses. Five pumping wells were used to pump a total of 50, 500 and 5,000 m^3/day in three sensitivity tests. As observed in Figure 7-46, increasing the pumping rate to 500 m^3/day resulted in shift of the 0.1 isochlor by less than 500 m, while pumping at 5,000 m^3/day resulted in complete intrusion of the aquifer. During the pumping sensitivity analysis, the flux at the left hand boundary was kept at 15 m^3/day/m of seasthne, which is 3,000 m^3/day of flow for the 200 m cell width used. Accelerated intrusion was observed when the amount of pumped water exceeded the magnitude of flux. This type of sensitivity analysis in addition to other optimal management methods helps to determine the amount of water that could safely be withdrawn for use.

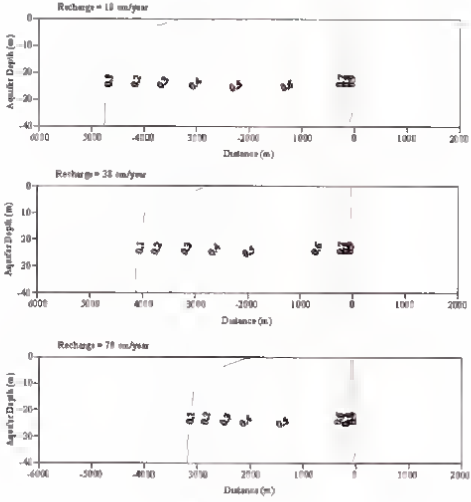

Figure 7-45 Sensitivity plots for uniform recharge

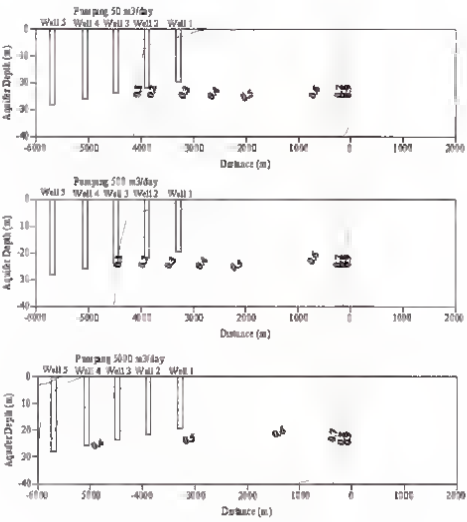

Figure 7-46. Sensitivity plots for pumping

Numerical Stability and Sensitivity to Solution Techniques

The solutions of groundwater flow and solute transport equations primarily depend on the accuracy and stability of the numerical methods used to approximate the governing flow and advection-dispersion equations. Experience has shown that solutions obtained from traditional finite difference methods quite often exhibit numerical damping

or spurious oscillations. This numerical dispersion could be brought about by more than one factor. The widely held opinion is that the numerical dispersion is caused by the inadequate approximation of the advection terms in the governing transport equation (Bear and Verruijt, 1987; Domenico and Schwartz, 1998; Zheng and Bennet, 1995). There are also some researchers who argue that the problem can also arise due to inaccurate approximation of the dispersive fluxes, more specifically, traditional finite difference methods like the ones used in MT3D, SEAWAT, RT3D can lead to significant unphysical oscillations and negative concentrations when dispersion is strongly anisotropic and the principal direction of anisotropy deviates significantly from the grid orientation (Bear, 1972; Bear and Bachmat, 1967; Domenico and Schwartz, 1998).

Numerical solutions of both the groundwater flow and transport equations are based on a number of solution techniques. Modeling techniques used to solve the flow and transport problems in the past include analog models, finite difference, finite elements, analytic elements, method of characteristics and random walk.

The finite difference method implemented in both MODFLOW and MT3DMS is used in SEAWAT as well. The finite difference approximation quite often exhibits numerical dispersion, which is caused by truncation of the terms that approximate the flow in the formulation. In order to ensure numerical stability and accuracy of the advection-dispersion solution certain stability analysis criteria need to be satisfied. One such criterion involves performing eigenvalue analysis.

In order to successfully complete a simulation, it is necessary to spend time experimenting with the various solution techniques and alter parameters to encourage convergence and minimize numerical dispersion. The general set of conditions for

convergence and minimal numerical dispersion are set in terms of flow velocity, flow time step, and aquifer spatial discretization. The discretization criteria used in SEAWAT are based on that of MT3DMS. The stability constraints and accuracy requirements for the transport of conservative species with the explicit finite-difference scheme as (Zheng and Wang, 1998)

$$\text{advection, } \Delta t \le \frac{1}{\frac{v_x}{\Delta x}+\frac{v_y}{\Delta y}+\frac{v}{\Delta z}}, \tag{7-3}$$

$$\text{dispersion, } \Delta t \le \frac{0.5}{\frac{D_{xx}}{\Delta x^2}+\frac{D_{yy}}{\Delta y^2}+\frac{D_{zz}}{\Delta z^2}}, \tag{7-4}$$

$$\text{sink/source } \Delta t \le \frac{\theta}{|q_s|}, \tag{7-5}$$

where Δt is the length of the time step, and Δx, Δy, and Δz represent the model cell dimensions in the x, y, and z directions. The stability criteria implemented in MT3DMS are given in equations 7-3 to 7-5. The inherent formulation of the explicit finite difference scheme allows the program to calculate the length of transport time step. The stability constraint for advection requires flow velocities in order to calculate transport step lengths.

If the implicit iterative procedure called the GCG (generalized conjugate gradient) solver is used, then the user has the option of specifying transport time step lengths. Although the implicit solver may reduce the number of transport steps required for a simulation, there will be limitations due to convergence and accuracy requirements. Generally the user has to specify smaller time steps in order to encourage convergence. Using the implicit scheme also requires observing the stability criteria set in terms of the

dimensionless grid Peclet number and Courant number which are given in equations 7-6 and 7-7

$$P_e = \frac{V\,\Delta x}{D_x} \leq 2 \tag{7-6}$$

$$C_r = \frac{V\,\Delta t}{\Delta x} \leq 1 \tag{7-7}$$

where V is flow velocity and D_x is dispersion coefficient. In advection dominated problems the Peclet number has to be kept sufficiently higher to ensure stability

The solution schemes provided in MT3DMS include Finite Difference (FD), Method of Characteristics (MOC), Modified Method of Characteristics (MMOC), Hybrid Method of Characteristics (HMOC), and Total Variation Diminishing (TVD) Generally the FD technique is faster to run and more vulnerable to convergence problems while the MOC, MMOC, and HMOC have slightly better sensitivity to numerical convergence and take longer time to run The ultimate method, TVD ensures convergence in many cases but takes a considerably longer time to run compared to others Also the FD method exhibits more numerical disperson compared to MOC and TVD, although the TVD is essentially a higher order FD technique based on the premise of a diminishing sum of concentration differences between adjacent nodes. Sensitivity analysis was performed for the Coconut Grove model using all the solution techniques. The results are presented in figure 7-44 and 7-45.

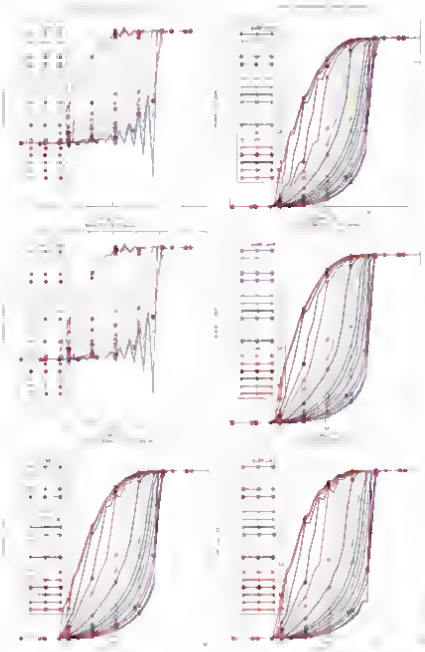

Figure 7-47 Sensitivity of monitored concentration to solution technique.

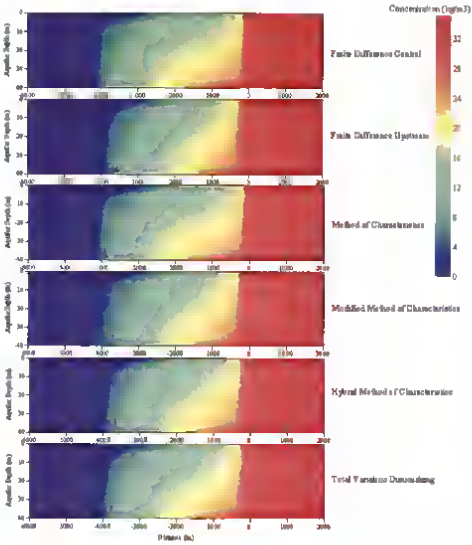

Figure 7-48 Sensitivity of concentration profile to solution technique

Application of the Genetic Algorithms Based Optimization Model

The optimization modeling was tested on a surficial unconfined aquifer of extent 3000m in both width and length. The aquifer has three layers and a total depth of 60 m. The model was discretized into 30 columns by 30 rows of each 100 m cell size (see Figure 7-49). The seaside boundary is set to have a time variant constant head and seawater concentration of 35 kg/m^3. The intrinsic aquifer parameters include a horizontal hydraulic conductivity of 1000 m/day, vertical hydraulic conductivity of 10 m/day, porosity of 0.35, longitudinal dispersivity of 300 m, transverse dispersivity of 30 m and vertical dispersivity of 3 m. A uniform recharge rate of 1320 mm/year was applied.

Two sets of simulations were performed by operating four wells at a time. The optimization well on/off status was utilized to turn four wells off at a given time and perform the optimization. In the second set of optimization the other set was turned on while the first four were turned off. The pumping wells were spaced 1000 m apart horizontally in order to minimize the chance of well interference. In order to satisfy the well interference criteria wells 1 to 4 were turned on initially. During the second optimization run, wells 5 to 8 were turned on. The model does not support a moving well option, but this approach makes it possible to perform optimization where the spatial location of the well plays a role in determining the optimal strategy. In all the optimization runs, pumping wells 1, 2, 5, and 6 pump from layer 2, while wells 3, 4, 7, and 8 pump from layers 3 and 4.

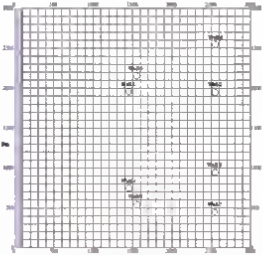

Figure 7-49 Model configuration and location of pumping wells

The management period considered in this model is 20 years and initial simulations were performed to see the level of salinity in each well and generate the required inputs for the optimization model The initial pumping and salinity data are presented in Table 7-9

Table 7-9 Initial pumping and salinity data for the pumping wells.

Well ID	Distance from sea (m)	Pumping rate (m^3/day)	Observed salinity range (kg/m^3)
Well 1	1000	1800	0 – 1.2
Well 2	2000	2400	0
Well 3	2000	2800	0
Well 4	1000	3000	0 – 2.9
Well 5	1500	1800	0 – 0.88
Well 6	2500	2400	0
Well 7	2500	2800	0
Well 8	1500	3000	0 – 2.4

In order to proceed with the optimization the minimum and maximum pumping and concentration values had to be set The minimum concentration value is set to be 0 while the maximum concentration value is set to be 0.5 kg/m^3 The maximum value is based on

the requirements for potable water supply Also the minimum pumping rate was set to be 0 while the maximum pumping rate was set to be 10^4 m^3/day In order to estimate the global maximum pumping value, the net recharge was calculated and divided for the existing four wells The resulting figure was higher than $1x10^4$ m^3/day so it was assumed that a $1x10^4$ m^3/day maximum pumping was reasonable to use Perhaps in other situations this figure could be set depending on additional factors such as forecasted demand.

Optimal Pumping Strategy

The optimizations performed for the two layouts of wells required an average of 700 generations with a crossover probability of 0 85 and the option of no elitism. The results of optimal pumping strategy are presented in Table 7-10

Table 7-10 Results of optimal pumping strategy and observed aquifer salinity

Well ID	Initial pumping rate (m^3/day)	Optimal pumping rates (m^3/day)		Range of Salinity (kg/m^3)	
		Layout 1	Layout 2	Layout 1	Layout 2
Well 1	1800	800	-	0 – 0 5	-
Well 2	2400	3000	-	0	-
Well 3	2600	3000	-	0	-
Well 4	3000	200	-	0 – 0 57	-
Well 5	1800	-	1000	-	0 – 0.3
Well 6	2400	-	2400	-	0
Well 7	2600	-	2600	-	0
Well 8	3000	-	1000	-	0.55

The distribution of salinity isochlors and hydraulic heads for pre and post optimization periods are presented in Figures 7-50 and 7-51 for layout 1, and Figures 7-52 and 7-53 for layout 2

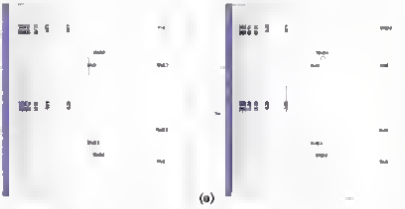

Figure 7-50. Distribution of salinity isochlors for the current (a) and optimal (b) pumping strategy at the end of 20 years management period for Layout 1

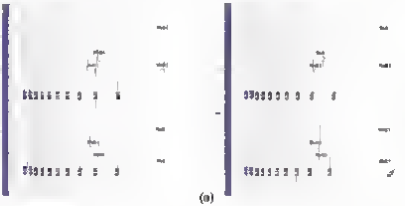

Figure 7-51. Distribution of groundwater head for the current (a) and optimal (b) pumping strategy at the end of 20 years management period for Layout 1

From the concentration plots presented in Figure 7-50 a and b, it is possible to see the impact of optimized withdrawal on the process of saltwater intrusion. If layout 1 is to be adopted, the current pumping rate of 10 000 m^3/day has to be reduced to 7 000 m^3/day. This results in a slower rate of saltwater intrusion by maintaining the 0.5 ppm isochlor at a maximum distance of about 1,500 m inland. Layout 2 on the other hand gave an optimal pumping rate of 7,200 m^3/day for the same criteria of lower salinity at the

monitoring/pumping points. The plot of changes in concentration for both layouts is presented in Figure 7-54.

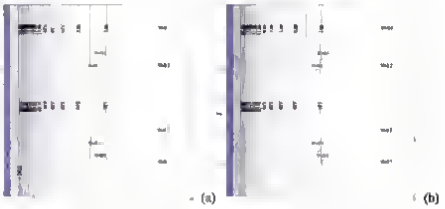

(a) (b)

Figure 7-52 Distribution of salinity isochlors for the current (a) and optimal (b) pumping strategy at the end of 20 years management period for Layout 2

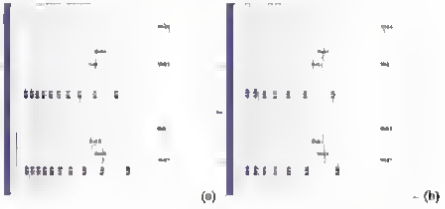

(a) (b)

Figure 7-53 Distribution of groundwater head for the current (a) and optimal (b) pumping strategy at the end of 20 years management period for Layout 2.

From the concentration plots presented in Figure 7-50 a and b, it is possible to see the impact of optimized withdrawal on the process of saltwater intrusion. If layout 1 is to be adopted, the current pumping rate of 10 000 m^3/day has to be reduced to 7,000 m^3/day. This results in a slower rate of saltwater intrusion by maintaining the 0.5 ppm isochlor at

a maximum distance of about 1 500 m inland. Layout 2 on the other hand gave an optimal pumping rate of 7,200 m^3/day for the same criteria of lower salinity at the monitoring/pumping points. The plot of changes in concentration for both layouts is presented in Figure 7-54.

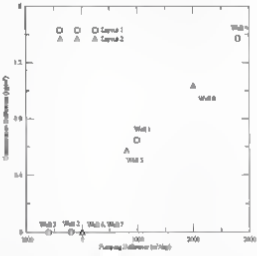

Figure 7-54 Plot of change in concentration and pumping for Layout1 and Layout 2

The plot of changes in pumping and monitored concentration are plotted in Figure 7-54, exhibiting an increasing trend. It is also possible to conclude that location of the wells plays a significant role in the solution of the optimization problem. The pumping values presented are by no means global optimum values, but rather close to what could be global maximum given the nature of the algorithm used in the solution.

The salt mass extracted through pumping was one of the constraining variables. As presented in Table 7-11, the salt mass extracted during post optimization simulation is considerably lower than the pre-optimization simulation. A tradeoff curve was also

plotted for both layouts to see the variation between salt mass and pumped volume for both (see Figure 7-55).

Table 7-11. Salt mass extracted and volume of water pumped

Layout	Pre/Post	Salt Mass Extracted (kg)	Volume Pumped (m^3)
1	Pre	26,027,920	73,000,000
1	Post	1,519,254	51,100,000
2	Pre	18,838,650	73,000,000
2	Post	2,321,123	52,560,000

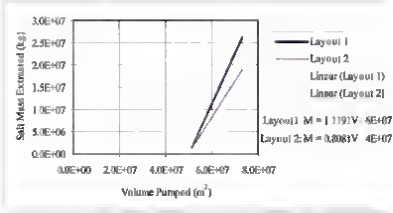

Figure 7-55. Tradeoff curve for salt mass extracted vs volume of water pumped.

As observed from the slopes of the linear equations in Figure 7-55, layout 2 provides a smaller amount of salt for the volume of water pumped. The equations represent salt mass M and volume of water V.

Optimal Pumping as a Decision Support System Tool

Optimal pumping is a vital component of a decision support system for sustainable management of coastal aquifers. Understanding the nature of the flow process through simulations and analyzing a set of scenarios to arrive at an optimal solution make possible a well informed decision.

It is also important to incorporate non-quantifiable socio-economic factors in the development of the decision support system. This could be achieved by involving the various stakeholders in the management of the water resources of the area.

CHAPTER 8
SUMMARY AND CONCLUSIONS

An Evaluation of the Research Presented in this Dissertation

This research is the result of about three and half years of work that had the purpose of establishing a sound understanding of the issues of climate change induced sea level rise, saltwater intrusion in coastal aquifers and integrated management strategy for coastal aquifers on the basis of optimal withdrawal of freshwater.

On the basis of the objectives, a GIS based tool that can be used to investigate the impacts of climate change induced sea level rise was developed. This approach also leaves room for further expansion of research to include integration of other components of coastal hydrologic processes. The three-dimensional, variable density, groundwater flow modeling code SEAWAT was modified to incorporate a sea level rise component that dynamically updates the coastal boundary to simulate the rise in sea level as part of the hydrostatic time variant specified head sea boundary. An optimization code also was developed on the basis of the mechanics of genetic algorithms. The optimization code uses the outputs of the simulation model to compute optimal pumping values.

The three simulation-optimization modeling tools are combined in a shell program that enables seamless running of each component within a user-friendly graphical user interface. In addition, a framework that could be used to develop a decision support system for optimal management of coastal aquifers subject to climate change impacts also was developed. Detailed summary and conclusions drawn from the research are presented under the following subheadings.

Global Climate Change, Sea Level Rise, and Seawater Intrusion

There is a compelling evidence suggesting the significance of anthropogenic factors in global climate and change. One of the primary manifestations of anthropogenic climate change is the rise in the global sea level. The sea level is expected to rise mainly due to global warming and the subsequent melting of ice caps and thermal expansion. The most recent climate change impacts assessment (IPCC, 2001) concluded that the global sea level is projected to rise by 0.09 to 0.88 meters between 1990 and 2100 for the full range of SRES scenarios. The projections made by the IPCC are slightly lower than the earlier forecasts made on the basis of the IS92 marker scenarios, which projected the sea level to rise globally by 0.13 to 0.94 meters.

Climatic anomalies such as El Niño are expected to continue with little or no change in their amplitude. The impacts of El Niño are primarily extremes of dry weather and heavy rainfall depending on the geographic location of the area. Extremely dry weather will have significant impacts on the estimation of actual and potential evapotranspiration while the high rainfall will pose a serious flooding threat. Global sea level rise, on the other hand, has a delayed response time to such an intense spell of wet period, and may not be significantly affected in the short run. However, the development of a management model for coastal aquifers with a management period of decadal to century scale has to consider the impacts of El Niño and other climatic anomalies in the form of changes in precipitation and evaporation.

Sea level rise is likely to cause accelerated seawater intrusion on a scale of century or more. When the aquifer is subject to additional stresses due to pumping and reduced recharge, the rate of intrusion is accelerated even faster. The influence of sea level rise and freshwater withdrawal on the process of seawater intrusion is dependent on a number

of factors. The factors include aquifer hydraulic properties, aquifer geometry, the location of pumping wells, and the magnitude of pumping.

Based on the analysis conducted for the surficial aquifer system of south Florida, climate change and sea level rise pose a serious threat to the ecosystem. Within the next 100 years or more, the primary forms of changes in the ecosystem are likely to be accelerated translation of the shoreline. Vulnerability assessments for the three counties considered in this study indicate that at a scale of a century the relative sea level rise estimate for the south Florida coast will be about 0.5 m. For the entire range of IPCC scenarios considered for select tidal stations, the relative sea level rise was estimated to be between 0.4 to 0.6 m. Depending on the slope of the local area considered, the corresponding shoreline translation for Palm Beach County could range from a few meters to about 200 meters or more. Similarly, for Broward County, the estimated shoreline translation could be as high as 1,000 m. For coastal areas of Miami-Dade County, the shoreline translation could be more than 100 m.

This study serves as indicator of the vulnerability of coastal areas to sea level rise. Detailed assessments should include mapping of existing infrastructure, settlement patterns, natural habitat, wildlife, and water resources. The study should also be performed at a smaller scale to enhance the visibility of the different GIS data layers to be used in the analysis. A detailed study should also consider that a range of scenarios and selection has to be made on the basis of likelihood of occurrence.

The analysis of available topographic data for Goksu Delta in Turkey indicated that sea level rise is a factor that needs to be considered in future studies. Detailed sea level rise and shoreline translation analyses were not conducted for the Goksu Delta due to

unavailability of a DEM for the area. As a result it is not possible to make specific conclusions

Sea level rise is also noted to have a significant impact on the movement of the transition zone For the cross-section model studied in south Florida, portion of the aquifer that extends from 3,000 to 4 200 meters from the coast is expected to undergo significant changes in ambient aquifer salinity due to sea level rise. In general there will be increased levels of salinity and shift of the transition zone The general trend of flow is not expected to show significant changes. The groundwater flow regime will be affected in terms of slightly higher levels of hydraulic head and a more dynamic exchange of freshwater saltwater near the coast

The surficial aquifer system of south Florida is not likely to attain a state of dynamic equilibrium within the next millennium Pumping stresses and the system of canals that exist in the area are the primary factors that make it difficult to attain dynamic equilibrium Detailed analyses that consider pumping withdrawals and the full range of sea level rise scenarios are expected to give a more practical management scenario for the next century

The study conducted on the Goksu Delta aquifer indicated that the change in aquifer salinity is expected to cover a cross-section that is about 1,000 meters wide on average in the X-X section (north-south orientation) The Y-Y section (east-west orientation) exhibited a much wider zone of influence due to the existence of a seaside on both ends A strip of aquifer that has a width of about 10,000 meters and a depth that extends from 200 to 400 meters is expected to undergo significant changes in salinity due to sea level rise The significance of geometry is also very noticeable in the Goksu Delta

as observed by the shape of the transition of the zone Conclusions similar to the one for the surficial aquifer cross-section of south Florida could be made for the Goksu Delta aquifer

Application of Genetic Algorithms Based Optimization in Coastal Aquifers Management

Genetic algorithm based search and optimization methods provide a very robust alternative to the existing optimization methods The nonlinear nature of most water resources problems makes non gradient-based search and optimization methods more appealing. The selection of parameters and seeding of the random number generation scheme require careful understanding and experimentation The stopping criterion needs to be defined on the basis of a more efficient method Generally, genetic algorithm based optimization requires longer processing time Therefore, access to faster processors makes the process run smoothly

The research presented in this dissertation is based on external coupling However, the process of simulation-optimization runs much better if the two processes are coupled internally With internal coupling, the simulation results are transferred dynamically to the optimization program and vice-versa.

Modeling Issues:Objectives and Scale Considerations

There are a number of approaches to modeling seawater intrusion One dimensional, steady state, analytical expressions such as the Ghyben-Herzberg approximation, are simple to use and do not require much data. They also have little computational requirements The premise of this analysis is the existence of steady state; however that is not quite the case as seen in the sensitivity analyses. These types of

analyses involve limiting assumptions and could be performed in a relatively short period of time

Two-dimensional, transient numerical models on the other hand can handle more complex situations and provide a more realistic representation of the processes and can account for variability in physical situations They have the ability to forecast and develop scenarios by considering temporal variability Two-dimensional models require computer modeling and involve moderate to large computational effort. There are some analytical approximations for two-dimensional problems Being numerical representations, they could have numerical stability problems and require proper understanding of solution methods and techniques. The processing time is relatively greater than for the one-dimensional models generally ranging from a few hours to several days depending on the processor speed.

Three-dimensional numerical models provide a much more accurate representation of the aquifer system to be modeled. Three-dimensional models require intensive computational efforts and considerably longer simulation time. The results are much more sensitive to temporal and spatial discretization and solution techniques and more vulnerable to numerical dispersion. As it is normally the case with variable density three-dimensional models of moderate extent, the computing needs are also coupled with input data and output file storage needs They generally require a thorough understanding of the numerical methods involved in order to obtain a numerically stable solution The results are more useful and accurate in predicting the future and developing scenarios.

Sharp interface models are useful alternatives that provide insight into the flow regime and characteristics in coastal aquifers However, the development of sharp

interface models needs to be performed with care and understanding of the characteristics of both the area that needs to be modeled and the underlying assumptions of the sharp interface approach Perhaps the two most significant factors that need to be considered are the thickness of the interface and equilibrium in the aquifer Generally sharp interface modeling should not be applied if the interface is thick compared to the depth of the aquifer The second significant factor is the assumption of a hydrostatic equilibrium, which in effect is not easy to achieve as aquifers are generally in a dynamic equilibrium state

Experience has shown that most coastal aquifers have a significantly broad transition zone Thus, using the sharp interface approach does not provide an accurate representation of the flow process In situations where there is a freshwater lens or a transition zone that extends to a few meters, then the sharp interface could be used by assuming the Ghyben-Herzberg relationship

Management models for coastal aquifers can have varying time scales If the management time frame is not more than a few decades, then the impacts of climate change can be approximated by the variability in recharge and evapotranspiration If on the other hand the time frame is on a scale of a century then the impacts of sea level rise need to be incorporated in addition to variability in recharge and evapotranspiration

Water resources management has to follow an integrated approach that considers both surface and groundwater sources as an integral unit. Depending on the scale of management time, the cumulative impact of climate change and consumptive use has to be incorporated in the development of a regional water resources analysis model

Development of a framework for management of coastal water resources has to be focused on optimal withdrawal of freshwater from both surface and groundwater. Since the problem of seawater intrusion is evident in most coastal aquifers, the management practice needs to have a component of impact mitigation. This could be accomplished by utilizing a number of techniques such as a hydraulic barrier, physical barrier, and surface recharge. Development of a regional model helps to formulate a decision support tool that enables management of water resources based on a sound policy that ensures sustainable use of water resources. A flowchart for a decision support system that could be used to formulate a water resources management policy for coastal areas is presented in Figure 8-1.

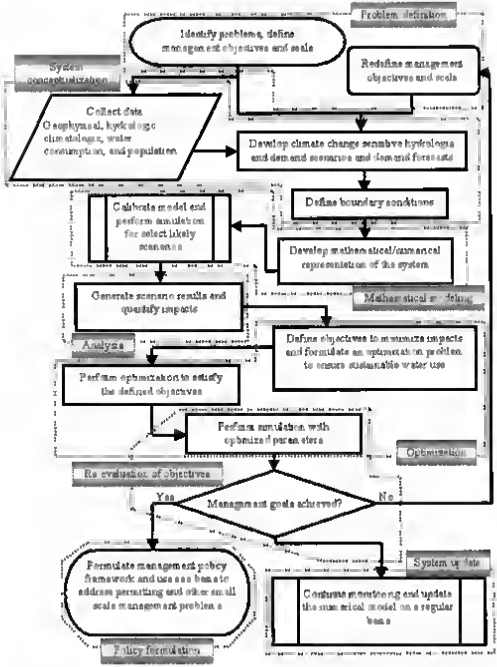

Figure 8-1 Coastal water resources management decision support system flowchart.

APPENDIX A
DEVELOPMENT OF INTEGRATED MODELING ENVIRONMENT

CSCAMM: Climate Sensitive Coastal Aquifer Management Model

CSCAMM is a shell program written in Visual Basic to serve as a Graphical User Interface (GUI) and facilitate the calling of the various components of the model CSCAMM provides the user the ability to select and run a specific model of choice by calling the executables specified in a selected working directory

CCGEN is a GIS tool written in the programming language Avenue and designed to work in ArcView therefore the user has to make sure the computer used for the modeling exercise has ArcView and the Spatial Analyst extension is activated The current release is a fully functional program to be run as a project in ArcView In the future CCGEN will be recompiled to be an ArcView extension, thus ensuring ease in portability

SEAWATSLR is a Fortran code designed to enable consideration of climate change in terms of sea level rise The code has an additional routine to import and analyze sea level rise data and modify the algorithm for Time Varying Constant Head (CHD) which needs to be defined along the seaside boundary During the modeling process variability in recharge and evapotranspiration will have to be included as required for the area of study.

GENOPT is a multi-objective, multi-management period groundwater flow optimization code written in Fortran. The inputs for GENOPT are obtained from either SEAWAT or SEAWATSLR

INTERFACE is a Fortran code written to read the binary outputs of SEAWAT or SEAWATSLR and calculate environmental groundwater heads. It also isolates specified isochlors of choice and enable exporting them into an ASCII file which could easily be imported into any plotting software for display.

Software and Data Requirements

The software requirements for CSCAMM are primarily of two types. The first type of software is a pre and post processor suited for MODFLOW and MT3DMS based models. In this research the pre and post processing was accomplished by Groundwater Vistas, a commercial software developed by Environmental Simulations Inc.

The second type of software is the Environmental Systems Research Institute (ESRI) product ArcView. The primary advantage of ArcView is its availability and the ease with which it could be modified.

The data required to run the various components of CSCAMM are the following,

1. Global climate change scenario to be selected from the IPCC 2001 documentation. This is included in the database of CSCAMM.
2. Digital Elevation data to be obtained from appropriate DEM data repository.
3. Local sea level rise trend and possibly submergence data which has to be obtained from NOAA and/or other agencies.
4. Hydrogeologic data required to construct a variable density groundwater flow model.
5. Water demand and population forecast data required to analyze the demand during simulation and optimization.

The methodology and data requirements are outlined in figure AA-1.

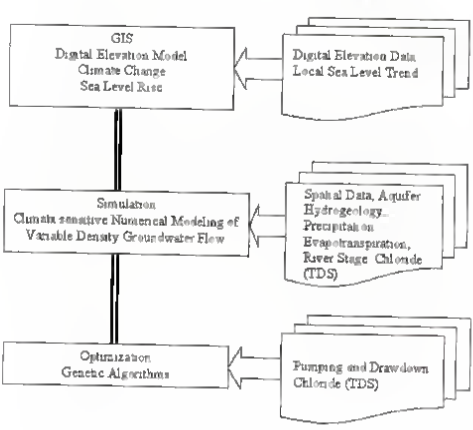

Figure A-1 Methodology and data requirement for CSCAMM

Computing Requirements

The computer codes used in this research are all designed to utilize the computing capacity of desktop computers in a more efficient manner However, due to the magnitude of data that needs to be processed there are minimal requirements that need to be met for the models to run smoothly

All models require a Pentium® or equivalent processor of at least 400 MHZ processing speed for the simulations to run efficiently In addition CCGEN requires a memory of at least 128 MB in order to be able to run a series of simulations. Depending

on the size of the raster file that is being processed the storage capacity of the disk might sometimes be not sufficient resulting in a very common error message of not being able to create grid file from the theme Unless the data has some inherent problems this usually comes from insufficient disk space or not the theme active in the active document When this happens the ASCII file that are necessary for the new grid files to be created will not be successfully created thus giving the error message

The user has the option of defining the analysis side depending on the orientation of the coast Since the translation of coast is calculated from the sea level to the inland the user has to specify which direction during the execution of the program The code is designed to be interactive to allow the user to make the necessary selections The simulation using CCGEN also creates a file named "rise.sir" by default. This file contains the necessary information required to run SEAWATSLR Upon successful execution of the program the intermediate ASCII files will be deleted thus freeing up space that could unnecessarily be held by slope and elevation ASCII files.

Screen Captures from Simulations

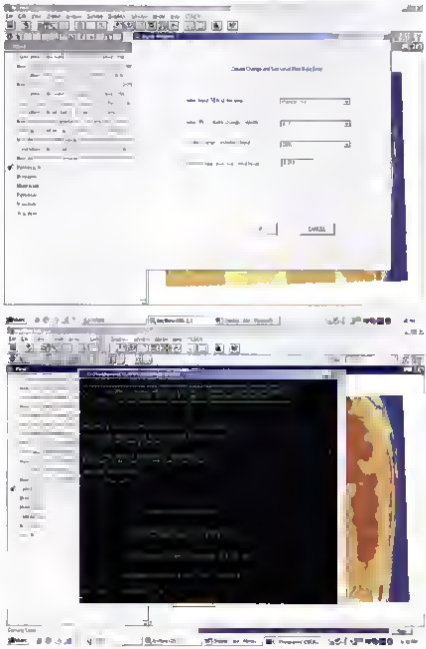

Figure A-2. Screen capture of CCGEN simulation

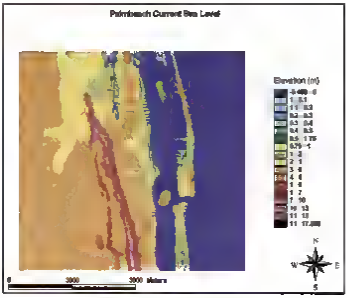

Figure A-3. Current sea level for Palmbeach coast

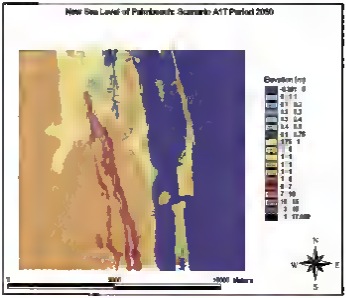

Figure A-4 Palmbeach coast sea level forecast for the year 2050

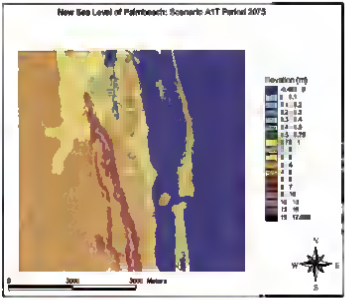

Figure A-5 Palmbeach coast sea level forecast for the year 2075

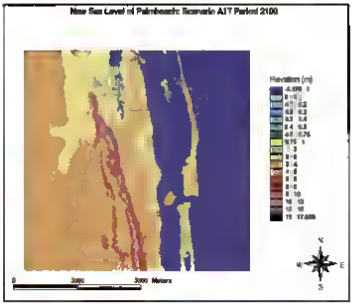

Figure A-6 Palmbeach coast sea level forecast for the year 2100

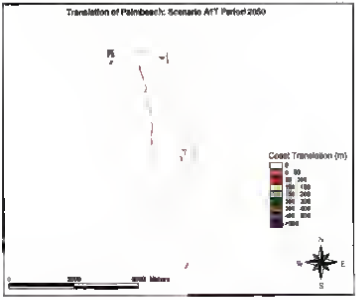

Figure A-7 Palmbeach coast shoreline translation forecast for the year 2050

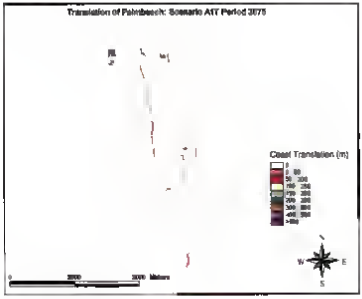

Figure A-8 Palmbeach shoreline translation forecast for the year 2075

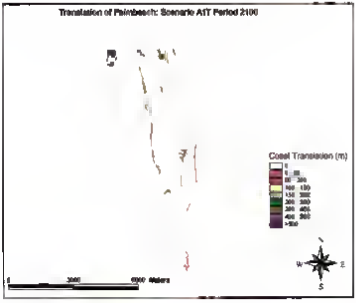

Figure A 9 Palmbeach shoreline translation forecast for the year 2100

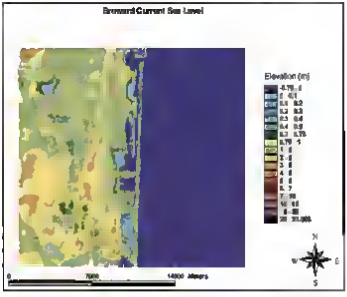

Figure A-10 Current sea level for Broward coast

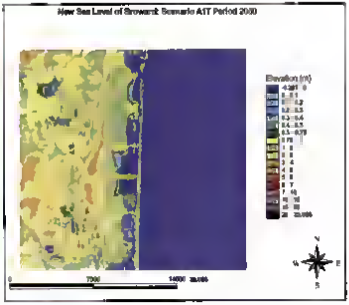

Figure A-11 Broward coast sea level forecast for the year 2050

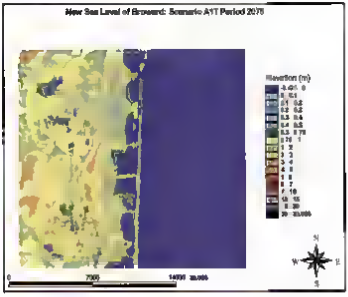

Figure A-12. Broward coast sea level forecast for the year 2075

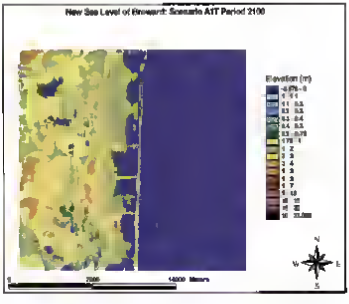

Figure A-13 Broward coast sea level forecast for the year 2100

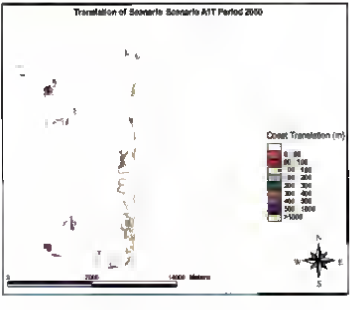

Figure A-14 Broward shoreline translation forecast for the year 2050

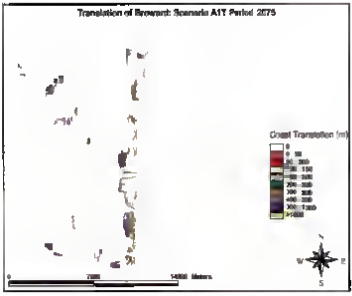

Figure A-15 Broward shoreline translation forecast for the year 2075

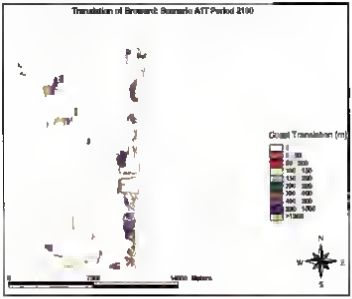

Figure A-16 Broward shoreline translation forecast for the year 2100

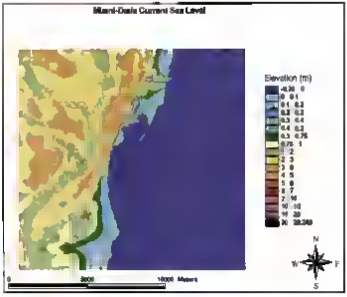

Figure A-17 Current sea level for Miami-Dade coast.

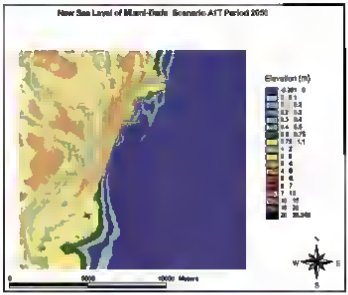

Figure A-18. Miami-Dade coast sea level forecast for the year 2050

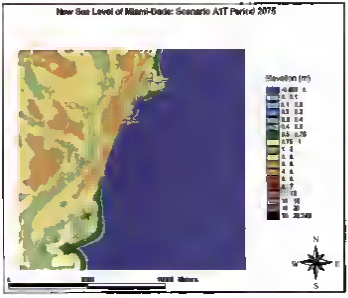

Figure A-19 Miami Dade coast sea level forecast for the year 2075

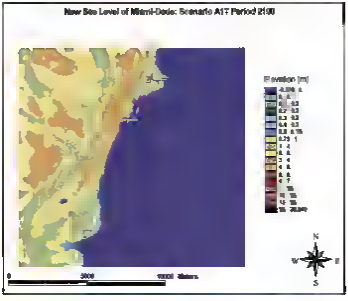

Figure A-20 Miami Dade coast sea level forecast for the year 2100

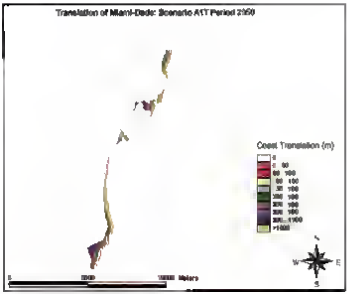

Figure A-21 Miami-Dade shoreline translation forecast for the year 2050

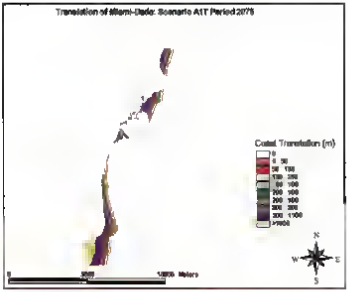

Figure A-22 Miami-Dade shoreline translation forecast for the year 2075

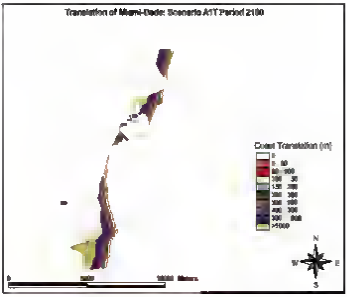

Figure A 23 Miami-Dade shoreline translation forecast for the year 2100.

LIST OF REFERENCES

Adeli H and Hung, S -L (1995) Machine Learning Neural Networks Genetic Algorithms and Fuzzy Systems Addison Wesley New York pp 128 135

Aguado E., Remson I (1974) Groundwater hydraulics in aquifer management. Journal of Hydraulics Div , Am Soc Civ Eng HY1 100 103-118

Aguado E., Remson I (1980) Groundwater management with fixed charges Journal of Water Resources Planning and Management Div Am Soc Civ Eng WR2-106 375 382

Alley, W M. (ed) (1993) Regional Ground-water Quality Van Norstrand Reinhold, New York, NY

Andersen, M P , and Woessner, W W (2002) Applied Groundwater Modeling Simulation of Flow and Advective Transport. Academic Press, San Diego CA

Appelo C A J and Geirnart, W (1991) Processes accompanying the intrusion of saltwater Hydrogeology of Saltwater-a Selection of SWIM Papers II, 291 304

Back W (1986) Geologic significance of the groundwater mixing zone associated with seawater intrusion Proceedings of the 5th International Symposium on Water Rock Interaction. Reykjavik, Iceland pp 25-28

Battaglin W A , Hay, L E , Parker R S and Leavesly G H (1993) Application of a GIS for modeling the sensitivity of water resources to alterations in climate in the Gunnison River basin, Colorado Water Resources Bulletin, 29(6), 43-69

Bear J (1972) Dynamics of Fluids in Porous Media. American Elsevier New York, 64p.

Bear J (1979) Hydraulics of Groundwater. McGraw-Hill, New York, 567 p

Bear, J and Dagan G (1964a) Some exact solutions of interface problems by means of hodograph method Journal of Geophysical Research, 69, 1563-1572.

Bear, J , and Dagan, G (1964b) Moving interface in coastal aquifers Journal of Hydraulics Div , Am. Soc Civ Eng 90, 193-216

Bear, J and Bachmat, Y (1967) A generalized theory on hydrodynamic dispersion in porous media IASH Symp Artificial Recharge and Management of Aquifers, IASH.

Bear, J and Verruijt, A. (1987) (Reprinted, 1998). Modeling Groundwater Flow and Pollution Theory and Applications of Transport in Porous Media D Reidel Publishing Co Dordrecht

Bear, J , Cheng, A H -D , Sorek, S , Ouazar, D and Herrera, I , (Eds.) (1999) Theory and Applications of Transport in Porous Media Sea Water Intrusion in Coastal Aquifers-Concepts Methods and Practices Kluwer Academic Publishers, Dordrecht.

Benachmi, M K., Ouazar, D., Naji, A. Cheng, A H-D , El Harrouni, K (2003) Pumping Optimization in Saltwater Intruded Aquifers by Simple Genetic Algorithm Deterministic Model Proceedings of the Second International Conference on SaltwaterIntrusion adn Coastal Aquifers-Monitoring, Modeling, and Management Merida, Mexico, (CD-ROM)

Bennett G D and Giusti, E V. (1971) Coastal Ground water Flow near Ponce, Puerto Rico U S Geological Survey Professional Paper 750-D, D 206-D211 Reston, VA

Berger, A , Dickinson, R E , and Kidson, J W (1989) Understanding Climate Change (Geophysical Monograph 52), American Geophysical Union

Bogardi, J.L., Das Gupta, A ,and Jiang H Z. (1991) Search beam method, a promising way to define non-dominated solution in multiojective groundwater development. International Journal of Water Resources Development. 7 247-258

Bruun P (1954) Coastal Erosion and Developmeot of Beach Profiles, Beach Erosion Board Technical Memorandum No 44 U S Army Cops of Engineers Washington, O C

Bruun P (1962) Sea-level rise as a cause of shore erosion. Journal of Waterways and Harbors Div ASCE 88 117-130

Chang, L C , Shoemaker, C A., Liu P L F (1992) Optimal time varying pumping rates for groundwater remediation. applicatioo of a constrained optimal cootrol algorithm Water Resources Research 28 3157-3173

Chen, C X and Jiao, J (1999) Numerical simulation of pumping tests in multilayer wells with non-darcian flow in the wellbore Ground Water 37(3) 465-575

Chang A.H D , Halhal, D , Naji, A , Ouazar, D (2000) Pumping optimization in saltwater-intrudad coastal aquifers. Water Resources Research, 36(8). 2155-2165

Chemical Rubber Company (1982) CRC Handbook of Chemistry and Physics (63rd ed) CRC Press Boca Raton, FL, pp D227-D258

Coello, C.A , Van Veldhuizen, D.A.V , and Lamont, G B (2002) Evolutionary Algorithms for Solving Multi-Objective Problems Kluwer Academic Publishers, New York

Cohon J.L., Marks, D H (1975) A review and evaluation of multiobjective programming techniques. Water Resources Research. 11 208-220

Colarullo, S J., Heidari, M., Maddock, T III (1984) Identification of an optimal groundwater strategy in a contaminated aquifer Water Resources Bulletin. 20 747-760

Collette, Y and Siarry, P (2003) Multiobjective Optimization Principles and Case Studies Springer-Verlag Berlin Germany

Culver T.B , Shoemaker, C A (1992) Dynamic optimal control for groundwater remediation with flexible management periods. Water Resources Research 28 629-641

Das, A., and Datta, B (1999a) Development of multiobjective management models for coastal aquifers Journal of Water Resources Planning and Managment 125 76-87

Das A , and Datta, B (1999b) Development of management models for sustainable use of coastal aquifers Journal of Irrigation and Drainage Engineering. 125 112 121

Das, A , Datta, B (2001) Application of optimisation techniques in groundwater quantity and quality management Sadhana, 26(4) 293 316

Datta, B , Dhuman S D. (1996) Chance constrained optimal monitoring network design for pollutants in groundwater Journal of Water Resources Planning Management. Div , Am Soc Civ Eng 122 180-188

Dean, R G (1983) Shoreline Erosion Due to Extreme Storms and Sea Level Rise 58 pp Department of Coastal and Oceanographic Engineering, University of Florida, Gainesville

Dean, R.G., Darlymple, R.A., Fairbridge R W Leatherman S P Nummedal D O'Brien M P Pilkey, O H , Sturges III, W , Wiegel, R L (1987) Responding to Changes in Sea Level Engineering Implications National Research Council (U S) Committee on Engineering Implications of Changes in Relative Mean Sea Level Washington, DC

Domenico, P.A. and Schwartz, F W (1998) Physical and Chemical Hydrogeology (2nd ed) John Wiley and Sons, New York.

Douglas B C (1991) Global sea level rise, Journal of Geophysical Research, 96(C4), 6981-6992

Dougherty, D. E., Marryott, R. A. (1991). Optimal groundwater management 1. Simulated annealing. Water Resources Research, 27, 2493-2508.

Emch, P. G., and Yeh, W. W-G. (1998). Management Model for Conjunctive Use of Coastal Surface Water and Ground Water. Journal of Water Resources Planning and Management, 124-3, 129-139.

Erskine, A.D. (1991). The effect of tidal fluctuation on a coastal aquifer in the U.K. Ground Water, 29, 556-562.

Essaid, H. I. (1999). In Bear, J., Cheng, A. H.-D., Sorek, S., Ouazar, D. and Herrera, I. (Eds.) (1999). Theory and Applications of Transport in Porous Media: Sea Water Intrusion in Coastal Aquifers-Concepts, Methods and Practices. Kluwer Academic Publishers, Dordrecht.

Essaid, H.I. (1990a). The Computer Model SHARP, a Quasi-Three-Dimensional Finite Difference Model to Simulate Freshwater and Saltwater Flow in Layered Coastal Aquifer Systems. U.S. Geological Survey Open File Report 90-4130, Reston, VA.

Essaid, H.I. (1990b). A multilayered sharp interface model of coupled freshwater and saltwater flow in coastal systems: Model development and application. Water Resources Research, 8(5):1307-1315.

Everts, C. (1985). Effects of sea level rise and net sand volume change on shoreline position at Ocean City, Maryland. Pp 67-98 in Potential Impacts of Sea Level Rise on the Beach at Ocean City, Maryland, Titus, J.G. (ed). U.S. Environmental Protection Agency, Washington, D.C.

Fetter, C.W. (1972). Position of the saline water interface beneath oceanic islands. Water Resources Research, 8(5):1307-1315.

Fetter, C.W. (2001). Applied Hydrogeology. Prentice-Hall, New Jersey.

Finney, B., Samsuhadi, A., and Willis, R. (1992). Quasi-three-dimensional optimization model of Jakarta Basin. Journal of Water Resources Planning and Management, 118:18-31.

Flemming, N. C. (1978). Holocene eustatic changes and coastal tectonics in the northeast Mediterranean: implications for models of crustal consumption. Phil. Trans. Royal Soc. London, 289, no. 1362, 405-458.

Flemming, N. C., and C. O. Webb, (1986). Tectonic and eustatic coastal changes during the last 10,000 years derived from archeological data. Zeit.-F. Geomorph. Suppl. Bd. 62, 1-29, Berlin.

Franke, O.L., Reilly, T.E., and Bennett, G.D. (1987) Definition of boundary and initial conditions in the analysis of saturated ground-water flow systems - an introduction Techniques of Water-Resources Investigations of the United States Geological Survey Book 3, Chapter B5 Washington, DC

Fried J.J. and Combarnous, M.A. (1971) Dispersion in porous media Advances in Hydroscience 7 169–282

Galeati G., Gambolati, G. (1988) Optimal dewatering schemes in the foundation design of an electronuclear plant. Water Resources Research 24 541-552

Gleick, P.H. (ed.) 1993 Water in Crisis A Guide to the World's Fresh Water Resources Oxford University Press, New York.

Glover, F. (1986) Future paths for integer programming and links to artificial intelligence Computers and Operations Research, 13 533-549

Glover, F. (1990) Artificial intelligence, heuristic frameworks and tabu search. Managerial and Decision Economics, 11 365-375

Glover, F. and Laguna, M. (1997) Tabu Search Kluwer Academic Publishers, Dordrecht.

Glover, R.E. (1959) The pattern of fresh-water flow in a coastal aquifer Journal of Geophysical Research, 64(4) 457-459

Goodchild, M.F., Haining, R., Wise, S. (1995) Integrating GIS and Spatial Analysis. problems and possibilities International Journal of Geographical Information Systems 6 407-23

Gordu, F. (2000) Simulation of Seawater Intrusion and Optimization of Groundwater Use in the Goksu Delta at Silifke Turkey ME Thesis University of Florida

Gorelick, S.M. (1983) A Review of Distributed Parameter Groundwater Management Models Water Resources Research 19(2) 305-319

Gorelick S.M., Voss C.I., Gill P.E., Murray W., Saunders M.A., Wright M.H. (1984) Aquifer reclamation design The use of contaminant transport simulation combined with nonlinear programming Water Resources Research 20 415-427

Gornitz, V. (1993) Mean sea level changes in the recent past, in Climate and sea level change Observations projections and implications, edited by R.A. Warrick, E.M. Barrow, and T.M.L. Wigley, Cambridge University Press

Gornitz, V. and A. Solow. (1991) Observations of long term tide-gauge records for indicators of accelerated sea level rise in Greenhouse Gas-Induced Climatic change A Critical Appraisal of Simulations and Observations M.E. Schlesinger (ed.), pp. 347-367. Elsevier Amsterdam

Gornitz, V , and L. Seeber, (1990) Vertical crustal movements along the east coast, North America, from historic and late Holocene sea level data, Tectonophysics 178

Guo, W , and Langevin, C D (2002) User's Guide to SEAWAT A Computer Program for Simulation of Three-Dimensional Variable-Density Groundwater Flow U S Geological Survey Open File Report 01-434 Tallahassee, FL

Guswa, J H and LeBlanc, D R. (1985) Digital Models of Ground-Water Flow in the Cape Cod Aquifer System, Massachusetts. U S Geological Survey Water Supply Paper 2209, Reston, VA

Hallaji, K., Yazicigil, H (1996) Optimal management of a coastal aquifer in southern Turkey Journal of Water Resources Planning and Management Div Am Soc Civ Eng. 122 233-244

Hennecke, W G and Cowell, P J (2000) GIS Modeling of Impacts of an Accelerated Rate of Sea-Level Rise on Coastal Inlets and Deeply Embayed Shorelines Environmental Geosciences 7(3)

Horn, J (1997) The Nature of Niching Genetic Algorithms and The Evolution of Optimal, Cooperative Populations. Ph.D Thesis , University of Illinois Urbana-Champaign.

Hubbert, M K (1940) The theory of ground-water motion Journal of Geology, 48(8) 785-944

Huyakorn, P S., Andersen, P.F., Mercer, J W , and White, H.O (1987) Saltwater in Aquifers Development and Testing of a Three-Dimensional Finite Element Model Water Resources Research, 23(2), pp 293-312

Intergovernmental Panel on Climate Change (IPCC) (2001a) Climate Change 2001 The Scientific Basis Contribution of WorkingGroup I to the Third Assessment Report of the Intergovernmental Panel on Climate Change Houghton, J T , Ding, Y , Griggs, D J , Noguer, M., Van der Linden, P J , and Xiaosu, D (eds) Cambridge University Press, Cambridge, U K , and New York, N.Y , U S A 944 pp.

Intergovernmental Panel on Climate Change (IPCC) (2001b) Climate Change 2001 Impacts Adaptations and Vulnerability Contribution of Working Group II to the Third Assessment Report of the Intergovernmental Panel on Climate Change. McCarthy, J.J , Canziani, O F., Leary, N.A., Dokken, D.J , White, K.S (eds) Cambridge University Press, Cambridge, U.K and New York, N Y , U S.A. 1000 pp

Intergovernmental Panel on Climate Change (IPCC). (2001c) Climate Change 2001 Mitigation Contribution of Working Group III to the Third Assessment Report of the Intergovernmental Panel on Climate Change

Intergovernmental Panel on Climate Change (IPCC) (2000) Emissions Scenarios Special Report of the Intergovernmental Panel on Climate Change Nakicenovic, N and Swart, R. (eds) Cambridge University Press, Cambridge U K , and New York, N Y., U S.A, 599 pp

Intergovernmental Panel on Climate Change (IPCC) (1998) Regional Impacts of Climate Change-An Assessment of Vulnerability--A special Report of IPCC Working Group II Cambridge University Press, Cambridge, U.K., and New York, N Y , U S.A,

Intergovernmental Panel on Climate Change (IPCC) (1996a) Climate Change 1995 The Science of Climate Change Contribution of Working Group I to the Second Assessment Report of the Intergovernmental Panel on Climate Change Houghton, J T., Meira Filho, L G , Callander, B A Harris N , Kattenberg A , and Maskell K. (eds) Cambridge University Press, Cambridge U K , and New York, N Y , U S A, 572 pp

Intergovernmental Panel on Climate Change (IPCC) (1996b) Climate Change 1995 Impacts, Adaptations and Mitigation of Climate Change Scientific Technical analyses Contribution of Working Group II to the Second Assessment Report of the Intergovernmental Panel on Climate Change Watson, R.T , Zinyowera M C , and Moss, R.H (eds) Cambridge University Press, Cambridge, U.K., and New York, N Y., U.S A, 878 pp.

Intergovernmental Panel on Climate Change (IPCC) (1996c) Climate Change 1995 Economic and Social Dimensions of Climate Change Contribution of Working Group III to the Second Assessment Report of the Intergovernmental Panel on Climate Change Bruce, J P., Lee, H., and Haites, E.F (eds) Cambridge University Press, Cambridge, U K., and New York, N Y , U S A, 448 pp

Intergovernmental Panel on Climate Change (IPCC) (1990) The IPCC Scientific Assessment Houghton, J T , Jenkins G.J. Ephraums J J (eds). Cambridge University Press, Cambridge, U K , and New York, N Y , U S.A, 365 pp

Jacob, C E (1940) On the flow of water in an elastic artesian aquifer Transactions American Geophysical Union 21 574-586

Jacob, C.E. (1950) Flow of ground water In Engineering hydraulics, Ed. (Hunter Rouse) John Wiley, New York, pp 321-386

Jiao, J. and Tang, Z. (1999) An analytical solution of groundwater response to tidal fluctuation in leaky confined aquifer Water Resources Research. 35(3) 747-751

Johnson, V M. Rogers, L.L. (2000) Accuracy of Neural Network Approximators in Simulation Optimization Journal of Water Resources Planning and Management, 126(2) 48-56

Jones, L Willis, R., Yeh W W G (1987) Optimal control of nonlinear groundwater hydraulics using differential dynamic programming. Water Resources Research 23 2097-2107.

Josselin de Jong, G de (1969) Generating functions in the theory of flow through porous media, in R J M de Wiest (ed.) Flow though Porous M Academic Press, New York, pp 75-82.

Kana, T W., Michel, J., Hayes, M O., Jensen, J.R. (1984) The Physical impact of sea level rise in the area of Charleston, S C pp 105-150 in Greenhouse Effect and Sea Level Rise, Barth, M C., and Titus J G., (eds) New York Van Norstrand Reinhold.

Karatzas G P., Pinder, G F (1996) Groundwater management using numerical simulation and the outer approximation method for global optimization Water Resources Research. 29 3371-3378

Kearney, M.S., and J C Stevenson, (1991). Island land loss and marsh vertical accretion rate evidence for historical sea-level changes in Chesapeake Bay. Journal of Coastal Research. 7(2) 403-415

Kirkpatrick, S., Gelatt, C.D., Vecchi, M.P (1983) Optimization by simulated annealing Science 220 pp 671-680

Knuth, D E (1981) Seminumerical Algorithms, 2nd ed. vol 2 of The Art of Computer Programming Addison Wesley: Reading, MA

Kondratyev, K Ya., and Cracknell, A P (1998) Observing Global Climate Change. Taylor and Francis, London

Laarhoven, P J M v, Aarts, E H L (1987) Simulated Annealing. Theory and Applications. Dordrecht, Kluwer Academic Publishers

Langevin, C D., Shoemaker, W.B and Guo W (2003) MODFLOW-2000, the U.S. Geological Survey Modular Ground-Water Model Documentation of the SEAWAT 2000 Version with the Variable-Density Flow Process (VDF) and the Integrated MT3DMS Transport Process (IMT) U S Geological Survey Open-File Report 03-426 Tallahassee, Florida.

Langley P A., Goodchild, M F., Maguire, D.J., and Rhind, D W., (eds) (1999) Geographical Information Systems. John Wiley and Sons, New York

Leatherman, S P (1984) Coastal geomorphologic responses to sea-level rise Galveston Bay, Texas Pp 151-178 in Greenhouse Effect and Sea Level Rise, Barth, M C, Titus, J G (eds) Van Norstrand Reinhold, New York.

Lefkoff, L. J., Gorelick, S. M. (1986) Design and cost analysis of rapid aquifer restoration systems using flow simulation and quadratic programming. Ground Water 24: 777-790.

Loucks, D. W. F., Yeh, W. W.-G., and Hsu, N.-S. (1984) Multiobjective water resources management planning. Journal of Water Resources Planning and Management Div. Am. Soc. of Civ. Eng. 110(1): 39-56.

Lyon, J. G., McCarthy, J., (eds). (1995) Wetland and environmental applications of GIS. Lewis Publishers, New York.

Maddock, T. III. (1972a) Algebraic technological function from a simulation model. Water Resources Research. 8: 129-134.

Maddock, T. III. (1972b) A groundwater planning model: A basis for a data collection network. Presented at the Int. Symp. on Uncertainties in Hydrologic and Water Resource Systems (Tucson, AZ. Int. Assoc. Sci. Hydrol.). Michener, W. K., Brunt, J. W., Stafford, S. G. (eds). (1994) Environmental Information Management and Analysis: ecosystem to global scales. Taylor and Francis: London.

Marryott, R. A., Dougherty, D. E., Stollar, R. L. (1993) Optimal groundwater management: 2. Application of simulated annealing to a field-scale contamination site. Water Resources Research. 29: 847-860.

Mercer, J. W., Larson, S. P., and Faust, C. R. (1980) Finite-Difference Model to Simulate the Areal Flow of Saltwater and Freshwater Separated by an Interface. U. S. Geological Survey Open File Report 80-407. Reston, VA.

Metropolis, N., Rosenbluth, A. W., Rosenbluth, M. N., Teller, A. H., and Teller, E. (1953) Equation of State Calculations by Fast Computing Machines. Journal of Chemical Physics. 21(6): 1087-1092.

Michener, W. K., Brunt, J. W., Stafford, S. G., (eds). 1994. Environmental Information Management and Analysis: ecosystem to global scales. Taylor and Francis: London, UK.

Millham, N. P., and Howes, B. L. (1995) A comparison of methods to determine K in a shallow coastal aquifer. Ground Water. 33: 49-57.

Misirli, F., Yazicigil, H. (1997) Optimal ground water pollution containment with fixed charges. Journal of Water Resources Planning and Management. Am. Soc. Civ. Eng. 123: 212.

Morshed, J., Kaluarachchi, J. J. (1998) Application of artificial neural network and genetic algorithm in flow and transport simulations. Advances in Water Resources. 22(2): 145-158.

Murtagh, B.A., and Saunders, M.A. (1987) MINOS 5.1 user's guide. Technical Report #83-20R, Systems Optimization Lab., Dept. of Operations Research, Stanford University, Stanford, CA.

Osyeka, A. (1985) Multicriteria optimization for engineering design. In Gero, J.S., (eds.) Design and Optimization. Academic Press, San Diego.

Oude Essink, G.H.P. (1996) Impact of Sea Level Rise on Groundwater Flow Regimes, Ph.D. Thesis, Delft University of Technology, Delft, The Netherlands.

Peltier, W.R., and A.M. Tushingham. (1989) Global Sea Level Rise and the Greenhouse Effect. Might They be Connected? Science 244(4906): 806-810.

Pinder, G.F. and Page, R.H. (1977). Finite element simulation of salt water intrusion on the south fork of Long Island. Finite Elements in Water Resources. Proceedings of the First International Conference on Finite Elements in Water Resources. Pentech Press, London, pp 2.51-2.70.

Press, W.H., Teukolsy, S.A., Vetterling, W.T., and Flannery, B.P. (1992) Numerical Recipes in Fortran 77: The Art of Scientific Computing (second edition). Cambridge University Press, New York, NY.

Reilly, T.E. and Goodman, A.S. (1985) Quantitative Analysis of Saltwater-Freshwater Relationships in Groundwater Systems-A Historical Perspective. Journal of Hydrology, 80: 125-160.

Reilly, T.E. and Goodman, A.S. (1987) Analysis of saltwater upconing beneath pumping well. Journal of Hydrology 89: 169-204.

Reilly, T.E., Frimpter, M.H., LeBlanc, D.R., and Goodman, A.S. (1987b) Analysis of steady-state saltwater upconing with applications at Truro Well Field, Cape Cod, Massachusetts. Ground Water 25(2): 194-206.

Reilly, T.E. (1993) In Ailey, W.M. (ed.) Regional Ground water Quality. Van Norstrand Reinhold, New York, NY.

Reilly, T.E. (2001) System and Boundary Conceptualization in Ground-Water Flow Simulation. Techniques of Water Resources Investigations of the United States Geological Survey, Book 3, Applications of Hydraulics, Chapter B8. Reston, VA.

Rosenwald, G.W., Green, D.W. (1974) A method for determining the optimum location of wells in a reservoir using mixed-integer programming. Soc. Pet. Eng. J. 14: 44-54.

Saffman, P.G. (1960) Dispersion due to molecular diffusion and macroscoping mixing in flow through network of capillaries. Journal of Fluid Mechanics 7(2): 194-208.

Shamir, U., Bear, J., and Gamliel, A. (1984) Optimal annual operation of a coastal aquifer. Water Resources Research, 20: 435-444.

Scheidegger, A.E. (1961) General theory of dispersion in porous media. Journal of Geophysical Research 66, 3273-3278

Sherman, I., and P. L. Woodworth, (1992) A comparison of late Holocene and twentieth century sea-level trends from the UK and North Sea region, Geophys. J. Int. 109(1) 96-105

Simmers, I. (ed.) 1987 Estimation of Groundwater Recharge (1988) NATO ASI Series, D. Reidel Publishing Co., Dordrecht. The Netherlands.

Singh, V.P. and Fiorentino, M. (1996) Geographical Information Systems in Hydrology Kluwer Academic Publishers. Dordrecht, The Netherlands.

Solomon, S.I., Berna, M., and Hogg, W., (eds.) (1987) The Influence of Climate Change and Climatic Variability on The Hydrologic Regime and Water Resources. (IAHS Publication No. 168) IAHS Press Wallingford, U.K.

Spall, J.C. (2003) Introduction to Stochastic Search and Optimization: Estimation, Simulation, and Control. Wiley-Interscience, Hoboken, NJ

Stewart, M.T. (1999) In Bear, J., Cheng, A.H.-D., Sorek, S., Ouazar, D., and Herrera, I. (Eds.) (1999). Theory and Applications of Transport in Porous Media: Sea Water Intrusion in Coastal Aquifers-Concepts, Methods and Practices. Kluwer Academic Publishers, Dordrecht

Stuyfzand, P.J. (1986) A new hydrochemical classification of water types: principles and application to the coastal dunes aquifer system of the Netherlands. Proceedings of the 9th Saltwater Intrusion Meeting. Delft, the Netherlands, pp 641-655

Tang, A., and Mays, L.W. (1998) Genetic Algorithms for Optimal Operation of Soil Aquifer Treatment Systems. Water Resources Management. 12. 375-396. Kluwer Academic Publishers.

Tiruneh, N.D., and Motz, L.H. (2003) Three-Dimensional Modeling of Saltwater Intrusion Coupled with the Impact of Climate Change and Pumping. Proceedings of the World Water and Environmental Resources Congress 2003 (CD-ROM). Philadelphia, PA, (CD-ROM)

Tiruneh, N.D., Motz, L.H. (2003) Sensitivity of Seawater Intrusion in Coastal Aquifers to a Hydraulic Barrier. American Geophysical Union Fall 2003 Conference presentation (CD-ROM). San Francisco, CA.

Tiruneh, N.D., Motz, L.H. (2001) Climate change Sea Level Rise and Saltwater Intrusion. Bridging the Gap: Meeting the World's Water and Environmental Resources Challenges. Proceedings of the World Water and Environmental Resources Congress (CD-ROM). Orlando, FL

Titus J G and Narayanan, V.K. (1995) The Probability of Sea Level Rise Washington D C , Environmental Protection Agency

Tooley M J (1993) Long term changes in eustatic sea level, in Warrick, R.A , Barrow, E M and Wigley, T M L (eds) Climate and sea Level Change Observations, Projections Implications Cambridge University Press.

Tooley, M.J and Jelgersma, S (eds.) (1992) Impacts of Sea-Level Rise on the European Coastal Lowlands. The Institute of British Geographers Special Publications Series Blackwell Pubbshers, Cambridge MA.

Trupin A and J Wahr (1990) Spectroscopic analysis of global tide gauge sea level data, Geophys. J Int , 100 441-453

Van Dam, J C. (1999) In Bear, J , Cheng, A H -D., Sorek, S., Ouazar, D and Herrera, I., (eds.) Theory and Applications of Transport in Porous Media Sea Water Intrusion in Coastal Aquifers-Concepts, Methods and Practices. Kluwer Academic Publishers, Dordrecht.

Varekamp, J C., E. Thomas, and O Van de Plassche, (1992) Relative sea level rise and climate change over the last 1500 years, Terra Nova 4 293 304

Voss, C.I. (1984a) AQUIFEM-SALT A Finite Element Model for Aquifers Containing a Seawater Interface U S Geological Survey Water Resources Investigations Report 84-4263 Reston, VA.

Voss C I (1984b) SUTRA-A Finite-Element Simulation Model for Saturated Unsaturated Fluid-Density-Dependent Ground Water Flow with Energy Transport or Chemically Reactive Single Species Solute Transport. U.S Geological Survey Water Resources Investigations Report 844369 Reston, VA.

Waggoner, P E (Ed) (1990) Climate Change and U S Water Resources. John Wiley and Sons, New York

Walker F J Saad, D F and Krohelski, J T (1998) Optimization of Ground-Water Withdrawal In the Lower Fox River Communities Wisconsin. U S Geological Survey Water Resources Investigation Report. 97-4218

Wang W , Ahlfeld, D P (1994) Optimal groundwater remediation with well location as a decision variable Model development. Water Resources Research. 30 1605-1618.

Wang, H F , and Andersen, M.P (1982) Introduction to Groundwater Modeling Finite Difference and Finite Element Methods Academic Press Inc San Diego, CA

Warrick, R A (1993) Climate and sea level change- a synthesis. Warrick, R.A., Barrow E M and Wigley, T M L (eds) (1993) Climate and sea Level Change, Observations, Projections Implications Cambridge University Press.

Warrick R A , Barrow, E M and Wigley T M L (eds) (1993) Climate and sea Level Change Observations Projections Implications. Cambridge University Press

Watson, R.T , Zinyowera, M.C., and Moss, R.H., (eds) (1998) The Regional Impacts of Climate Change An Assessmeot of Vulnerability Intergovernmental Panel on Climate Change Cambridge University Press

White J K and Roberts T O L (1994) The significance of groundwater tidal fluctuations Groundwater Problems in Urban Areas Proceedings of the International Conference organized by the Institution of Civil Engineers, Wilkinson, W B (ed) June 2-3, 1993 London. pp 31-42

Willis R (1976) Optimal groundwater quality management Well injection of waste water Water Resources Research. 12 47-53

Willis R, Liu P (1984) Optimization model for groundwater planning J Water Resources Planning and Management. Div , Am Soc Civ Eng. 110 333-347

World Health Organization (1996) Guidelines for drinking-water quality, 2nd ed Vol. 2 Health criteria and other supporting information, pp 367-370

Yakowitz, S J (1982) Dynamic programming applications in water resources Water Resour Res. 18 637-696

Yazicigil, H (1990) Optimal planning and operation of multiaquifer system. Journal of Water Resources Planning and Management. 116 435-454

Yazicigil H Rasheeduddin, M (1987) Optimization model for groundwater management in multi-aquifer systems Journal of Water Resources Planning and Management 113 257-273

Yeh W W G , Becker, L , Liang W K , Sun, N Z, Davert, M W , and Jeng, M C (1992) Development of multi-objective optimization model for water quality management planning in the upper Santa Ana basin Santa Ana Watershed Project Authority Report, Dept of Civil and Environ. Engrg , UCLA. Los Angeles, CA

Zheog, C and Wang P (1996) Parameter structure identification using tabu search and simulated annealing Advances in Water Resources 19(4) 215-224

Zheng, C , and Bennett, G D (1995) Applied contaminant transport modeling, theory and practice Van Nostrand Reinhold

BIOGRAPHICAL SKETCH

Nebiyu Daniel Tirunch graduated from Menelik II Comprehensive Secondary School in Addis Ababa, Ethiopia. He was then admitted to Arba Minch Water Technology Institute from which he graduated in 1992 with a Bachelor of Science degree in hydraulic engineering.

After working in the field of water supply design and construction for four years, he decided to go back to graduate school. He was awarded a full scholarship by the Netherlands fellowship program to study at the University of Dar Es Salaam. He obtained his Master of Science degree in water resources engineering from the University of Dar Es Salaam in 1997.

He started working on his Ph.D. in the Department of Civil and Coastal Engineering at the University of Florida in Fall 1999. In the past five years he worked under the supervision of Dr. Louis H. Motz in the field of numerical modeling of groundwater flow.

I certify that I have read this study and that in my opinion it conforms to acceptable standards of scholarly presentation and is fully adequate, in scope and quality, as a thesis for the degree of Doctor of Philosophy

Louis H. Motz, Chairman
Associate Professor of Civil and Coastal Engineering

I certify that I have read this study and that in my opinion it conforms to acceptable standards of scholarly presentation and is fully adequate, in scope and quality, as a thesis for the degree of Doctor of Philosophy

Kirk Hatfield, Cochairman
Associate Professor of Civil and Coastal Engineering

I certify that I have read this study and that in my opinion it conforms to acceptable standards of scholarly presentation and is fully adequate in scope and quality, as a thesis for the degree of Doctor of Philosophy

Scott E. Smith
Associate Professor of Forest Resources and Conservation

I certify that I have read this study and that in my opinion it conforms to acceptable standards of scholarly presentation and is fully adequate in scope and quality as a thesis for the degree of Doctor of Philosophy

William R. Wise
Associate Professor of Environmental Engineering and Sciences

I certify that I have read this study and that in my opinion it conforms to acceptable standards of scholarly presentation and is fully adequate in scope and quality, as a thesis for the degree of Doctor of Philosophy

Elizabeth J. Screaton
Assistant Professor of Geological Sciences

This thesis was submitted to the Graduate Faculty of the College of Engineering and to the Graduate School and was accepted as partial fulfillment of the requirements for the degree of Doctor of Philosophy

December 2004

Pramod P Khargonekar
Dean College of Engineering

Kenneth J Gerhardt
Interim Dean, Graduate School